Summer 8-15-2018

Dualities, Topological Properties, and Degeneracies of Classical and Quantum Lattice Models

Seyyed Mohammad Sadegh Vaezi
Washington University in St. Louis

WASHINGTON UNIVERSITY IN ST. LOUIS

Department of Physics

Dissertation Examination Committee:
Zohar Nussinov, Chair
Carl Bender
Gerardo Ortiz
Alexander Seidel
Li Yang

Dualities, Topological Properties, and Degeneracies of Classical and Quantum Lattice Models

by

Seyyed Mohammad Sadegh Vaezi

A dissertation presented to
The Graduate School
of Washington University in
partial fulfillment of the
requirements for the degree
of Doctor of Philosophy

August 2018
Saint Louis, Missouri

Contents

List of Figures

List of Tables

Acknowledgments

Foremost, I would like to express my sincere gratitude to my advisor Prof. Zohar Nussinov for the continuous support of my Ph.D study and research, for his patience, motivation, enthusiasm, and immense knowledge. His guidance helped me in all the time of research and writing of this thesis.

My sincere gratitude also goes to Prof. Gerardo Ortiz. It was a great pleasure for me to collaborate with him during my doctoral studies. I have benefited a lot from his knowledge, experience, priceless ideas and inspiration discussions.

I would also like to thank my defense committee members, Prof. Alexander Seidel, Prof. Carl Bender, and Prof. Li yang for serving as my committee members.

Finally, I must express my very profound gratitude to my parents, my brother Dr. Abolhassan Vaezi, and other family members for providing me with unfailing support and continuous encouragement throughout my years of study and through the process of researching. This accomplishment would not have been possible without them. Thank you.

Seyyed Mohammad Sadegh Vaezi

Washington University in Saint Louis

August 2018

Dedication

to my family

ABSTRACT OF THE DISSERTATION

Dualities, Topological Properties, and Degeneracies of Classical and Quantum Lattice Models

by

Seyyed Mohammad Sadegh Vaezi

Doctor of Philosophy in Physics

Washington University in St. Louis, 2018

Zohar Nussinov, Chair

We study various nontrivial facets of "degeneracy"- a concept of paramount importance in numerous physical systems.

In the first part of this thesis, we challenge the folklore that if the ground state degeneracy of a physical system depends on topology then this system must necessarily realize an unconventional, so-called "topological quantum", order. To this end, we introduce a classical rendition of the Toric Code model that displays such a topological degeneracy yet exhibits conventional Landau order. As the ground states of this classical system may be distinguished by local measurements, this example illustrates that, on its own, topological degeneracy is not a sufficient condition for topological quantum order. This conclusion is generic and applies to many other models.

In the second part of this thesis, we prove that under fairly modest conditions, all "dualities" are conformal. This general result has enormous practical consequences. For example, one

can establish that weak- and strong-coupling series expansions of arbitrarily large finite size systems are trivially related. As we explain, this relation partially solves or, equivalently, localizes the computational complexity of evaluating the series expansions to only a subset of those coefficients. The coefficients in the strong-coupling series expansions are related to the degeneracy of the system. Thus, our results may facilitate the computation of the degeneracies of the various levels.

We end this thesis by establishing a unified framework for studying general disordered systems with either discrete or continuous coupling distributions. We introduce a "*binomial*" spin glass wherein the couplings are the sum of "m" identically distributed Bernoulli random variables. In the continuum limit $m \to \infty$, this system reduces to a model with Gaussian couplings, while $m = 1$ corresponds to the $\pm J$ spin glass. We demonstrate that for short-range Ising spin glass models on d-dimensional hypercubic lattices, the ground-state entropy density for N spins is bounded from above by $(\sqrt{d/2m} + 1/N) \ln 2$. This confirms the longheld suspicion that the degeneracy of real (finite dimensional) spin glasses with Gaussian couplings is not extensive. Exact calculations reveal the presence of a crossover length scale $L^*(m)$ below which the binomial spin glass is indistinguishable from the Gaussian system. Our analytical and numerical results underscore the non-commutativity of the thermodynamic and continuous coupling limits.

Chapter 1

Introduction

Condensed matter physics explores microscopic and macroscopic properties of "condensed" materials (including, principally, solids and fluids of various types). One of the most important and fundamental issues in condensed matter (and other branches of) physics is to understand the different phases of matter and what occurs during transitions between these phases. The tools of statistical mechanics are crucial to the understanding of phase transitions in various systems. A fundamental concept in the study of phase transitions and other general physical questions is that of "degeneracy" which is the cornerstone of this thesis. The concept of degeneracy threads all of the chapters of this thesis. In what follows, I will first briefly review the subject of phase transitions and then discuss the importance of degeneracy.

1.1 Phase transitions

Throughout the decades, there has been a flurry of activity in studying phase transitions and critical phenomena. This quest has been driven both by fundamental questions as

well as possible applications. It is very important to develop a good understanding of this phenomena [1–5].

Different states of matter are associated with different internal structures which in many case can be related to "order parameters". Phase transitions occur upon a variation of an external control parameter (e.g., temperature or pressure). To understand this better, we may compare three states of matter, i.e., gas, liquid, and solid. At low enough temperatures that most materials become solid, atoms form a very regular pattern and develop crystalline order. Solids have a very ordered internal structure. As the temperature is raised, atoms start moving with increasing energies. Ultimately, the solid melts into a fluid. At even higher temperatures the system transforms into a gas. Gases and fluids lack clear structured orders. In this example, the external parameter is temperature and thermal fluctuation is responsible for the phase transition. The above discussed transitions, where temperature is the control variable, are examples of "classical phase transitions". Phase transitions can also occur at zero temperature where quantum fluctuations (arising from Heisenberg's uncertainty principle) play an important role. In this case, a physical and non-thermal parameter such as magnetic field or pressure is varied to access the phase transition. These types of transitions are inherently quantum in nature. In "quantum phase transitions", the ground states change in response to a variation of an external parameter of the Hamiltonian. For example, in the superconductor-insulator transition, the control parameter could be the parallel or perpendicular magnetic field, disorder, or charge density.

According to the conventional taxonomy, phase transitions can be grossly divided into discontinuous or continuous. Discontinuous transitions generally feature an entropy jump and a phase coexistence. The change in entropy corresponds to latent heat. During this process, the temperature of a system remains unchanged despite absorbing (or releasing) a fixed amount

of energy per unit volume. In such a transition, an appropriately defined order parameter may change abruptly from zero to a non-vanishing finite value. Examples are afforded by solid-liquid (e.g., melting of ice, where ice and water coexist at 273.15 K) and fluid-superfluid transitions. By contrast, in continuous phase transitions the entropy changes continuously (no latent heat is present) and no phase coexistence is seen. A continuous phase transition is characterized by a divergent susceptibility, divergent correlation length, and power-law decay of correlations at the ("critical") transition point. In continuous transitions, the order parameter changes continuously from zero to a finite value.

1.2 Novel aspects of degeneracies: A synopsis of this thesis

We briefly summarize various nontrivial facets of degeneracy that will be elaborated on in the following chapters.

1.2.1 Degeneracy and Topological Order (Chapter 2)

For many decades, it was believed that the Landau symmetry-breaking paradigm can explain all different phases of matter [1,6]. As we explained earlier, in different materials, atoms can organize to display various orders. When a system undergoes a phase transition, the order of its constituent atoms changes. Each order typically breaks one or more symmetries. The "order parameter" measures the degrees of symmetry breaking in the ordered phase. The order parameter is non-zero in the ordered phase (lower-symmetry state) and vanishes in the disordered phase (symmetric phase). For example, a liquid is invariant under continuous

symmetries such as global rotations and translations while the crystalline phase typically exhibits only discrete symmetries such as specific rotations, translations, or reflections. Such systems are known as Landau ordered. Their main characteristic is that the state of the system can be determined by performing finite number of local measurements.

However, in 1982, Horst Störmer and Daniel Tsui found a new quantum state, by cooling down a two-dimensional electron gas to very low temperatures and subjecting it to strong magnetic fields. It was named the Fractional Quantum Hall (FQH) state [6–9]. FQH states cannot not be described using conventional symmetries and order parameters; a new approach rather than Landau symmetry-breaking theory is needed. To explain the new states of matter, the concept of "Topological Quantum Order" (TQO) [6,10] was introduced. Most textbook examples of such systems exhibit topological degeneracy- i.e., the ground state degeneracy depends on the topology of the manifold on which the system is embedded. For instance, on a genus g manifold, the FQH system at filling fraction $\nu = 1/3$ has a degeneracy equal to 3^g. For such systems, we cannot define Landau order (local order) parameter and the state of the system cannot be determined by performing finite number of local measurements. Common lore asserted that a topological ground state degeneracy implied topological order.

In chapter 2, we challenge this hypothesis by introducing some classical models which are Landau ordered despite having topological degeneracy. We further discuss the definition of the topological order as follows. Consider a set of $n_{g.s.}$ orthonormal ground states $\{|g_\alpha\rangle\}(\alpha = 1, ..., n_{g,s},)$ with a spectral gap to all other (excited) states. Topological order exists at $T = 0$, if and only if for any quasi-local operator $\mathcal{V}$ [11, 12],

$$\langle g_\alpha|\mathcal{V}|g_\beta\rangle = v\delta_{\alpha,\beta} + c, \tag{1.1}$$

where v is a constant, independent of α and β, and c is a correction that is zero in the thermodynamic limit. For different classical models that we have studied, in spite of finding a topological ground state degeneracy, Eq. (1.1) is violated. These models are Landau ordered in spite of having topological degeneracy.

1.2.2 Degeneracy and duality transformations (Chapter 3)

Consider a system with states l, energy E_l, and associated degeneracy D_l. By definition, the partition function is the Laplace transformation of the density of states. The partition function

$$\mathcal{Z} = \sum_l D_l e^{-E_l/k_B T}, \tag{1.2}$$

where k_B and T are the Boltzmann's constant and temperature, respectively, and the summation is over all allowed states l of the system. The free energy A is given by

$$A = -k_B T \ln \mathcal{Z}. \tag{1.3}$$

One should note that since $\mathcal{Z}$ is a sum of exponentials of $e^{-E/k_B T}$, the non-analytic behavior of the free energy may become apparent only in the "thermodynamic limit" [5].

The thermodynamic properties of the system can be obtained by differentiation of A or $\mathcal{Z}$. For example the internal energy $U = \langle E \rangle$ is defined as,

$$U = \frac{\sum_l E_l D_l e^{-E_l/k_B T}}{\mathcal{Z}}. \tag{1.4}$$

It is trivial to show (as is well known) that

$$U = k_B T^2 \frac{\partial \ln \mathcal{Z}}{\partial T} = -T^2 \frac{\partial (A/T)}{\partial T}. \tag{1.5}$$

Similarly, the entropy S is given by

$$S = -\frac{\partial A}{\partial T}. \tag{1.6}$$

Unfortunately, especially in more than one spatial dimension, the number of models for which the free energy may be calculated exactly is very small [13]. There are numerous models (e.g., Ising model) for which the energy levels (E_l's) can be determined yet the associated degeneracies (D_l) are not known in general. Thus, any method that can help with the computation of the individual level degeneracies is very welcome. In chapter 3, we demonstrate that the implementation of "duality" transformations can indeed facilitate the computation of D_l's and consequently $\mathcal{Z}$ (and general observables).

Duality (as it appears in physics) was first introduced in 1886 by the British autodidact engineer Oliver Heaviside [14]. The basic realization of Heaviside was that Maxwell's equations of electromagnetism in vacuum are invariant under a duality transformation that exchange the electric field with the magnetic field (and vice versa). In statistical mechanics and field theory, notable duality transformations relate physical systems at very high temperatures (weak coupling) to those of low temperatures (strong coupling). The basic virtue of nearly all dualities is that they often connect hard to examine problems with strong interactions (or low temperatures) to nearly free particle systems (or high temperature systems).

The key idea of chapter 3 is that if two dual or complementary points of view exist of a given physical problem, then this implies an equality between functions computed in the two dual representations. These equalities give rise to the linear equations.

In the first part of this chapter, we demonstrate that under fairly general mild constraints, all dualities are "conformal". In mathematics, conformal maps in the complex plane preserve angles locally. For example, if F (i.e., acting on parameter w in the complex plane) represents a duality transformation, then it can be written as

$$F(w) = \frac{a_1 w + a_2}{a_3 w + a_4}, \tag{1.7}$$

with a_1, a_2, a_3, and a_4 complex coefficients, and determinant

$$\Delta = \det \begin{pmatrix} a_1 & a_2 \\ a_3 & a_4 \end{pmatrix} = a_1 a_4 - a_2 a_3 \neq 0. \tag{1.8}$$

In the remaining of this chapter, we use duality as a tool to relate the high temperature ($\mathsf{H}-\mathsf{T}$) and low temperature ($\mathsf{L}-\mathsf{T}$) series expansions of the partition function in different systems such as Ising models, Potts model, Ising spin glass models, and Wegner models. By studying these models, we realize that duality leads to partial solvability and facilitates the computation of the coefficients (D_l, i.e., the degeneracies) in Eq. (1.2).

Here, I briefly explain the essentials of our method for the Ising model. Consider a general bipartite lattice (in any finite number of dimensions d) of size N, endowed with periodic

boundaries, with an Ising spin s_{x} at each lattice site x. The Hamiltonian is given by

$$H = -J \sum_{\langle \mathsf{xy} \rangle} s_{\mathsf{x}} s_{\mathsf{y}} \equiv -J \sum_{\alpha=1}^{dN} z_\alpha. \tag{1.9}$$

The summation in Eq. (1.14) is over nearest-neighbor spins at sites x and y sharing the link $\alpha = \langle \mathsf{xy} \rangle$, $z_\alpha = \pm 1$. The $\mathsf{H}-\mathsf{T}$ and $\mathsf{L}-\mathsf{T}$ series expansions [15] of the partition function are given by

$$\begin{aligned} \mathcal{Z}_{\mathsf{H}-\mathsf{T}} &= 2^N (\cosh K)^{dN} \sum_{l=0}^{dN/2} C_{2l} (\tanh(K))^{2l}, \\ \mathcal{Z}_{\mathsf{L}-\mathsf{T}} &= 2 e^{KdN} \sum_{l=0}^{dN/2} C'_{2l} (e^{-2K})^{2l}, \end{aligned} \tag{1.10}$$

where $K = \beta J$, with $\beta = \frac{1}{k_B T}$ the inverse temperature. The coefficients C'_{2l} provide the degeneracy (i.e., D_l) of the l-th level ($l = 0, 1, ..., dN/2$) with energy $E_l = -J(dN - 4l)$. Defining $w = \tanh(K)$ and $w' = e^{-2K}$, it is trivial to check the identities

$$\begin{aligned} w &= F(w') = \frac{1-w'}{1+w'}, \\ w' &= F(w) = \frac{1-w}{1+w}. \end{aligned} \tag{1.11}$$

Invoking Eqs. (1.10) and (1.11), we can rewrite Z_{H-T} and Z_{H-T} as,

$$\begin{aligned} \mathcal{Z}_{\mathsf{H}-\mathsf{T}} &= 2 e^{KdN} \Big[\sum_{m=0}^{dN} \Big(\frac{\sum_{l=0}^{dN/2} C_{2l} A^d_{\frac{m}{2},l}}{2^{(d-1)N+1}} \Big) (e^{-2K})^m \Big], \\ \mathcal{Z}_{\mathsf{L}-\mathsf{T}} &= 2^N (\cosh K)^{dN} \Big[\sum_{m=0}^{dN} \Big(\frac{\sum_{l=0}^{dN/2} C'_{2l} \; A^d_{\frac{m}{2},l}}{2^{N-1}} \Big) (\tanh(K))^m \Big], \end{aligned} \tag{1.12}$$

where $A^d_{k,l} = \sum_{i=0}^{2l} (-1)^i \binom{2l}{i} \binom{dN-2l}{2k-i}$.

Since partition functions of finite size systems are analytic (i.e., all expansions are convergent), equating the $\mathcal{Z}_{\mathsf{H-T}}$ ($\mathcal{Z}_{\mathsf{L-T}}$) in Eq. (1.10) with the $\mathcal{Z}_{\mathsf{L-T}}$ ($\mathcal{Z}_{\mathsf{H-T}}$) in Eq. (1.12) leads to a linear relation among expansion coefficients,

$$\begin{aligned}
\sum_{l=1}^{dN/2} A^d_{k,l} C_{2l} + \binom{dN}{2k} &= 2^{(d-1)N+1} C'_{2k}, \\
\sum_{l=1}^{dN/2} A^d_{k,l} C'_{2l} + \binom{dN}{2k} &= 2^{N-1} C_{2k}.
\end{aligned} \tag{1.13}$$

Eq. (1.13) is a "duality" relation connecting the weak and strong coupling coefficients (or degeneracies D_l) $\{C_{2l}\}$ and $\{C'_{2l}\}$. Our analysis in chapter 3 reveals that one needs to compute only $1/4$ of the combined coefficients $\{C_{2l}\}$ and $\{C'_{2l}\}$ and the rest are given by Eq. (1.13). These results are correct for any arbitrary large finite size system.

1.2.3 Degeneracy and the spin glass model (Chapter 4)

One of the outstanding problems in physics is understanding the nature and complexity of spin glasses [5, 16–18]. These systems are extremely rich and relate to deep questions in computational complexity theory. Although this problem is decades old by now, our understanding of short-range spin glass models remains poor. In chapter 3 we briefly study the spin glass model, but because of its importance, the entirety of chapter 4 is devoted to this model.

Sherrington, Kirkpatrick, Parisi, Nishimori, and many others have significantly increased our understanding of infinite dimensional and infinite range spin glasses [18–20]. However, what occurs in physical finite dimensional short-range spin glasses is not clear. While the Parisi solution and various related (effective infinite dimension or infinite range) mean-field

treatments raise the possibility of an exponentially large number of ground states, other considerations [16, 21–25] suggest that in typical short-range spin glasses, there are (similar to ferromagnets) only two symmetry related ground states. Understanding of this question is not merely of academic importance; the behavior of real finite dimensional magnetic spin glass systems has long been of direct experimental pertinence, e.g., [17, 26].

The quintessential short-range Ising spin glass system is the Edwards-Anderson(EA) model [27]. The EA spin glass Hamiltonian is similar to that of Eq. (1.9) but with varying couplings. That is,

$$H = -\sum_{\langle \mathsf{xy} \rangle} J_{\mathsf{xy}} s_{\mathsf{x}} s_{\mathsf{y}} \equiv -\sum_{\alpha=1}^{dN} J_\alpha z_\alpha. \tag{1.14}$$

In various standard Ising spin glass models, the spin couplings $\{J_\alpha\}$ in Eq. (1.14) are customarily drawn from one of several well studied distributions. For instance, in the "binary Ising spin glass model" [28], the couplings $\{J_\alpha\}$ are random variables that assume the two values ± 1 with probabilities $P(J_\alpha = 1) = p$, $P(J_\alpha = -1) = 1 - p$ (i.e., a Bernoulli distribution). In the continuous EA model, the couplings $\{J_\alpha\}$ are drawn from a Gaussian distribution of vanishing mean and variance equals to unity.

Unfortunately, the nature of real spin glasses with continuous couplings remains ill-understood. While the extensive ground state degeneracy is well established for various binary distributions [29, 30], the situation for the continuous EA model has been mired by controversy [31–33].

In chapter 4, we introduce a new class of ("Binomial") spin glass models, which enables us to interpolate between the well understood discrete spin glasses and the enigmatic continuous spin glasses in arbitrary space dimensionality. In this model the *binomial coupling* for each

link α, $\mathcal{J}_\alpha^m \equiv \frac{1}{\sqrt{m}} \sum_{k=1}^m J_\alpha^{(k)}$, is a sum of m copies (or "layers") of binary couplings $J_\alpha^{(k)} = \pm 1$, each with probability p of being $+1$ and $1-p$ of being -1. The probability distribution of $\mathcal{J}_\alpha^m$,

$$\tilde{P}(\mathcal{J}_\alpha^m) = \sum_{j=0}^{m} \binom{m}{j} p^{m-j}(1-p)^j \delta\left(\mathcal{J}_\alpha^m - \frac{m-2j}{\sqrt{m}}\right), \tag{1.15}$$

is a binomial. In the large-m limit, for general p, the distribution (1.15) approaches a Gaussian of mean $\sqrt{m}(2p-1)$ and variance $\sigma^2 = 4p(1-p)$. In particular, for $p = 1/2$, the distribution $\tilde{P}(\mathcal{J}_\alpha^m)$ approaches the standard normal distribution usually considered for the EA model.

We further demonstrate that the ground-state entropy density is bounded from above by $(\sqrt{d/2m} + 1/N) \ln 2$. This confirms the long hand suspicion that the degeneracy of real (finite dimensional) spin glasses with Gaussian couplings is not extensive. Exact calculations reveal the presence of a crossover length scale $L^*(m)$ below which the binomial spin glass is indistinguishable from the Gaussian system. These results confirm that depending on how the continuous spin glass models are approached (i.e., how the continuum limit is taken), both an exponentially large number of low energy states or systems with rigorously provable two-fold degenerate ground states are possible. That is, taking the thermodynamic and continuum limits in different orders leads to different results. Therefore, this model reveals to us the root of disagreement between two different camps of the spin glass divide. In the end, it's worth mentioning that this model enables us to control the precision of computations by a tunable parameter m.

References

[1] R. Peierls, Proc. Cambridge Phil. Soc. **32**, 477 (1936); L. D. Landau and E. M. Lifshitz, Statistical Physics - Course of Theoretical Physics Vol 5 (Pergamon, London, 1958); J. Frolich, B. Simon, and T. Spencer, Commun. Math. Phys. **50**, 79 (1976); R. Peierls, Contemporary Physics **33**, 221 (1992).

[2] N. Goldenfeld, *Lectures On Phase Transitions And The Renormalization Group* (CRC Press, 2018).

[3] S.-K. Ma, *Modern Theory of Critical Phenomena* (Routledge, 2018)

[4] S. Sachdev, *Quantum Phase Transitions* (Cambridge University Press, Cambridge, 2000)

[5] H. Nishimori and G. Ortiz *Elements of Phase Transitions and Critical Phenomena* (Oxford University Press, Oxford, 2011).

[6] X.-G. Wen, *Quantum Field Theory of Many-Body Systems* (Oxford University Press, Oxford, 2004).

[7] D. C. Tsui, H. L. Stormer, and A. C. Gossard, Phys. Rev. Lett. 48, 1559 (1982).

[8] R. B. Laughlin, Phys. Rev. Lett. 50, 1395 (1983).

[9] E. Fradkin, *Field Theories of Condensed Matter Physics*, second Edition (Cambridge University Press, Cambridge, 2013).

[10] A. Yu. Kitaev, Ann. of Phys. **303**, 2 (2003); arXiv:quant-ph/9707021 (1997).

[11] Z. Nussinov and G. Ortiz, Ann. of Phys.(N.Y.) **324**, 977 (2009); arXiv:cond-mat/0702377 (2007).

[12] Z. Nussinov and G. Ortiz, Proceedings of the National Academy of Sciences, **106**, 16944 (2009); arXiv:cond-mat/0605316 (2006).

[13] R. J. Baxter, *Exactly solved models in statistical mechanics* (Academic Press, New York, 1982).

[14] O. Heaviside, "On the Forces, Stresses, and Fiuxes of Energy in the Electromagnetic Field", Phil. Trans. Roy. Soc. London. **183A**, 423-480 (1892).

[15] *Phase Transitions and Critical Phenomena*, vol. 3, *Series Expansions for Lattice Models*, ed. C. Domb and M. S. Green (Academic Press, London, 1974).

[16] D. L. Stein and C. M. Newman, *Spin Glasses and Complexity* (Princeton University Press, 2013).

[17] J. A. Mydosh, *Spin Glasses: An Experimental Introduction* (Taylor and Francis, London, Washington D. C., 1993).

[18] H. Nishimori, *Statistical Physics of Spin Glasses and Information Processing: An Introduction* (Oxford University Press, Oxford, 2011).

[19] D. Sherrington and S. Kirkpatrick, Phys. Rev. Lett. **35**, 1792 (1975).

[20] G. Parisi, Phys. Rev. Lett. **43**, 1754 (1979); G. Parisi, J. Phys. A **13**, L115 (1980; G. Parisi, J. Phys. A **13**, 1101 (1980); G. Parisi, J. Phys. A **13**, 1887 (1980); G. Parisi, Phys. Rev. Lett. **50**, 1946 (1983).

[21] W. L. MacMillan Phys. Rev. B **31**, 340 (1985).

[22] A. J. Bray and M. A. Moore, Phys. Rev. B **31**, 631 (1985).

[23] R. G. Calfish and J. R. Banavar, Phys. Rev. B **32**, 7617 (1985).

[24] M. A. Moore and A. J. Bray, J. Phys C: Solid State Phys. **18**, L699 (1985).

[25] D. S. Fisher and D. A. Huse, J. Phys. A: Math. Gen. **20**, L1005 (1987).

[26] V. Cannella and J. A. Mydosh Phys. Rev. B **6**, 4220 (1972).

[27] S. Edwards and P. W. Anderson, J. Phys. F **5**, 965 (1975).

[28] J. Lukic, A. Galluccio, E. Marinari, Olivier C. Martin, and G. Rinaldi, Phys. Rev. Lett. **92**, 117202 (2004).

[29] J. E. Avron, G. Roepstorff, and L. S. Schulman, J. Stat. Phys. **26**, 25 (1981).

[30] M. Loebl and J. Vondrak, Discrete Mathematics **271** (1-3), 179 (2003).

[31] J. W. Landry and S. N. Coppersmith, Phys. Rev. B **65**, 134404 (2002).

[32] E. Marinari and G. Parisi, Phys. Rev. B **62**, 11677 (2000).

[33] H. Rieger, *Frustrated Systems: Ground State Properties via Combinatorial Optimization*, Lecture Notes in Physics Vol. 501 (Springer-Verlag, Heidelberg, 1998).

Chapter 2

Robust Topological Degeneracy of Classical Theories

This chapter contains the materials published in a paper [1].

2.1 Introduction

The primary purpose of this chapter is to show that, as a matter of principle, contrary to discerning lore that is realized in many fascinating systems, e.g., [1–3], the appearance of a *topological* ground state degeneracy *does not* imply that these degenerate states are "topologically ordered", in the sense that local perturbations can be detected without destroying the encoded quantum information [4]. Towards this end, we introduce various models, including a classical version of Kitaev's Toric Code [3], that exhibit robust genus dependent degeneracies but are nonetheless Landau ordered. Those models do not harbor long-range entangled ground states that cannot be told apart from one another by local measurements. Rather,

[1] M.-S. Vaezi, G. Ortiz, and Z. Nussinov, Phys. Rev. B **93**, 205112 (2016).

they (as well as all other eigenstates) are trivial classical states. Along the way we will discover that these two-dimensional classical models (including rather mundane clock and $U(1)$ gauge like theories with four spin interactions (specifically, Toric Clock and $U(1)$ theories that we will define) may not only have genus dependent symmetries and degeneracies but, for various lattice types, may also exhibit *holographic* degeneracies that scale exponentially in the system perimeter. Similar degeneracies also appear in classical systems having two spin interactions. Thus, the classical degeneracies that we find may be viewed as analogs of those in quantum models such as the Haah Code model on the simple cubic lattice [5–7], a nontrivial theory with eight spin interactions that is topologically quantum ordered, and other quantum systems. To put our results in a broader context, we first succinctly review current basic notions concerning the different possible types of order.

The celebrated symmetry-breaking paradigm [8, 9] has seen monumental success across disparate arenas of physics. Its traditional textbook applications include liquid to solid transitions, magnetism, and superconductivity to name only a few examples out of a very vast array. Within this paradigm, distinct thermodynamic phases are associated with local observables known as order parameter(s). In the symmetric phase(s), these order parameters must vanish. However, when symmetries are lifted, the order parameter may become non-zero. Phase transitions occur at these symmetry breaking points at which the order parameter becomes non-zero (either continuously or discontinuously). Landau [9] turned these ideas into a potent phenomenological prescription. Indeed, long before the microscopic theory of superconductivity [10], Ginzburg and Landau [11] wrote down a phenomenological free energy form in the hitherto unknown complex order parameter with the aid of which predictions may be made. Albeit its numerous triumphs, the symmetry-breaking paradigm might not directly account for transitions in which symmetry breaking cannot occur. Pivotal examples

are afforded by gauge theories of the fundamental forces and very insightful abstracted simplified renditions capturing their quintessential character, e.g., [12]. Elitzur's theorem [13] prohibits symmetry breaking in gauge theories. Another notable example where the symmetry breaking paradigm cannot be directly applied is that of the Berezinskii-Kosterlitz-Thouless transition [14] in two-dimensional systems with a global $U(1)$ symmetry. By the Mermin-Wagner-Hohenberg-Coleman theorem and its extensions [15–18], such continuous symmetries cannot be spontaneously broken in very general two-dimensional systems.

Augmenting these examples, penetrating work illustrated that something intriguing may happen when the quantum nature of the theory is of a defining nature [1]. In particular, strikingly rich behavior was found in Fractional Quantum Hall (FQH) systems [1, 19–21], chiral spin liquids [1, 21, 22], a plethora of exactly solvable models, e.g., [3, 23–25], and other systems. One curious characteristic highlighted in [1] concerns the number of degenerate ground states in FQH fluids [26], chiral spin liquids [27, 28], and other systems. Namely, in these theories, the ground state (g.s.) degeneracy is set by the topology alone. For instance, regardless of general perturbations (including impurities that may break all the symmetries of the Hamiltonian), when placed on a manifold of genus number g (the determining topological characteristic), the FQH liquid at a Laughlin type filling of $\nu = 1/q$ (with $q \geq 3$ an odd integer) universally has

$$n_{\text{g.s.}}^{\text{Laughlin}} = q^g \tag{2.1}$$

orthogonal ground states [26]. *Equation (2.1) constitutes one of the best known realization of topological degeneracy.* Exact similarity transformations connect the second quantized FQH systems of equal filling when these are placed on different surfaces sharing the same

genus [29]. Making use of the archetypal topological quantum phenomenon, the Aharonov-Bohm effect [30], it was argued that, when charge is quantized in units of $(1/q)$ (as it is for Laughlin states), the minimal ground state degeneracy is given by the righthand side of Eq. (2.1) [31]. This may appear esoteric since realizing FQH states on Riemann surfaces is seemingly not feasible in the lab. Recent work [32] proposed the use of an annular superconductor-insulator-superconductor Josephson junction in which the insulator is (an electron-hole double layer) in a FQH state (of an identical filling) for which this degeneracy is not mathematical fiction but might be experimentally addressed. Associated fractional Josephson effects of this type in parafermionic systems were advanced in [33].

Historically, the robust topological degeneracy of Eq. (2.1) for FQH systems and its counterparts in chiral spin liquids suggested that such a degeneracy may imply the existence of a novel sort of order — "topological quantum order" present in Kitaev's Toric Code model [3], Haah's code [5, 6], and numerous other quantum systems [26–28, 34] — a quantum order for which no local Landau order parameter exists. As we will later review and make precise (see Eq. (2.3)), in topologically ordered systems, no local measurement may provide useful information.

As it is of greater pertinence to a model analyzed in this chapter, we note that similar to Eq. (2.1), on a surface of genus g the ground state degeneracy of Kitaev's Toric Code model [3], an example of an Abelian quantum double model representing quantum error correcting codes (solvable both in the ground state sector [3] as well as at all temperatures [35–37]), is

$$n_{\text{g.s.}}^{\text{Toric}-\text{Code}} = 4^g. \tag{2.2}$$

Thus, for instance, on a torus ($g = 1$), the model exhibits 4 ground states while the system has a unique ground state on a topologically trivial ($g = 0$) surface with boundaries. By virtue of a simple mapping [35–37], it may be readily established that an identical degeneracy appears for all excited states; that is the degeneracy of each energy level is an integer multiple of 4^g. Thus, the minimal degeneracy amongst all energy levels is given by 4^g. Same ground state degeneracy [38] appears in Kitaev's honeycomb model [23, 24]. As is widely known, an identical situation occurs in the quantum dimer model [35, 36, 39]. Invoking the well-known "$n-$ality" considerations of $SU(n)$, leading to a basic spin of $1/2$ in $SU(2)$ and a minimal quark charge of $1/3$ in $SU(3)$, it was suggested [35, 36] that in many systems, fractional charges (quantized in units of $1/n$) are a trivial consequence of the $\mathbb{Z}_n$ phase group center structure of a system endowed with an $SU(n)$ symmetry, which is associated with the n states comprising the ground state manifold. This n-ality type phase factors and other considerations, prompted Sato [40] to suggest the use of topological degeneracy (akin to that of Eqs. (2.1) and (2.2)) as a theoretical diagnosis delineating the boundary between the confined and the topological deconfined phases of QCD in the presence of dynamical quarks. Other notable examples include, e.g., the BF action for superconductors (carefully argued to not support a local order parameter [41]).

References [35, 36] examined the links between various concepts surrounding topological order with a focus on the absence of local order parameters. In particular, building on a generalization of Elitzur's theorem [42, 43] it was shown how to construct and classify theories for which no local order parameter exists both at zero and at positive temperatures; this extension of Elitzur's theorem unifies the treatment of classical systems, such as gauge and Berezinskii-Kosterlitz-Thouless type theories in arbitrary number of space (or space-time) dimensions, to topologically ordered systems. Moreover, it was demonstrated that a sufficient condition for the existence of topological quantum order is the explicit presence,

or emergence, of symmetries of *dimension d lower* than the system's dimension D, dubbed d-dimensional gauge-like symmetries, and which lead to the phenomenon of *dimensional reduction*. The topologically ordered ground states are connected by these low-dimensional operator symmetries [35, 36]. All known examples of systems displaying topological quantum order host these low dimensional symmetries, thus providing a unifying framework and organizing principle for such an order.

As underscored by numerous pioneers, features such as fractionalization and quasiparticle statistics, e.g., [1, 3, 20, 23, 44–54], edge states [3, 23, 53, 55, 56], nontrivial entanglement [35, 36, 57], and other fascinating properties seem to relate with the absence of local order parameters and permeate topological quantum order. While all of the above features appear and complement the topological degeneracies found in, e.g., the FQH (Eq. (2.1)), the Toric Code (Eq. (2.2)), and numerous other systems, it is not at all obvious that one property (say, a topological degeneracy such as those of Eqs. (2.1) and (2.2)) implies another attribute (for instance, the absence of meaningful local observables). This chapter will indeed precisely establish the absence of such a rigid connection between these two concepts (viz., topological degeneracy is not at odds with the existence of a local order parameter).

We will employ the lack of local order parameters (or, equivalently, an associated robustness to local perturbations) as the defining feature of topological quantum order [35–37]. This robustness condition implies that local errors can be detected, and thus corrected, without spoiling the potentially encoded quantum information. To set the stage, in what follows, we consider a set of $n_{\mathsf{g.s.}}$ orthonormal ground states$\{|g_\alpha\rangle\}_{\alpha=1}^{n_{\mathsf{g.s.}}}$ with a spectral gap to all other (excited) states. Specifically [35, 36], a system will be said to exhibit topological order at

zero temperature if and only if for *any quasi-local operator* $\mathcal{V}$,

$$\langle g_\alpha|\mathcal{V}|g_\beta\rangle = v\ \delta_{\alpha,\beta} + c, \tag{2.3}$$

where v is a constant, independent of α and β, and c is a correction that is either zero or vanishes (typically exponentially in the system size) in the thermodynamic limit. The physical content of Eq. (2.3) is clear: no possible quantity $\mathcal{V}$ may serve as an order parameter to differentiate between the different ground states in the "algebraic language" [58] where $\mathcal{V}$ is local [35,36,59]. That is, all ground states look identical locally. Similarly, no local operator $\mathcal{V}$ may link different orthogonal states – the ground states are immune to all local perturbations. Notice the importance of the physical, and consequently mathematical, language to establish topological order: A physical system may be topologically ordered in a given language but its dual (that is isospectral) is not [35, 36, 59].

Couched in terms of the simple equations that we discussed thus far, the goal of this chapter is to introduce systems for which the ground state sector has a genus dependent degeneracy (as in Eqs. (2.1) and (2.2)) while, nevertheless, certain local observables (or order parameters) $\mathcal{V}$ will be able to distinguish between different ground states (thus violating Eq. (2.3)). Moreover, they will be connected by global symmetry operators as opposed to low-dimensional ones. Our conclusions are generic and, as shown, they apply to many classical models. The paradigmatic counterexample that we will introduce is a new classical version of Kitaev's Toric Code model [3].

We now turn to the outline of this chapter. In Section 2.2, we generalize the standard (quantum) Toric Code model. After a brief review and analysis of the ground states of Kitaev's Toric Code model (Section 2.3), we exclusively study our classical systems. In

Section 2.4, we extensively study the ground states of the classical variant of the model for different square lattices on Riemann surfaces of varying genus numbers $g \geq 1$. A principal result will be that this and many other *classical systems exhibit a topological degeneracy*. We will demonstrate that an intriguing holographic degeneracy may appear on lattices of a certain type. As will be explained, topological as well as exponentially large in system linear size ("holographic") degeneracies can appear in numerous systems, not only in this new classical version of Kitaev's Toric Code model [60]. We further study the effect of lattice defects. The partition function of the classical Toric Code model is revealed in Section 2.5 and Section 2.11.

In Section 2.6, we introduce related classical clock models. Generalizing the considerations of Section 2.4, we will demonstrate that these clock models may exhibit topological or holographic degeneracies. The ensuing analysis is richer by comparison to that of the classical Toric Code model. Towards this end, we will construct a new framework for broadly examining degeneracies. We then derive lower bounds on the degeneracy that are in agreement with our numerical analysis. These bounds are *not confined to the ground state sector*. That is, all levels may exhibit topological degeneracies (as they do in the classical Toric Code model (Section 2.5)).

In Section 2.7, we will relate our results to $U(1)$ models and to $U(1)$ lattice gauge theories in particular. The fact that simple lattice gauge systems, that constitute a limiting case of our more general studied models, such as the conventional classical Clock and $U(1)$ lattice gauge theories *on general Riemann surfaces* (and their Toric Code extensions), *exhibit topological* (or, in some cases, holographic) *degeneracies* seems to have been overlooked until now. In Section 2.8, we will study honeycomb and triangular lattice systems embedded on surfaces of different genus. In Section 2.9, we will discuss yet three more regular lattice classical systems

that exhibit holographic degeneracies. We summarize our main message and findings in Section 2.10.

Before embarking on the specifics of these various models, we briefly highlight the organizing principle behind the existence of degeneracies in our theories. Irrespective of the magnitude and precise form of the interactions in these theories, the number of independent constraints between the individual interaction terms sets the system degeneracy. As such, the degeneracies that we find are, generally, *not a consequence of any particular fine-tuning*.

2.2 The general Toric Code Model

We start with a general description of a class of two-dimensional stabilizer models defined on lattices embedded on closed manifolds with arbitrary genus number g (the number of handles or, equivalently, the number of holes). The genus of a closed orientable surface is related to a topological invariant known as Euler characteristic

$$\chi = 2 - 2g, \tag{2.4}$$

which, for a general tessellation of that surface, satisfies the (Euler) relation

$$\chi = V - E + F. \tag{2.5}$$

In Eq. (2.5), V is the number of vertices in the closed tessellating polyhedron, or graph, E is the number of edges, and F the number of polygonal faces. Assume that on each of the E edges of the graph there is a spin S degree of freedom, defining a local Hilbert space of

size $\dim \mathcal{H} = \mathsf{d}_Q$, and that on each of the V vertices and F faces we will have a number of conditions to be satisfied by the ground states of a model that we define next.

We now explicitly define, on a general lattice or graph Λ, the "General Toric Code model". Towards this end, we consider the Hamiltonian

$$H^{\mu,\nu} = -J \sum_s A_s^\mu - J' \sum_p B_p^\nu, \tag{2.6}$$

where J and J' are coupling constants (although it is immaterial, in the remainder of this chapter we will assume these to be positive). The interaction terms of edges in Eq. (2.6) are so-called "star" ("s") terms (A_s^μ) associated with the V vertices (labelled by the letter i) and the F "plaquette" ("p") terms (B_p^ν). In the $S = 1/2$ case, these are given by the following products of Pauli operators σ_{ij}^μ, $\mu, \nu = x, y, z$,

$$\begin{aligned} A_s^\mu &= \prod_{i \in \mathsf{vertex}(s)} \sigma_{is}^\mu, \\ B_p^\nu &= \prod_{(ij) \in \mathsf{face}(p)} \sigma_{ij}^\nu. \end{aligned} \tag{2.7}$$

The product defining A_s^μ spans the spins on all edges (is) that have vertex s as an endpoint, and the plaquette product B_p^ν is over all spins lying on the edges (ij) that form the plaquette p (see Fig. 2.1 for an illustration). A key feature of this system (both the well known [3] quantum variant ($\mu = x \neq \nu = z$) as well as, even more trivially, the classical version that we introduce in this chapter ($\mu = \nu = z$)) is that each of the bonds A_s^μ and B_p^ν can assume $\mathsf{d}_Q = 2S + 1 = 2$ independent values. Apart from global topological constraints [35, 36] that we will expand on below, the bonds $\{A_s^\mu\}$ and $\{B_p^\nu\}$ are completely independent of one another. Not only, trivially, in the classical but also in the quantum (q) rendition of the

model [3] all of these operators commute with one another. That is $\forall s, p \in \Lambda$,

$$[A_s^\mu, B_p^\nu] = 0. \tag{2.8}$$

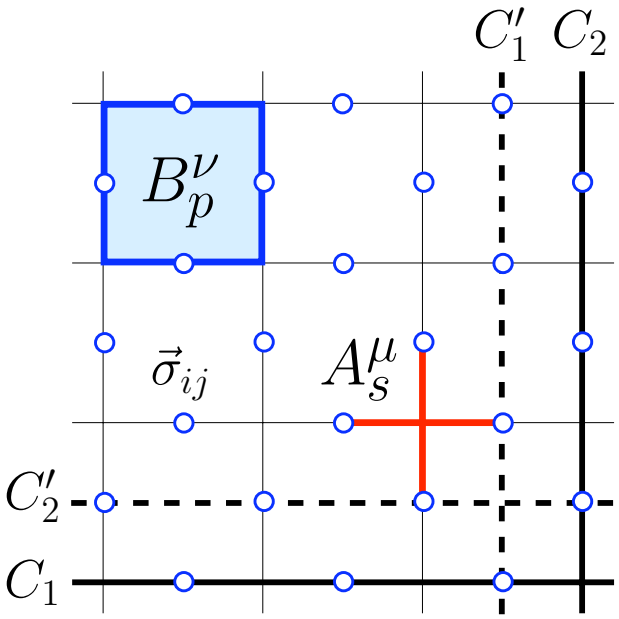

Figure 2.1: General Toric Code lattice model with spins $S = 1/2$ placed on the edges (bonds). The red cross-shape object corresponds to the star operator A_s^μ. The plaquette operator B_p^ν is depicted in the top-left corner in blue color. Dark solid and dashed lines represent the loops C_1, C_2 and C_1', C_2', defining the symmetry operators Z_1, Z_2, and X_1, X_2, respectively.

In the quantum version of the model, these terms commute as the products defining the star and plaquette operators must share an even number of spins. As the individual Pauli operators σ^x and σ^z appearing in the product of Eq. (2.7) anticommute, an even number of such anticommutations trivially gives rise to the commutativity in Eq. (2.8). Even more simply, one observes that

$$[A_s^\mu, A_{s'}^\mu] = [B_p^\nu, B_{p'}^\nu] = 0. \tag{2.9}$$

Lastly, from Eq. (2.7), it is trivially seen that

$$(A_s^{\mu})^2 = (B_p^{\nu})^2 = \mathbb{1}. \tag{2.10}$$

Apart from a number (C_g^{Λ}) of constraints, Eqs. (2.8), (2.9), and (2.10) completely specify all the relations amongst the operators of Eq. (2.7). As we will illustrate, $H^{\mu,\nu}$ is a *minimal model that embodies all of the elements in Eq. (2.5)* such that its minimum degeneracy will only depend on the genus number g. As all terms in the Hamiltonian $H^{\mu,\nu}$ commute with one another, the general Toric Code model can be related quite trivially to a classical model. Intriguingly, as may be readily established by a unitarity transformation (a particular case of the bond-algebraic dualities [66]), the quantum version, which includes Kitaev's Toric Code model as a particular example, on a graph having E edges spanning the surface of genus $g \geq 1$ is identical [35–37], i.e. *is isomorphic, to two decoupled* **classical** *Ising chains* (with one of these chains having V classical Ising spins and the other chain composed of F Ising spins) augmented by $2(g-1)$ decoupled single Ising spins. Perusing Eq. (2.6), it is clear that, if globally attainable, within the ground state(s), $|g_\alpha\rangle$,

$$A_s^{\mu}|g_\alpha\rangle = (+1)|g_\alpha\rangle \ , \ B_s^{\nu}|g_\alpha\rangle = (+1)|g_\alpha\rangle, \tag{2.11}$$

on all vertices s and faces p and, thus, the ground state energy is $E_0 = -JV - J'F$. The algebraic relations above enable the realization of Eq. (2.11) for all s and p.

We now turn to the constraints that augment Eqs. (2.8), (2.9), and (2.10). For any lattice Λ on any closed surface of genus $g \geq 1$, there are $C_{g\geq 1}^{\mathsf{universal}} = 2$ universal constraints given

by the equalities

$$\prod_s A_s^\mu = \prod_p B_p^\nu = \mathbb{1}. \tag{2.12}$$

For the quantum variant [3] no further constraints appear beyond those of Eq. (2.12) (that is, $C_g^\Lambda = 2$ irrespective of the lattice Λ). By contrast, for the classical variant of the theory realized on the relatively uncommon "commensurate" lattices, additional constraints will augment those of Eq. (2.12) (i.e., for classical systems, $C_g^\Lambda \geq 2$). Invoking the C_g^Λ constraints as well as the trivial algebra of Eqs. (2.8) and (2.9), we may transform from the original variables – the spins on each of the E edges – $\{\sigma_{ij}^\mu\}$ to new basic degrees of freedom – all $\mathsf{N}_{\text{ind. bonds}}$ independent *"bonds"* $\{A_{s\neq s'}^\mu\}, \{B_{p\neq p'}^\nu\}$ that appear in the Hamiltonian and $N_{\text{redundant}} = (E - \mathsf{N}_{\text{ind. bonds}})$ remaining redundant spins of the original form $\{\sigma_{ij}^\mu\}$ on which the energy does not depend (and thus relate to symmetries). If the bonds A_s^μ and B_p^ν do not adhere to any constraint apart from that in Eq. (2.12) then $\mathsf{N}_{\text{ind. bonds}} = (V + F - 2)$ of the $(V + F)$ bonds in the Hamiltonian of Eq. (2.6) will be independent of one another. Correspondingly, $N_{\text{redundant}} = [E - (V + F - 2)] = 2g$. As all bonds must satisfy the constraint of Eq. (2.12) and thus $\mathsf{N}_{\text{ind. bonds}} \leq (V + F - 2)$, the number of redundant spin degrees of freedom $N_{\text{redundant}} \geq 2g$. In the general case, if there are $(C_g^\Lambda - 2)$ constraints that augment the two restrictions already present in Eq. (2.12), then we may map the original system of E spins to $\mathsf{N}_{\text{ind. bonds}} = (V + F - C_g^\Lambda)$ independent bonds in Eq. (2.6) and $N_{\text{redundant}} = (E - \mathsf{N}_{\text{ind. bonds}}) = 2(g-1) + C_g^\Lambda$ spins that have no impact on the energy. Thus, for genus $g \geq 1$ surfaces, the degeneracy of each energy level is an integer multiple of the *minimal* degeneracy possible,

$$\min(n_{\text{g.s.}}) = 2^{N_{\text{redundant}}} = n_{\text{g.s.}}^{\min} \times 2^{C_g^\Lambda - 2}, \tag{2.13}$$

with $n_{\mathsf{g.s.}}^{\mathsf{min}} = 4^g$. Equation (2.13) will lead to a global redundancy factor in the partition function $\mathcal{Z} = \mathsf{Tr}\exp(-\beta H^{\mu,\nu})$ with β the inverse temperature.

We now focus on the ground state sector. If there are no constraints apart from Eq. (2.12), then to obtain the ground states it suffices to make certain that $\mathsf{N}_{\mathsf{ind.\ bonds}}$ of the bonds are unity in a given state. Once that occurs, we are guaranteed a ground state in which each bond in the Hamiltonian of Eq. (2.6) is maximized (i.e., Eqs. (2.11) are satisfied). A smaller number of bonds fixed to one will not ensure that only ground states may be obtained. Thus the values of all $\mathsf{N}_{\mathsf{ind.\ bonds}}$ independent bonds need to be fixed in order to secure a minimal value of the energy. The lower bound of the degeneracy on each level (Eq. (2.13)) is saturated for the ground state sector where it becomes an equality. That is, very explicitly, the ground state degeneracy is given by

$$n_{\mathsf{g.s.}}^{\mathsf{General\ \ Toric-Code}} = 4^g \times 2^{C_g^\Lambda - 2}. \tag{2.14}$$

The equalities of Eqs. (2.13) and (2.14) are basic facts that will be exploited in the present chapter. The degeneracy of Eq. (2.14) is in accord with the general result

$$n_{\mathsf{g.s.}}^{\mathsf{g}\geq 1} = \mathsf{d}_Q^{-\chi+(C_g^\Lambda - C_1^\Lambda)} n_{\mathsf{g.s.}}^{\mathsf{g}=1}, \tag{2.15}$$

and differs from that of Kitaev's Toric Code model [3] (Eq. (2.2)) by a factor of $2^{C_g^\Lambda - 2}$. As each of the C_g^Λ constraints as well as increase in genus number leads to a degeneracy of the spectrum, a simple "correspondence maxim" follows: *it must be that we may associate a corresponding independent set of symmetries with any individual constraint.* Similarly, as Eqs. (2.13, 2.14) attest, elevating the genus number g must introduce further symmetries. Thus, the global degeneracy of Eq. (2.13) is a consequence of all of these symmetries.

Given Eq. (2.6) it is readily seen that the system has a gap of magnitude $\Delta = 4(J + J')$ between the ground state E_0 and the lowest lying excited state E_1. All energy levels E_ℓ, defining the spectrum of $H^{\mu,\nu}$, are quantized in integer multiples of J and J'.

2.3 Ground states of the quantum Toric Code model

In Kitaev's Toric Code model [3] the symmetries associated with the constraints of Eq. (2.12) are rather straightforward, and cogently relate to the topology of the surface on which the lattice is embedded. An illustration for the square lattice is depicted in Fig. 2.1. For such a model on a simple torus (i.e., one with genus $g = 1$), the four canonical symmetry operators are

$$Z^q_{1,2} = \prod_{(ij)\in C_{1,2}} \sigma^z_{ij} \ , \ X^q_{1,2} = \prod_{(ij)\in C'_{1,2}} \sigma^x_{ij}. \tag{2.16}$$

These two sets of non-commuting operators [3]

$$\begin{aligned} \{X^q_1, Z^q_1\} = \quad 0 \quad &= \{X^q_2, Z^q_2\}, \\ [X^q_1, X^q_2] = \quad 0 \quad &= [Z^q_1, Z^q_2]\,, \\ [X^q_1, Z^q_2] = \quad 0 \quad &= [X^q_2, Z^q_1]\,, \end{aligned} \tag{2.17}$$

realize a $\mathbb{Z}(2) \times \mathbb{Z}(2)$ symmetry and ensure a four-fold degeneracy (or, more generally a degeneracy that is an integer multiple of four) of the whole spectrum.

To see this, we may, for instance, seek mutual eigenstates of the Hamiltonian $H^{x,z}$ along with the two symmetries Z^q_1 and Z^q_2 with which it commutes. Noting the algebraic relations

amongst the above operators, a moment's reflection reveals that a possible candidate for a normalized ground state is given by

$$|g_1\rangle = \frac{1}{\sqrt{2}} \prod_s \left(\frac{\mathbb{1} + A_s^x}{\sqrt{2}} \right) |\mathbf{F}\rangle, \tag{2.18}$$

where $\sigma_{ij}^z |\mathbf{F}\rangle = |\mathbf{F}\rangle$, for all E edges, and $\langle \mathbf{F}|\mathbf{F}\rangle = 1$. This corresponds to $Z_{1,2}^q |g_1\rangle = |g_1\rangle$. Now, because $X_{1,2}^q$ are symmetries, by the algebraic relations of Eq. (2.17), the three additional orthogonal states

$$|g_2\rangle = X_1^q |g_1\rangle \ , \ |g_3\rangle = X_2^q |g_1\rangle \ , \ |g_4\rangle = X_1^q X_2^q |g_1\rangle, \tag{2.19}$$

are the remaining ground states. That is, the $C_{g=1} = 2$ lattice (Λ) independent constraints of the quantum model (Eq. (2.12)) correspond to the 2 sets of symmetry operators associated with the $\gamma = 1, 2$ toric cycles ($\{Z_\gamma^q, X_\gamma^q\}$) of Eq. (2.16). This correspondence is in agreement with the simple maxim highlighted above. The symmetry operators X_1^q and Z_1^q are independent (and trivially commute) with the symmetry operators X_2^q and Z_2^q. Notice that in the spin (σ_{ij}^μ) language the ground states above are entangled, and they are connected by $d = 1$ symmetry operators [35, 36]. Moreover, the anyonic statistics of its excitations is linked to the entanglement properties of those ground states [35, 36]. As mentioned above, the model can be trivially related, by duality, to two decoupled classical Ising chains so that in the dual language the mapped ground states are unentangled [35, 36].

For a Riemann surface of genus g, we may write down trivial extensions of Eqs. (2.16) for the $(2g)$ cycles circumnavigating the g handles of that surface. That is, instead of the four operators of Eq. (2.16), we may construct $2g$ operators pairs with each of these pairs associated with a particular handle h (where $1 \leq h \leq g$), containing the four operators $\{Z_{\gamma,h}^q\}$

and $\{X^q_{\gamma,h}\}$ with $\gamma = 1, 2$. A generalization of Eqs. (2.17) leads to an algebra amongst the $2g$ independent pairs of symmetry operators. The multiplicity of independent symmetries leads to the first factor in Eq. (2.14). The number of constraints is, in the quantum case, lattice independent and given by $C_{g\geq 1} = 2$ (there are no constraints beyond those in Eq. (2.12)). It is rather straightforward to establish that when $g = 0$ (i.e., for topologically trivial surfaces), the ground state of the quantum model is unique. Putting all of these pieces together, the well known degeneracy of Eq. (2.2) follows.

2.4 Ground states of the classical Toric Code model

We now finally turn to the examination of the ground states of the classical rendering of Eq. (2.6) in which only a single component $\mu = \nu = z$ of all spins appears. We will explain how *the degeneracy of Eqs. (2.13) and (2.14) emerges*. The upshot of our analysis, already implicitly alluded to above, consists of two main results:

• In the most frequent lattice realization of this classical model, *its degeneracy will still be given by Eq. (2.2)*, i.e., 4^g. That is, in the most common of geometries, the number of ground states will depend on topology alone (i.e., the genus number g of the embedding manifold). For arbitrary square lattice or graph, as our considerations universally mandate, the *minimal* possible ground state degeneracy will be given by the topological figure of merit of Eq. (2.2).

• In the remaining lattice realizations, *the degeneracy of the system will typically be holographic*. That is, in these slightly rarer lattices, the ground state degeneracy will scale as $\mathcal{O}(2^L)$ where L is the length of one of the sides of the two-dimensional lattice.

As will be seen, for the square lattice, depending on the parity of the length of the lattice sides, the number of constraints C_g^Λ may exceed its typical value of two. This will then lead to an enhanced degeneracy vis a vis the minimal possible value of 4^g. In the next subsection we first broadly sketch the constraints and symmetries of the classical system. As it will be convenient to formulate our main result via the "correspondence maxim", we will then proceed to explicitly relate the constraints and symmetries to one another. The *symmetry* $\leftrightarrow$ *constraint* consonance, along with Eqs. (2.13) and (2.14), will then rationalize all of the degeneracies found for general square lattices embedded on Riemann surfaces of arbitrary genus number. Exhaustive calculations for these degeneracies will then be reported in the subsections that follow.

2.4.1 Symmetries and constraints

We next list the general symmetries and constraints of the classical Toric Code model in square lattices of varying sizes. Consider first a lattice Λ of size $L_x \times L_y$ on a torus (i.e., having $V = L_x L_y$ vertices and $E = 2L_x L_y$ edges). We will then examine more general lattices of arbitrary genus g. The square lattice on the torus will be categorized as being one of two types:

$$\begin{cases} \text{Type I,} & L_x \neq L_y \text{ where at least} \\ & \text{one of } L_x \text{ or } L_y \text{ is odd} \\ \text{Type II,} & \text{otherwise.} \end{cases} \tag{2.20}$$

Type I lattices, as defined for the $g = 1$ case above and their generalizations for higher genus numbers $g > 1$, only admit two constraints C_g^Λ and thus by the correspondence maxim only

two symmetries. For these lattices, we will show that the ground state degeneracy is 4^g. By contrast, Type II lattices have a larger wealth of constraints, $C_g^\Lambda > 2$, and therefore a larger number of symmetries and a degeneracy higher than 4^g.

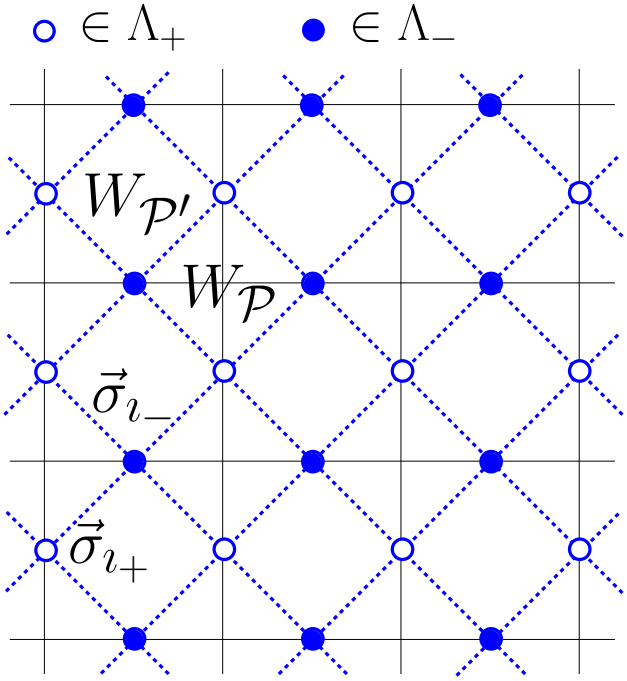

Figure 2.2: Dotted lines represent the rotated lattice Λ'. The spin degrees of freedom $\vec{\sigma}$ reside on the vertices of the rotated bipartite lattice Λ', formed out of two sublattices Λ_+ and Λ_-.

The centers of all nearest neighbor edges on the square lattice (of lattice constant a) form yet another square lattice $\Lambda^{'}$ (of lattice constant $a/\sqrt{2}$) at an angle of 45° relative to the original lattice (Fig. 2.2). The spins are located at the vertices of the rotated square lattice $\Lambda^{'}$. In order to describe the symmetries and constraints of this system, let us denote the two (standard) sublattices of the square lattice $\Lambda^{'}$ by $\Lambda_\pm$. That is, both Λ_+ and Λ_- are, on their own, square lattices with $\Lambda^{'} = \Lambda_+ \cup \Lambda_-$ and $\Lambda_+ \cap \Lambda_- = \emptyset$. Let us furthermore denote the sites of $\Lambda_\pm$ by $\imath_\pm$, respectively.

With these preliminaries, it is trivial to verify that

$$T_+^x = \prod_{\imath_+ \in \Lambda_+} \sigma_{\imath_+}^x,$$
$$T_-^x = \prod_{\imath_- \in \Lambda_-} \sigma_{\imath_-}^x, \tag{2.21}$$

are, universally, both symmetries of the classical ($\mu = \nu = z$) version of the Hamiltonian of Eq. (2.6). Most square lattices (those of Type I in Eq. (2.20)) will only exhibit the two symmetries of Eq. (2.21). The more commensurate Type II lattices admit diagonal contours (connecting nearest neighbors of sites $\imath$ of $\Lambda^{'}$) that close on themselves before threading all of the lattice sites of $\Lambda^{'}$. That is, in Type II lattices, it is possible to find diagonal loops Γ_m at a constant 45° angle (or a more non-trivial alternating contour) that contain only a subset of all sites of $\Lambda^{'}$ (or, equivalently, a subset of all edges (ij) of the original square lattice Λ). Associated with each such independent contour Γ_m, there is a symmetry operator,

$$T_m^x = \prod_{\imath \in \Gamma_m} \sigma_\imath^x, \tag{2.22}$$

augmenting the symmetries of Eq. (2.21).

The form of the symmetries suggests the distinction between Type I and Type II lattices on general surfaces. On Type II lattices, it is possible to find, at least, one diagonal contour Γ_m that contains a subset of all edges (ij) of the lattice Λ. Conversely, due to the lack of the requisite lattice commensurability, on Type I lattices, it is impossible to find any such contour.

We now turn to the constraints associated with Type I and II lattices. These are in one-to-one correspondence with the symmetries of Eqs. (2.21) and (2.22). Specifically for Type

I lattices, the only universal constraints present are those of Eq. (2.12) which we rewrite again for clarity,

$$\begin{aligned} \mathcal{C}_+ : \quad & \prod_s A_s^z = 1, \\ \mathcal{C}_- : \quad & \prod_p B_p^z = 1. \end{aligned} \tag{2.23}$$

These two constraints match the two symmetries of Eq. (2.21). In the case of the more commensurate lattices Λ, additional constraints appear. In order to underscore the similarities to the symmetries of Eq. (2.22), we will now aim to briefly use the same notation concerning the lattice $\Lambda^{'}$. Within the framework highlighted in earlier sections, the spin products $\{A_s^z\}$ and $\{B_p^z\}$ of Eq. (2.7) are associated with geometrical objects that look quite different (i.e., "stars" and "plaquettes"), see Fig. 2.1. If we now label the plaquettes of $\Lambda^{'}$ by $\mathcal{P}$ then, we may, of course, trivially express Eq. (2.6) as a sum of local terms,

$$H = -J \sum_{\mathcal{P}} W_{\mathcal{P}} - J' \sum_{\mathcal{P}'} W_{\mathcal{P}'}, \tag{2.24}$$

where $W_{\mathcal{P}} = \prod_{\imath \in \mathcal{P}} \sigma_\imath^z$ are the products of all Ising spins at sites $\imath$ belonging to plaquette $\mathcal{P}$. This trivial description renders the original star and plaquette terms of Eq. (2.6) on a more symmetric footing, see Fig. 2.2.

Associated with each of the symmetries of Eq. (2.22) there is a corresponding constraint,

$$\mathcal{C}_m : \quad \prod_{\imath \in \Gamma_m} W_m = 1. \tag{2.25}$$

In accordance with our earlier maxim, insofar as counting is concerned, we have the following correspondence between the symmetries and the associated constraints,

$$\begin{cases} T_+^x \leftrightarrow \mathcal{C}_+, \\ T_-^x \leftrightarrow \mathcal{C}_-, \\ T_m^x \leftrightarrow \mathcal{C}_m. \end{cases} \tag{2.26}$$

In Type I systems, wherein only the $C_g^\Lambda = 2$ universal constraints appear, the degeneracy of the spectrum is exactly 4^g. In Type II lattices, $C_g^\Lambda > 2$ (with the difference of $(C_g^\Lambda - 2)$ equal to the number of additional independent contours Γ_m that do not contain all edges of the original lattice Λ) and, as Eq. (2.14) dictates, the ground state degeneracy exceeds the minimal value of 4^g multiplied by two raised to the power of the number of the additional independent loops.

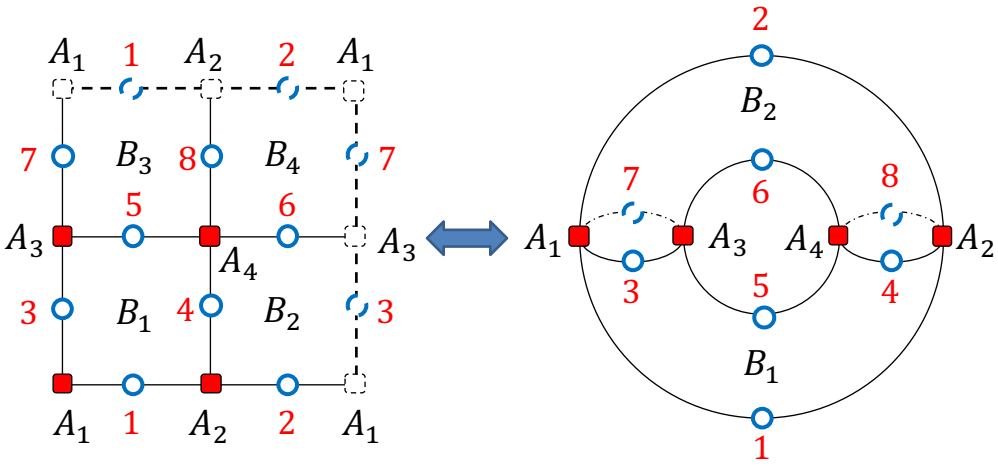

Figure 2.3: A square lattice with 8 spins along with its embedding on a torus. Because of periodic boundary conditions, spins on boundary edges (dashed-blue) display numbers identical to those in the bulk. In this figure $A_s = A_s^z$ and $B_p = B_p^z$. In the right panel, each edge has been labeled according to the left panel, and the solid red squares represent the vertices labeled by A_s. Since B_3 and B_4 are respectively behind B_1 and B_2, we cannot see them here.

2.4.2 Ground state degeneracy on $g = 1$ surfaces

Thus far, our discussion has been quite general and, admittedly, somewhat abstract. We now turn to simple concrete examples. We first consider the classical Toric Code model on a simple torus (i.e., a surface with genus $g = 1$), and examine small specific square lattices of dimension $L_x \times L_y$. We find that for general lattices Λ (with reference to Eq. (2.20)), the total number of independent constraints is

$$C^{\Lambda}_{g=1} = \begin{cases} 2, & \Lambda \text{ is a Type I lattice} \\ \\ 2\min\{L_x, L_y\}, & \Lambda \text{ is a Type II lattice.} \end{cases} \tag{2.27}$$

Thus, from Eq. (2.14), our two earlier stated main results follow: *while for the more "incommensurate" Type I lattices, the degeneracy will be "***topological***" (i.e., given by 4^g), for Type II lattices, the degeneracy will be "***holographic***" (viz., the degeneracy will be exponential in the smallest of the edges along the system boundaries).* As discussed in Subsection 2.4.1, the additional constraints in Type II lattices are of the form of Eq. (2.25). Expressed in terms of the four spin interaction terms A^z_s and B^z_p of Eq. (2.6), a constraint of the form of Eq. (2.25) states that there is a subset $\Gamma_m \subset \Lambda$ for which $\prod_{s,p\in\Gamma_m} A^z_s B^z_p = 1$. An illustration of a constraint of such a type is provided, e.g. in Fig. 2.3. Here, by virtue of the defining relations of Eq. (2.7), the product,

$$A^z_1 B^z_1 A^z_4 B^z_4 = 1. \tag{2.28}$$

Similarly, in panel a) of Fig. 2.4, colored arrows are drawn along the diagonals. These colors code the constraints on the specific A_s^z and B_p^z interaction terms. For example, along the *green* arrows,

$$A_1^z B_1^z A_4^z B_4^z = 1 \qquad \text{green (dashed)}, \tag{2.29}$$

and the constraints associated with the other diagonals

$$\begin{aligned} A_2^z B_2^z A_3^z B_3^z &= 1 \qquad \text{brown (dashed-dotted)}, \\ A_2^z B_1^z A_3^z B_4^z &= 1 \qquad \text{red (dashed-doubled-dotted)}, \\ A_1^z B_2^z A_4^z B_3^z &= 1 \qquad \text{black (dotted)}. \end{aligned} \tag{2.30}$$

We provide another example in panel b) of Fig. 2.4. The simplest visually appealing realization of Eq. (2.25) is that of the subset Γ_m being a trivial closed diagonal loop. Composites (i.e., products) of independent constraints of the form of Eq. (2.25) are, of course, also constraints. We aim to find the largest number $(C_g^\Lambda - 2)$ of such independent constraints. Non-trivial constraints formed by the product of bonds along real-space diagonal lines may appear. For example, in Fig. 2.3, the product $A_1^z B_1^z A_3^z B_2^z = 1$ is precisely such a constraint. These constraints are more difficult to determine due to the periodic boundary conditions. Generally, not all constraints are independent of each other (e.g., multiplying any two constraints yield a new constraint). The number of independent constraints, C_g^Λ may be generally found by calculating the "modular rank" of the linear equations formed by taking the logarithm of all constraints found. The qualified "modular" appears here as the A_s^z and B_p^z eigenvalues may only be (± 1) and thus, correspondingly, their phase is either 0 or π. Many, yet generally, not all, of the C_g^Λ independent constrains are naturally associated with products along the 45° lattice diagonals (as it appears on the torus). Table 2.1 lists the

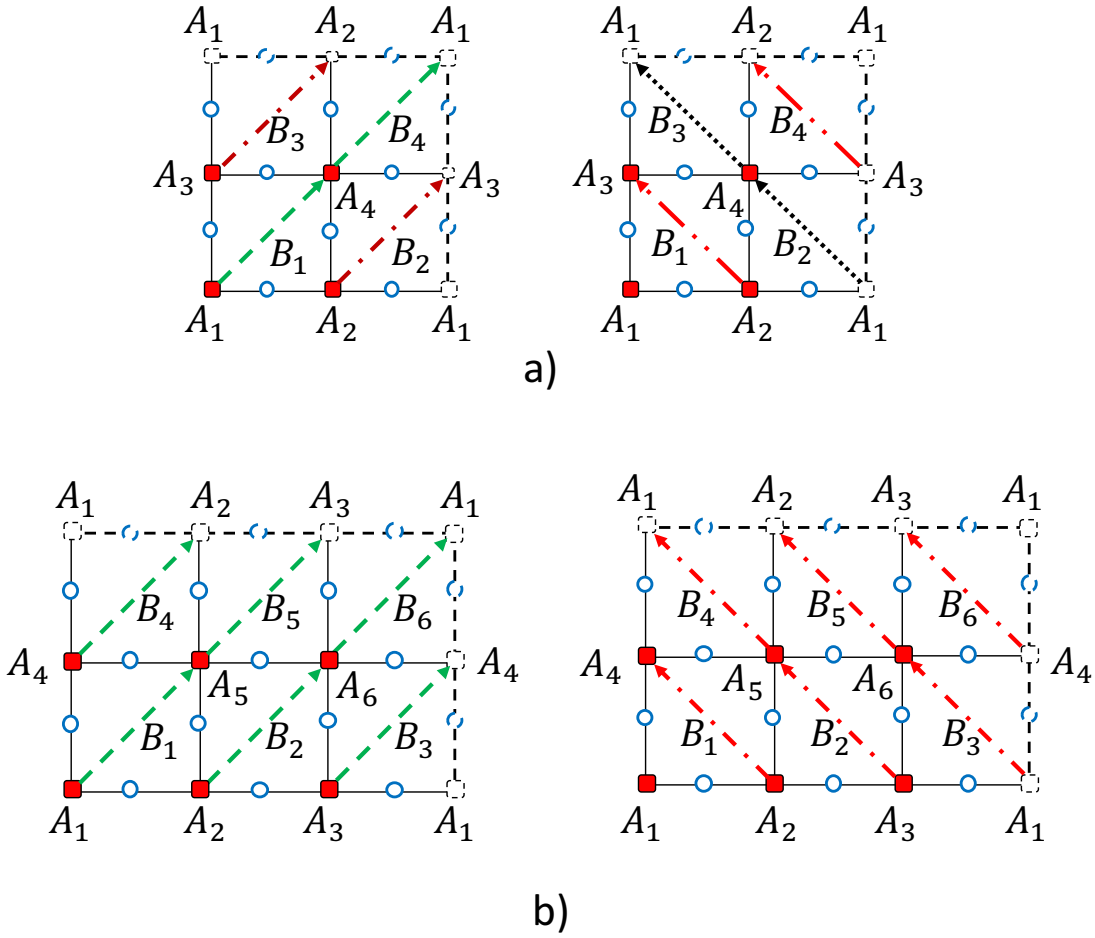

Figure 2.4: a) Lattice of size $L_x = 2$, $L_y = 2$, $E = 8$ and b) $L_x = 2$, $L_y = 3$, $E = 12$. Diagonal lines with arrows represent possible paths realizing constraints on $A_s = A_s^z$ and $B_p = B_p^z$.

numerically computed ground state degeneracies for numerous lattices of genus $g = 1$. All of these are concomitant with Eq. (2.27).

2.4.3 Construction of ground states

Given the symmetry operators of Eqs. (2.21) and (2.22), we may rather readily write down all ground states of the system. Denote the ferromagnetic ground state (i.e., one with all

Table 2.1: Computed ground state degeneracy ($n_{\text{g.s.}}$) for the classical Toric Code for different lattice sizes with genus one. Type I corresponds to the case $L_x \neq L_y$ where at least one of them is odd. We put any other possibility under Type II which in general covers the case $L_x \neq L_y$ where both L_x and L_y are even plus all cases with $L_x = L_y$. In this table, $C^{\Lambda}_{g=1}$ denotes the number of independent constraints (see text).

Type	L_x	L_y	E	$C^{\Lambda}_{g=1}$	$n_{\text{g.s.}}$
I	3	2	12	2	4
	5	2	20	2	4
	4	3	24	2	4
	5	3	30	2	4
II	2	2	8	4	4×2^2
	4	2	16	4	4×2^2
	6	2	24	4	4×2^2
	3	3	18	6	4×2^4
	4	4	32	8	4×2^6

spins up ($|\uparrow\rangle_{(ij)}$) on all edges (ij)) by

$$|\mathbf{F}\rangle \equiv \prod_{(ij)} |\uparrow\rangle_{(ij)}; \tag{2.31}$$

then, the four ground states of Type I lattices are

$$|G_{n_+,n_-}\rangle = (T^x_+)^{n_+}(T^x_-)^{n_-}|\mathbf{F}\rangle, \tag{2.32}$$

where $n_\pm = 0, 1$. Clearly, since $(T^x_\pm)^2 = 1$, only the parity of the integers $n_\pm$ is important. As (i) $[T^x_\pm, H] = 0$ and (ii) the ferromagnetic state $|\mathbf{F}\rangle$ minimizes the energy in Eq. (2.6), it follows that all four binary strings $(n_+, n_-) = (0,0), (0,1), (1,0), (1,1)$ in Eq. (2.32) lead to $n_{\text{g.s.}} = 2^2 = 4$ ground states. The situation for Type II lattices is a trivial extension of the above. That is, if there are $(C^{\Lambda}_{g=1} - 2)$ additional independent symmetries $T^x_{m=1}, T^x_{m=2}, \cdots, T^x_{m=(C^{\Lambda}_{g=1}-2)}$ of the form of Eq. (2.22) then, with the convention of Eq.

(2.31), the ground states will be of the form

$$|G_{n_+,n_-,n_1,n_2,\cdots,n_{C^{\Lambda}_{g=1}-2}}\rangle = (T^x_+)^{n_+}(T^x_-)^{n_-}(T^x_1)^{n_1} \times (T^x_2)^{n_2}\cdots(T^x_{C^{\Lambda}_{g=1}-2})^{n_{C^{\Lambda}_{g=1}-2}}|\mathbf{F}\rangle, \tag{2.33}$$

with $2^{C^{\Lambda}_{g=1}}$ binary strings $(n_+, n_-, n_1, n_2, \cdots, n_{C^{\Lambda}_{g=1}-2})$, where $n_m = 0, 1$. These strings span all possible $n_{\mathsf{g.s.}} = 2^{C^{\Lambda}_{g=1}}$ orthogonal ground states.

Given the set of all orthonormal ground states $\{|g_\alpha\rangle\}_{\alpha=1}^{n_{\mathsf{g.s.}}}$, it is possible to find quasi-local operators $\mathcal{V}$ composed of σ^z_{ij} "operators" on a small number of edges such that

$$\langle g_\alpha|\mathcal{V}|g_\alpha\rangle = v_\alpha \tag{2.34}$$

assumes different values v_α in, at least, two different ground states. Equation (2.34) highlights that the expectation value of $\mathcal{V}$ is not state independent. In other words, Eq. (2.3) [35–37] is violated. Thus, our classical system is, rather trivially, not topologically ordered .

2.4.4 Ground state degeneracy on $g > 1$ surfaces

Having understood the case of the simple torus ($g = 1$), we will now study lattices on surfaces Σ of genus $g \geq 2$. We first explain how to construct a finite size lattice of genus g [67]. Such lattices on genus g ($g \geq 2$) surfaces may be formed by *"stitching together"* g simple parts a_j, $j = 1, \cdots, g$, each of which largely looks like that of a simple torus (i.e., each region a_j represents a set of vertices, edges and faces of Type I or II in the notation of Eq. (2.20)), via $(g-1)$ "bridges" $\{b_j\}_{j=1}^{g-1}$. In Figs. 2.5, and 2.6, the integer number b_j denotes the number of edges that regions a_j and a_{j+1} share.

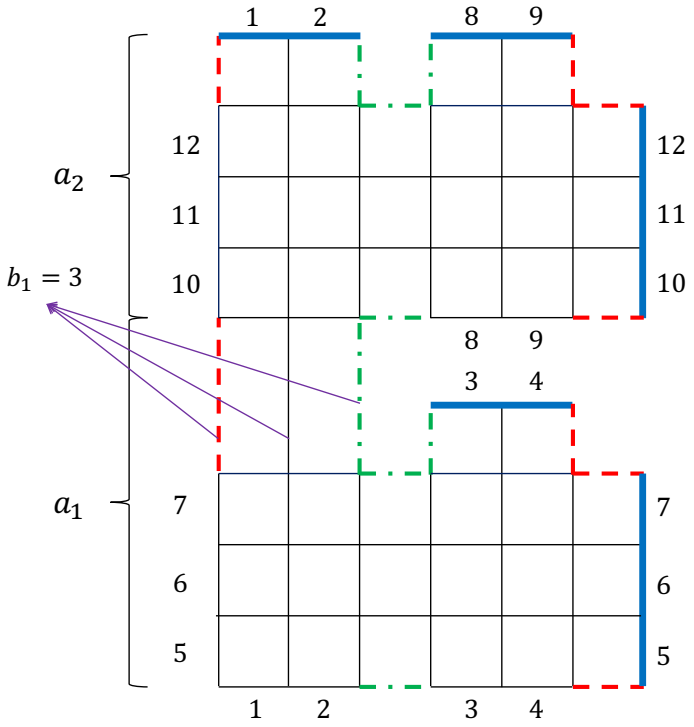

Figure 2.5: A genus two ($g = 2$) lattice. Identical bonds are labeled by the same number (as a result of periodic boundary conditions). Thick solid (blue) lines represent the boundary. The two plaquettes with 8 bonds are shown by dashed (red) and dashed-dotted (green) lines.

To lucidly illustrate the basic construct, we start first with a $g = 2$ lattice. In Fig. 2.5, identical edges are labeled by the same number as a consequence of the periodic boundary conditions. Here, there are $E = 96$ edges, $V = 48$ vertices, and $F = 46$ plaquettes. As in the case of the simple torus ($g = 1$), the typical vertices are endpoints of four edges. Similarly, in Fig. 2.5, all plaquettes (with the exception of two) are comprised of four edges as in the situation of the simple torus. The exceptional cases are colored green (dashed-dotted) and red (dashed). As seen in the figure, the lattice may be splintered into two regions (labeled by a_1 and a_2) where one end of some of the bonds belonging to a_1 are connected to a_2 as shown and labeled in the picture under b_1. Each of the regions a_1 and a_2 looks, by itself, like a square lattice on a genus $g = 1$ surface. Generally, the regions a_1 and a_2 may be composed

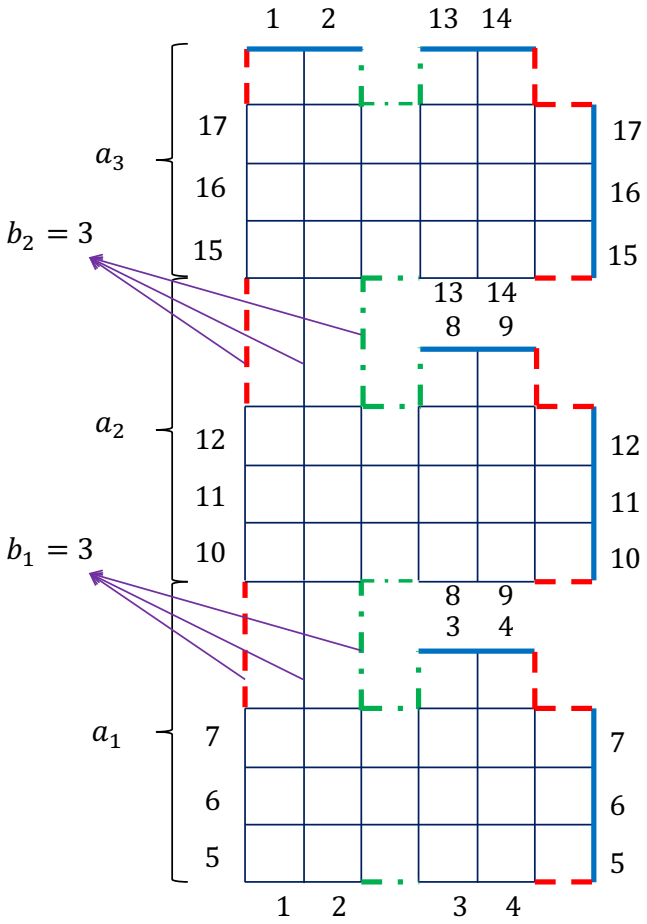

Figure 2.6: A genus three ($g = 3$) lattice. Identical bonds are labeled by the same number (as a result of periodic boundary conditions). Thick solid (blue) lines represent the boundary. The two plaquettes with 12 bonds are shown by dashed (red) and dashed-dotted (green) lines.

of a different number of edges. Employing the taxonomy of Eq. (2.20), we may classify these regions $\{a_j\}_{j=1}^{g}$ to be of either Type I or II. We remark that the number of edges b_1 must be always at least one less than the minimum of the number of bonds of a_1 and a_2 along the horizontal (x) axis. This algorithm trivially generalizes to higher genus number. The cartoon of Fig. 2.6 represents a lattice with $g = 3$.

A synopsis of our numerical results for the ground state degeneracy for surfaces of genus $2 \leq g \leq 5$ appears in Table 2.3. The ground state degeneracy depends on the type of each a_j and the number of bonds of each b_j. When all fragments $\{a_j\}$ are of Type I and are inter-connected by only *single* common edges, the degeneracy attains will its minimal possible value (Eq. (2.14)) of 4^g .

If, in Eq. (2.6), we set J to zero, we will obtain the Hamiltonian of the Ising gauge model. As this theory does not have a star term, this Hamiltonian involves more symmetries and, therefore, one expects the ground state subspace to have a larger degeneracy. We numerically verified it to be $n_{\mathsf{g.s.}}^{\mathsf{gauge}} = 4^g \times 2^{\mathsf{N_{site}}-1}$-fold degenerate ($\mathsf{N_{site}} = E/2$) [68].

2.4.5 Lattice Defects

When dislocations and/or any other lattice defects are present in the classical Toric Code model, the degeneracy is, of course, still bounded by the geometry independent result of 4^g. On Type I lattice (and their composites), the degeneracy is typically equal to this bound yet it may go up upon the introduction of defects. Similarly, in most cases introducing such lattice defects lowers the degeneracy of the more commensurate Type II lattices (and their composites).

Table 2.4 provides the numerical results for such defective lattices. For example, in Fig. 2.7 we see the original lattice, panel a), along with two types of defects as in panel b) and c). These are obtained by replacing 3 squares by 2 adjacent or separated pentagons as in panel b) and c), respectively. To avoid confusion, we will use "$\star$" sign for the first case and "$\star\star$" for the second case. By putting a "$\star$" ("$\star\star$") sign beside a 3×2 lattice, we mean it exhibits a defect of type one (two). That is, represented as "$3 \times 2\ \star$" ("$3 \times 2\ \star\star$").

2.5 Thermodynamics of the Classical Toric Code Model

Previous sections largely focused on the ground states of the classical Toric Code model. As our earlier considerations make clear, however, a minimal topology (and general constraint) dependent degeneracy $\mathcal{N}_{\mathsf{global}} \equiv \min(n_{\mathsf{g.s.}})$ appears for all levels (see, e.g., Eq. (2.13)). This "global" degeneracy must manifest itself as a prefactor in the computation of the partition function. That is, if the whole spectrum has a global degeneracy $\mathcal{N}_{\mathsf{global}}$ then the canonical partition function may be expressed as

$$\mathcal{Z} = \mathcal{N}_{\mathsf{global}} \sum_{\ell=0} n_\ell e^{-\beta E_\ell}, \tag{2.35}$$

where $\mathcal{N}_{\mathsf{global}}\, n_\ell \geq \mathcal{N}_{\mathsf{global}}$ is the number of states having total energy E_ℓ. In "incommensurate" lattices, when no constraints $\{\mathcal{C}_m\}$ augment those of Eq. (2.12), we find that, similar to the partition function of the quantum Toric Code model [35–37], the partition of the

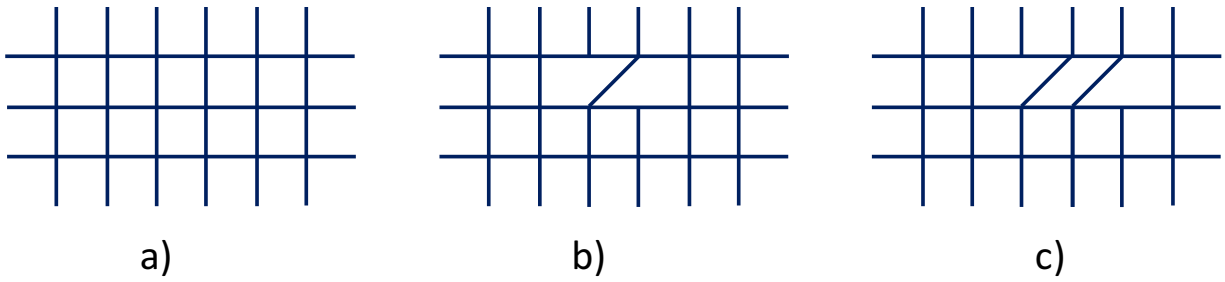

Figure 2.7: Sketch of a part of a square lattice a) with two types of defects b) and c). The defective lattices in b) and c) have one bond less than in a).

classical Toric Code model is given by

$$\begin{aligned} \mathcal{Z}_{\mathsf{inc.}} = \quad & 4^{g-1}[(2\cosh\beta J)^V + (2\sinh\beta J)^V] \\ & \times[(2\cosh\beta J')^F + (2\sinh\beta J')^F]. \end{aligned} \tag{2.36}$$

The prefactor of 4^{g-1} embodies the increase in degeneracy by a factor of four as g is elevated in increments $g \to (g+1)$ beyond a value of $g = 1$. On the simple torus (i.e., when $g = 1$), this partition function (similar to the partition function of the quantum Toric Code model [35–37]) is that of two decoupled Ising chains with one of these chains having V spins and the other composed of F spins. As each such Ising chain has a two-fold degeneracy, it thus follows that the degeneracy of the (more "incommensurate") Type I $g = 1$ system is four-fold and that the degeneracy of the classical Toric Code model on incommensurate lattices on Riemann surfaces of genus g is 4^g for all $g \geq 1$. The latter value saturates the lower bound on the degeneracy of Eq. (2.13). In Section 2.11, we list the partition function for several other more commensurate finite size lattice realizations.

2.6 Classical Toric Clock Models and their Clock gauge theory limits

In this section, we introduce and study a clock model ($\mathbb{Z}_{\mathsf{d}_Q}$) extension of the classical Toric Code model. To that end, we consider what occurs when each spin S may assume $\mathsf{d}_Q > 2$ values. Specifically, on every oriented $(i \to j)$ edge (that we will hereafter label as (ij)), we

set

$$\sigma_{ij} = \exp\Big[\mathrm{i}\,\frac{2\pi}{\mathsf{d}_Q}\alpha_{ij}\Big], \quad (\alpha_{ij} = 0, 1, \cdots, \mathsf{d}_Q - 1), \tag{2.37}$$

$$\sigma_{ji} = \sigma_{ij}^{*}. \tag{2.38}$$

The last equality reflects that a change in the orientation (i.e., a link in the direction from $j \to i$ as opposed to $i \to j$) is associated with complex conjugation. At each vertex "s", we define A_s as

$$\begin{aligned} A_s &= \frac{1}{2}(\sigma_{si}\sigma_{sj}\sigma_{sk}\sigma_{sl} + \text{H.c.}) \\ &= \cos\Big(\frac{2\pi}{\mathsf{d}_Q}(\alpha_{si} + \alpha_{sj} + \alpha_{sk} + \alpha_{sl})\Big), \end{aligned} \tag{2.39}$$

and for each plaquette p

$$B_p = \cos\Big(\frac{2\pi}{\mathsf{d}_Q}(\alpha_{ij} + \alpha_{jk} + \alpha_{kl} + \alpha_{li})\Big), \tag{2.40}$$

composed of edges $(ij), (jk), (kl), (li)$, such that the loop $i \to j \to k \to l$ is oriented counter-clockwise around about the plaquette center. Table 2.5 provides our numerical results for ground state degeneracy ($D^0_{\mathsf{d}_Q}$) for different size lattices of varying genus numbers g. The $\mathsf{d}_Q = 2$ case is that investigated in the earlier sections (i.e., that of the classical Toric Code model with Ising variables $\sigma_{ij} = \pm 1$).

It is readily observed that the *minimal* ground state degeneracy is set by the genus number,

$$n_{\mathsf{g.s.}}^{\mathsf{min}} = \min\{D_{\mathsf{d}_Q}^0\} = \begin{cases} \mathsf{d}_Q^{2g-1}, & \text{odd } \mathsf{d}_Q, \\ \\ 2\mathsf{d}_Q^{2g-1}, & \text{even } \mathsf{d}_Q. \end{cases} \tag{2.41}$$

We next introduce a simple framework that rationalizes Eq. (2.41) and enables us to furthermore derive the results of the previous sections (i.e., the Ising case of $\mathsf{d}_Q = 2$) in a unified way. Furthermore, this approach will allow us to better understand not only the degeneracies in the ground sector but also those of all higher energy states. In the up and coming, we will study the Hamiltonian

$$\begin{aligned} H_{\mathsf{d}_Q} &= -\sum_s A_s - \sum_p B_p \\ &= -\sum_s \cos\left(\frac{2\pi m_{s,\mathsf{d}_Q}}{\mathsf{d}_Q}\right) - \sum_p \cos\left(\frac{2\pi m_{p,\mathsf{d}_Q}}{\mathsf{d}_Q}\right). \end{aligned} \tag{2.42}$$

Here,

$$\begin{cases} m_{s,\mathsf{d}_Q} = \alpha_{si} + \alpha_{sj} + \alpha_{sk} + \alpha_{sl}, \\ \\ m_{p,\mathsf{d}_Q} = \alpha_{ij} + \alpha_{jk} + \alpha_{kl} + \alpha_{li}, \end{cases} \tag{2.43}$$

constitute a system of linear equations. A pair of fixed integers m_{s,d_Q}^ℓ and m_{p,d_Q}^ℓ defines an energy E_ℓ. There are $n_{\mathsf{d}_Q}^\ell$ such pairs.

For each fixed pair r, $r = 1, \cdots, n_{\mathsf{d}_Q}^\ell$, we may express these linear equations as

$$WX^r = Y^r, \tag{2.44}$$

where W is a rectangular $((V+F)\times E)$ matrix. The matrix elements of W are either 0 or ± 1. Generally, the form of the matrix W depends on both the size and type of lattice. The dimension of the vector X^r is equal to the number (E) of edges; Y^r is a $(V+F)-$component vector. Specifically, following Eq. (2.43), these two vectors are defined as: $X^r = \vec{\alpha}$, with components α_{ij}, and $Y^r = m^{\ell}_{s,\mathsf{d}_Q}$, for its first V components and $Y^r = m^{\ell}_{p,\mathsf{d}_Q}$, for the remaining F components.

The number of linearly independent equations (r_{d_Q}) is equal to the rank of the matrix W. Typically, the rank r_{d_Q} is less than the number of unknown α_{ij}. Therefore, we cannot determine all α_{ij} from Eq. (2.44). We should note that the rank of the matrix W is computed modularly, "mod d_Q". This latter modular rank is of pertinence as the edge variables α_{ij} may only take on particular modular values $(\alpha_{ij} = 0, 1, \cdots, \mathsf{d}_Q - 1)$.

Our objective is to calculate the degeneracy $D^{\ell}_{\mathsf{d}_Q}$ of each energy level ℓ (or sector of states that share the same energy of Eq. (2.42)). Equation (2.44) imposes r_{d_Q} constraints on the d_Q possible values of α_{ij}. Thus, for each set of integers $m^{\ell}_{s,\mathsf{d}_Q}$ and $m^{\ell}_{p,\mathsf{d}_Q}$, the degeneracy is equal to $\mathsf{d}_Q^{E-r_{\mathsf{d}_Q}}$. As there are $n^{\ell}_{\mathsf{d}_Q}$ such sets of integers (see Eq. (2.44)), the degeneracy of each level ℓ is

$$D^{\ell}_{\mathsf{d}_Q} = n^{\ell}_{\mathsf{d}_Q} \mathsf{d}_Q^{E-r_{\mathsf{d}_Q}}. \tag{2.45}$$

We may recast Eq. (2.45) to highlight the effect of topology and invoke the Euler relation (Eqs. (2.4) and (2.5)) to write the degeneracy as

$$D^{\ell}_{\mathsf{d}_Q} = n^{\ell}_{\mathsf{d}_Q} \mathsf{d}_Q^{2(g-1)+C_g^{\Lambda}}, \tag{2.46}$$

where we define

$$C_g^{\Lambda} \equiv V + F - r_{\mathsf{d}_Q}. \tag{2.47}$$

The modular rank of the matrix W lies in the interval $1 \leq r_{\mathsf{d}_Q} < V + F$. It thus follows that

$$1 \leq C_g^{\Lambda} \leq V + F - 1. \tag{2.48}$$

From Eqs. (2.46) and (2.48), it is readily seen that

$$D^{\ell}_{\mathsf{d}_Q} \geq \mathsf{d}_Q^{2g-1}. \tag{2.49}$$

The degeneracy of Eq. (2.49) (stemming from the spectral redundancy of each level ℓ seen in Eq. (2.46)) is consistent with an effective composite symmetry

$$G = \mathbb{Z}_{\mathsf{d}_Q} \otimes \mathbb{Z}_{\mathsf{d}_Q} \otimes \cdots \otimes \mathbb{Z}_{\mathsf{d}_Q}, \tag{2.50}$$

i.e., the product of $(2g-1)$ symmetries of the $\mathbb{Z}_{\mathsf{d}_Q}$ type. That is, if each element of such a $\mathbb{Z}_{\mathsf{d}_Q}$ symmetry gave rise to a d_Q-fold degeneracy then the result of Eq. (2.46) will naturally follow.

The non-local symmetry of Eq. (2.50) compound the standard local symmetries that appear in the gauge theory limit of Eq. (2.42) in which the A_s terms are absent, i.e., $H_{\mathsf{d}_Q} = -\sum_p B_p$. The latter gauge theory enjoys the local symmetries

$$\theta_{ij} \to \theta_{ij} + \phi_i - \phi_j, \tag{2.51}$$

with, at any lattice vertex (site) i, the angle ϕ_i being an arbitrary integer multiple of $2\pi/\mathsf{d}_Q$. In this case, we find that the ground state degeneracy ($D^{\mathsf{gauge},0}_{\mathsf{d_Q}}$) is purely topological (i.e., not holographic),

$$D^{\mathsf{gauge},0}_{\mathsf{d_Q}} = n^{\mathsf{gauge},0}_{\mathsf{d}_Q} \mathsf{d}_Q^{2(g-1)+\frac{E}{2}}, \tag{2.52}$$

where,

$$\begin{cases} 1 \leq n^{\mathsf{gauge},0}_{\mathsf{d}_Q} \leq \mathsf{d}_Q, & \text{odd } \mathsf{d}_Q, \\ \\ 2 \leq n^{\mathsf{gauge},0}_{\mathsf{d}_Q} \leq \mathsf{d}_Q, & \text{even } \mathsf{d}_Q. \end{cases} \tag{2.53}$$

These equations extend the degeneracy $\mathsf{n}^{\mathsf{gauge}}_{\mathsf{g.s.}}$ found in Subsection 2.4.4 for the Ising ($\mathsf{d}_Q = 2$) lattice gauge theory [68].

2.7 $U(1)$ Classical Toric Code Model and its gauge theory limit

We next turn to a simple $U(1)$ theory

$$H = -J \sum_s \cos(\Phi_s) - J' \sum_p \cos(\Phi_p), \tag{2.54}$$

where the "fluxes"

$$\Phi_s = \sum_i \theta_{si}, \quad \Phi_p = \sum_{ij \in p} \theta_{ij}, \tag{2.55}$$

are, respectively, the sums of the angles on all edges emanating from site s and the sum of all angles θ_{ij} on edges that belong to a plaquette p. In the continuum limit (in which the lattice constant a tends to zero), the $\cos \Phi_p$ term may be Taylor expanded as the flux is small, $\cos \Phi_p \approx (1 - \frac{1}{2}\Phi_p^2 + \cdots)$ in the usual way. Then, omitting an irrelevant constant additive term, the Hamiltonian becomes in the standard manner

$$H = \frac{1}{2} \int \Phi_p^2(x) d^2x \approx a^2 \int B_3^2 d^2x, \tag{2.56}$$

where $B_3 = \partial_1 A_2 - \partial_2 A_1$ (with $\vec{A}$ a vector potential) is the conventional magnetic field along the direction transverse to the plane where the lattice resides. In the $\mathsf{d}_Q \to \infty$ limit, the $U(1)$ Hamiltonian of Eq. (2.54) follows from Eqs. (2.37), (2.39), and (2.40) where $\sigma_{ij} = e^{\mathrm{i}\theta_{ij}}$, and $\theta_{ij} = 2\pi\alpha_{ij}/\mathsf{d}_Q$ with $\alpha_{ij} = 0, 1, \cdots, \mathsf{d}_Q - 1$. In the $\mathsf{d}_Q \to \infty$ limit, the discrete clock symmetry becomes a continuous rotational symmetry, $\mathbb{Z}_{\mathsf{d}_Q} \to U(1)$. Rather trivially, yet notably, in this limit, the system becomes *gapless*. Repeating *mutatis mutandis* the considerations of Eqs. (2.46) and (2.49), in the continuous large d_Q limit, a genus dependent symmetry is naturally associated with the system degeneracy. Peculiarly, in this limit, similar to Eq. (2.50), a genus dependent

$$G = U(1) \otimes U(1) \cdots \otimes U(1) \tag{2.57}$$

symmetry may appear for the Toric $U(1)$ theory of Eq. (2.54). In the limiting case in which the star term does not appear in Eq. (2.54), i.e., that of $J = 0$, a symmetry of the type of

Eq. (2.57) compounds the known local $U(1)$ symmetry,

$$\theta_{ij} \to \theta_{ij} + \phi_i - \phi_j, \tag{2.58}$$

similar to Eq. (2.51) but with an arbitrary real phase ϕ_i at each lattice vertex (site) i. These local symmetries are lifted once the $\cos \Phi_s$ term is introduced, as in Eq. (2.54). Thus, similar to the Clock gauge theory (whose degeneracy was given by Eqs. (2.52), and (2.53)), this $U(1)$ *lattice gauge theory exhibits a genus dependent degeneracy.*

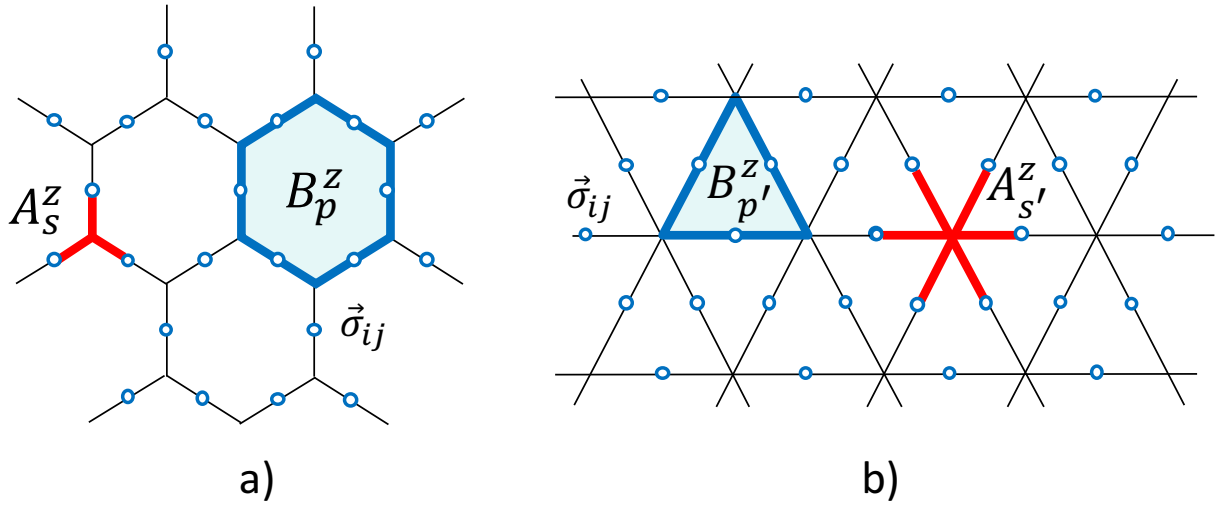

Figure 2.8: a) Hexagonal lattice and b) Triangular lattice. In panel a) the star terms A_s^z and plaquette terms B_p^z involve three and six spins S (circles) interactions, respectively, while the opposite happens in panel b).

2.8 Honeycomb and Triangular lattices

Thus far, we focused on square lattice realizations of the Ising, clock, and $U(1)$ theories. For completeness, we now examine other lattice geometries. Specifically, we study the honeycomb lattice (H) and triangular lattice (T) incarnations of our classical theory and determine

their ground state degeneracies. In Fig. 2.8, A_s^z and B_p^z are defined for each lattice. The Hamiltonians are given by

$$\begin{aligned} H_{\mathsf{H}} &= -J_h \sum_s A_s^z - J_h' \sum_p B_p^z, \\ H_{\mathsf{T}} &= -J_t \sum_{s'} A_{s'}^z - J_t' \sum_{p'} B_{p'}^z. \end{aligned} \tag{2.59}$$

Our numerical results are summarized in Table 2.2. These results are consistent with Eqs. (2.46) and (2.49).

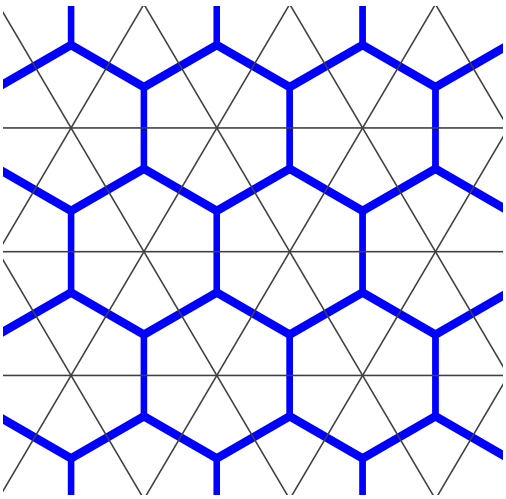

Figure 2.9: By connecting the centers of hexagons in an hexagonal lattice (thick solid lines), we obtain the corresponding dual lattice which is a triangular lattice (solid lines).

Table 2.2: Computed ground state degeneracy D^0_{M} for $\mathsf{d}_Q = \mathsf{M}$, for a hexagonal lattice (= triangular lattice).

g	E	D^0_2	D^0_3	D^0_4	D^0_5	D^0_6	D^0_7	D^0_8	D^0_9
1	6	8	27	64	125	216	343	512	729
	12	16	27						
	18	8							
	24	128							
2	24	128							
	30	64							

As is well known, the H and T lattices are dual lattices (Fig. 2.9). This duality implies that the classical Toric Code models of Eq. (2.59) yield the same results. From Figs. 2.8 and 2.9, as a consequence of duality, what is defined as A^z_s (B^z_p) in H corresponds to some $B^z_{p'}$ ($A^z_{s'}$) in T, and vice versa. This indicates that

$$\begin{aligned} A^z_s &\overset{\text{Duality}}{\longleftrightarrow} B^z_{p'}, \\ A^z_{s'} &\overset{\text{Duality}}{\longleftrightarrow} B^z_p. \end{aligned} \tag{2.60}$$

After this transformation we can rewrite Eqs. (2.59) as,

$$\begin{aligned} H_{\mathsf{H}} &= -J_h \sum_{p'} B^z_{p'} - J'_h \sum_{s'} A^z_{s'}, \\ H_{\mathsf{T}} &= -J_t \sum_{p} B^z_p - J'_t \sum_{s} A^z_s, \end{aligned} \tag{2.61}$$

and assuming $J_h = J'_t, J'_h = J_t$, it is seen that $H_{\mathsf{H}} = H_{\mathsf{T}}$. This simple analysis does not take into account potential boundary terms that may appear in finite lattices, as a result of the duality transformation.

2.9 Other classical models with holographic degeneracy

In this section, we dwell on a few more Ising type spin systems, similar to Type II commensurate lattice realizations of the classical Toric Code model (Eq. (2.27)), in which the degeneracy is holographic, i.e., exponential in the system's boundary.

2.9.1 Potts Compass Model

We now discuss a discretized version of the compass model [69], the "4-state Potts compass model" on an $L_x \times L_y$ square lattice with periodic boundary conditions. The Hamiltonian is given by,

$$H_{\mathsf{PC}} = -\sum_{i,\sigma,\tau} \Big(n_{i\sigma} n_{i+\hat{x},\sigma} \sigma_i \sigma_{i+\hat{x}} + n_{i\tau} n_{i+\hat{y},\tau} \tau_i \tau_{i+\hat{y}} \Big), \tag{2.62}$$

where at each site (vertex) i there are two Ising type spins $\sigma_i = \pm 1$, $\tau_i = \pm 1$, while the occupation numbers $n_{i\sigma} = 0, 1$ and $n_{i\tau} = 1 - n_{i\sigma}$. Then, at each site, there is either a σ or a τ degree of freedom. The Cartesian unit vectors $\hat{x}$ and $\hat{y}$ link neighboring sites of the square lattice. Spins of the σ type interact along the x-direction (horizontally) while those of the

τ variety interact along the y-direction (vertically). Minimizing the energy is equivalent to maximizing the number of products in the summand of Eq. (2.62) that are equal to $+1$. In a configuration in which at all sites there is a σ (and no τ) spin, the system effectively reduces to that of L_y independent Ising chains parallel to the x direction. For each such chain, there are two ground states: $\sigma_i = +1$ or $\sigma_i = -1$ for all lattice sites. As these chains are independent, there are 2^{L_y} ground states. Replacing some sites with τ spins some bonds turn into 0 and energy increases as a result. Repeating the same procedure where all sites are occupied by τ spins, we find out that there are L_x independent vertical Ising chains and so 2^{L_x} states giving the same minimum energy. The ground state degeneracy of Eq. (2.62) is $2^{L_x} + 2^{L_y}$. For a more general case with genus g (composed of regions $\{a_j\}$ connected by bridges $\{b_j\}$ (shared by regions a_j and a_{j+1})), the degeneracy again depends on the number of independent horizontal (L_y) and vertical (L_x) Ising chains. If each region a_j is of size $L_x^j \times L_y^j$ ($j = 1, \cdots, g$) and b_j ($j = 1, \cdots, g-1$) is the number of edges connecting a_j and a_{j+1}, then, the ground state degeneracy will be

$$n_{\text{g.s}}^{\text{Potts}-\text{compass}} = 2^{L_x} + 2^{L_y}, \tag{2.63}$$

where

$$L_x = \sum_{j=1}^{g} L_x^j - \sum_{j=1}^{g-1} b_j, \;\; L_y = \sum_{j=1}^{g} L_y^j. \tag{2.64}$$

This degeneracy depends on both the geometry and the topology of the lattice. We briefly highlight the effects of topology in the degeneracy of Eqs. (2.63) and (2.64). Panel a) of Fig. 2.10 depicts a genus one lattice for which $L_x = 5, L_y = 12$ and $N = V = 60$. By redefining the way spins are connected and boundary conditions, as we explained before, we may transform it into, e.g., $g = 2, 3$ lattices as in Fig. 2.10 (panels b) and c), respectively).

Here, one may readily verify that although $L_y = 12$ and the total number of spins do not change, L_x varies (increases) as a result of increasing the genus number.

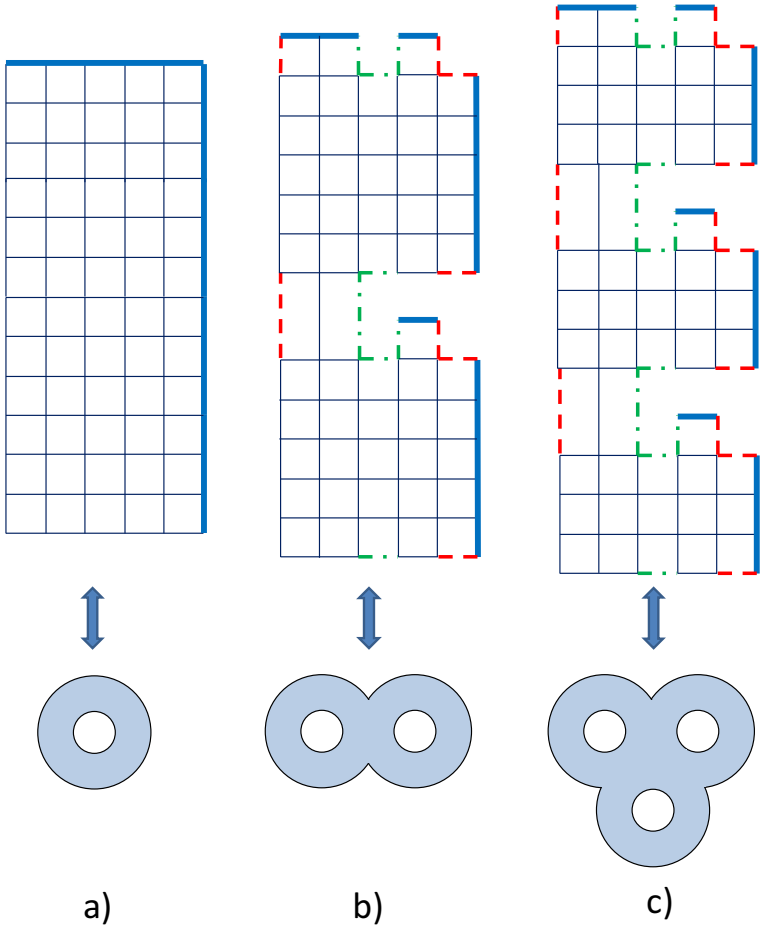

Figure 2.10: Three lattices with different genus numbers and their corresponding tori below. All have the same total number of spins, $N = 60$. Thick solid (blue) lines represent the boundary and spins are located at the vertices. We have, a) $g = 1$ and $L_x = 5, L_y = 12$. b) $g = 2$ and $L_x = 7, L_y = 12$. c) $g = 3$ and $L_x = 9, L_y = 12$.

2.9.2 Classical Xu-Moore Model

As discussed earlier, our classical Toric Code model of Eq. (2.6) is identical to the spin (defined on vertices) plaquette model of Eq. (2.24). This latter Hamiltonian is, as it turns

out, a particular limiting case of the so-called "Xu-Moore model" [70, 71], one in which its transverse field is set to zero and the model becomes classical. In its original rendition, this classical limit of the Xu-Moore model has a degeneracy exponential in the system's boundary. This degeneracy appears regardless of the parity of the system sides. We now discuss how to relate the degeneracy in our system to that of the classical Xu-Moore model. To achieve this, instead of applying periodic boundary conditions along the Cartesian directions as in the classical Toric Code model (i.e. along the solid lines of Fig. 2.2), we endow the system with different boundary conditions. Specifically, we examine instances in which periodic boundary conditions are associated with the diagonal x' and y' axis (45° angle rotation of the original square lattice) of Fig. 2.2. A simple calculation then illustrates that the ground state sector as well as all other energies have a global degeneracy factor,

$$\mathcal{N}_{\mathsf{global}} = 2^{L_{x'}+L_{y'}}. \tag{2.65}$$

where $L_{x'}$ and $L_{y'}$ are defined as in Eq. (2.64) but along the diagonal directions (dotted lines in Fig. 2.2). A similar (global) degeneracy appears in the classical 90° orbital compass model [24] (having only nearest neighbor two-spin interactions) to which the Xu-Moore model is dual.

2.9.3 Second and Third nearest neighbor Ising models

We conclude our discussion of holographic degeneracy in spin models with a brief review of an Ising system even simpler than the ones discussed above. Specifically, we may consider an Ising spin system on a square lattice with its lattice constant a set to unity when it is embedded on a torus ($g = 1$) with periodic boundary conditions along the x' and y' diagonals

with the Hamiltonian

$$H = \sum_{i,j} (2\delta_{|i-j|,\sqrt{2}} + \delta_{|i-j|,2})\sigma_i\sigma_j. \tag{2.66}$$

Here interactions are anti-ferromagnetic between next-nearest neighbors ($|i-j| = \sqrt{2}$) and next-next-nearest neighbors ($|i-j| = 2$). It is straightforward to demonstrate that this system has a ground state degeneracy scales as $2^{L_{x'}} + 2^{L_{y'}}$ where $L_{x',y'}$ are the lattice sizes along the x' and y' directions [18].

2.10 Summary

In this chapter, we demonstrated that a topological ground state degeneracy (one depending on the genus number of the Riemann surface on which the lattice is embedded) does not imply concurrent topological order (i.e., Eq. (2.3) is violated and distinct ground states may be told apart by local measurements). We illustrated this by introducing the classical Toric Code model (Eq. (2.6) with $\mu = \nu = z$). As we showed in some detail, under rather mild conditions (those pertaining to "Type I" lattices in the classification of Eq. (2.27)), the ground state degeneracy solely depends on topology. In these classical systems, however, the ground states (given by, e.g., Eqs. (2.32) and (2.33) on the torus) are distinguishable by measuring the pattern of σ^z_{ij} on a finite number of nearest neighbor edges; thus, the ground states do not satisfy Eq. (2.3) and are, rather trivially, not topologically ordered. They are Landau ordered instead and, most importantly, illustrate that the ground states are related by $d = 2$ (global) Gauge-like symmetries contrary to the $d = 1$ symmetries of Kitaev's Toric Code model [35–37].

In the more commensurate Type II lattice realizations of the classical Toric Code model as well as in a host of other systems, the ground state degeneracy is "holographic"- i.e., exponential in the linear size of the lattice [18,43]. This classical holographic effect is different from more subtle deeper quantum relations, for entanglement entropies, e.g., [72–74]. In all lattices and topologies, the minimal ground state degeneracy (and that of all levels in the system) of the classical model is robust and bounded from below by 4^g with g the genus number. We find similar genus dependent minimal degeneracies in clock and $U(1)$ theories (including *lattice gauge theories*). For completeness, we remark that a degeneracy of the form $2^{\eta(L)}$ with η a quantity bounded from above by the linear system size (viz., a holographic entropy) also appears in bona fide topologically ordered systems such as the "Haah code" [5–7].

Beyond demonstrating that such degeneracies may arise in classical theories, we illustrated that these behaviors may arise in rather canonical clock and $U(1)$ type theories. We provided a simple framework for studying and understanding the origin of these ubiquitous topological and holographic degeneracies.

We conclude with one last remark. Our results for classical systems enable the construction of simple *quantum models* with ground states that may be told apart locally (i.e., violating Eq. (2.3) for topological quantum order) yet, nevertheless, exhibit a topological ground state degeneracy). We present one, out of a large number of possible, routes to write such models exactly. Consider any one of the different theories studied in this chapter. Let us denote the classical Hamiltonian associated with any of these theories by $H_{\mathsf{Classical}}$ and corresponding local observables that may differentiate ground states apart by $\mathcal{V}$. One may then apply any product U of local unitary transformations to both the Hamiltonian and the corresponding "order parameter" local observable $\mathcal{V}$. That is, we may consider the

"quantum" Hamiltonian $H_{\mathsf{Quantum}} \equiv U^\dagger H_{\mathsf{Classical}} U$ and the corresponding local operator $\mathcal{V}_{\mathsf{Quantum}} \equiv U^\dagger \mathcal{V} U$. By virtue of the unitary transformation, both in the ground state sector (as well as at any finite temperature), the expectation value of the local observable $\mathcal{V}$ in the classical system given by $H_{\mathsf{Classical}}$ is identical to the expectation value of the $\mathcal{V}_{\mathsf{Quantum}}$ in the quantum system governed by H_{Quantum}. To be concrete, one may consider, e.g., the Classical Toric Code (CTC) model. That is, e.g., one may set $H_{\mathsf{Classical}} = H_{\mathsf{CTC}}$ that contains only classical Ising (σ_j^x) spins. Next, consider the unitary operator $U = \prod_{j\in\Lambda_+} \exp[i\frac{\pi}{4}\sigma_j^z]$ that effects a $\pi/2$ rotation of all spins at sites j that belong to the sublattice Λ_+ about the internal σ^z axis. (That is, indeed, $\frac{1}{\sqrt{2}}(1 - i\sigma_j^z)\sigma_j^x \frac{1}{\sqrt{2}}(1 + i\sigma_j^z) = \sigma_j^y$.) Thus, trivially, the resulting Hamiltonian H_{Quantum} contains non-commuting σ^x and σ^y and is "quantum" (just as the Kitaev Toric Code model of Section 2.3 [3] that may be mapped to two decoupled classical Ising spin chains [35–37]) contains exactly these two quantum spin components and is "quantum"). By virtue of the local product nature of the mapping operator U, the classical local observables $\mathcal{V}$ that we discussed in this chapter become now new local observables $\mathcal{V}_{\mathsf{Quantum}}$ in the quantum model. Thus, putting all of the pieces together, we may indeed generate quantum models with a topological degeneracy in which the ground state may be told apart by local measurements.

Acknowledgements

This work was partially supported by the National Science Foundation under NSF Grant No. DMR-1411229 and the Feinberg foundation visiting faculty program at the Weizmann Institute. We are very grateful to a discussion with J. Haah in which he explained to us the degeneracies found in his model [7].

2.11 Supplementary information

In Type I lattices (and their simplest composites), the canonical partition function of the classical Toric Code model is given by Eq. (2.36). The situation is somewhat richer for other lattices. Below, we briefly write the partition functions for several such finite size lattices. For simplicity we set $J = J' = 1$ and $\mathsf{d}_Q = 2$ in the classical rendition of Eq. (2.6) and perform a high temperature (H-T) and low temperature (L-T) series expansion which is everywhere convergent for these finite size systems. One can follow a similar procedure and find the partition functions for $\mathsf{d}_Q > 2$. We start with H-T series expansion,

$$\begin{aligned} \mathcal{Z}_{\mathsf{H-T}} &= \sum_{\{\sigma\}} e^{-\beta H^{z,z}} = \sum_{\{\sigma\}} e^{\beta \sum_s A_s^z + \beta \sum_p B_p^z} \\ &= \sum_{\{\sigma\}} \prod_s e^{\beta A_s^z} \prod_p e^{\beta B_p^z} \\ &= (\cosh \beta)^{V+F} \sum_{\{\sigma\}} \prod_s (1 + T\, A_s^z) \prod_p (1 + T\, B_p^z), \end{aligned} \tag{2.67}$$

where $T = \tanh \beta$ and $\beta = 1/(k_B T)$.

In Eq. (2.67) after expanding the products, and summing over all configurations, the only surviving terms are those for which the product of a subset of A_s^z's and B_p^z's is equal to 1 and this corresponds to one constraint or a product of two or more of them sharing no star or plaquette operators. Thus,

$$\begin{aligned} \mathcal{Z}_{\mathsf{H-T}} &= 2^E (\cosh \beta)^{V+F} \\ &\times \Big(1 + \text{terms from constraints on } A_s^z\text{'s and } B_p^z\text{'s}\Big), \end{aligned} \tag{2.68}$$

where F is the number of faces and V is the number of vertices. The factor of 2^E (with $E = N$ the number of spins or lattice edges) originates from the summation $\sum_{\{\sigma\}} 1$ (each σ_{ij}^z has two values (± 1), with $(ij) = 1, \cdots, E$). The sole non-vanishing traces in Eq. (2.67) originate from the constraints of Eqs. (2.23) and (2.25) and their higher genus counterparts. While this procedure trivially gives rise to the partition function of Eq. (2.36) for simple lattices, the additional constraints in other lattices spawn new terms in the partition functions.

In the following we develop the L-T series expansion for $\mathsf{d}_Q = 2$. From Eq. (2.36),

$$\begin{aligned} \mathcal{Z}_{\mathsf{L-T}} &= \mathcal{N}_{\mathsf{global}} \sum_{\ell=0} n_\ell e^{-\beta E_\ell} \\ &= \mathcal{N}_{\mathsf{global}} e^{-\beta E_0} \Big(1 + \sum_{\ell=1} n_\ell e^{-\beta (E_\ell - E_0)} \Big), \end{aligned} \tag{2.69}$$

where E_0 is the ground state energy and $\mathcal{N}_{\mathsf{global}}$ is the ground state degeneracy. Numerical results illustrate that the integers n_ℓ are larger than or equal to 1. One can generalize this form for $\mathsf{d}_Q > 2$

$$\mathcal{Z}_{\mathsf{L-T}} = \sum_{\ell=0} D_{\mathsf{d}_Q}^\ell e^{-\beta E_\ell}, \tag{2.70}$$

where E_ℓ and $D_{\mathsf{d}_Q}^\ell$ indicate energy and degeneracy of energy level ℓ for a given d_Q, respectively.

Below is a sample of our numerical results for $\mathcal{Z}_{\mathsf{H-T}}$ and $\mathcal{Z}_{\mathsf{L-T}}$ of lattices with different sizes, d_Q's and genus numbers ($g = 1, 2, 3$). From $\mathcal{Z}_{\mathsf{L-T}}$, we can easily see that exited states have a degeneracy "higher than or equal to" the ground state degeneracy ($J = J'$ and $\beta J = \mathrm{K}$).

(I) $\boldsymbol{g = 1}$:

(a) $\mathbf{3 \times 1, E = 6}$:

(i) $\underline{\mathsf{d}_Q = 2}$:

$$\begin{aligned}
\mathcal{Z}_{\mathsf{H-T}} &= (2\cosh\beta)^6\Big(1 + T^6 + 2T^3\Big), \\
\mathcal{Z}_{\mathsf{L-T}} &= 4(e^{6\mathrm{K}})\Big(1 + 9e^{-8\mathrm{K}} + 6e^{-4\mathrm{K}}\Big).
\end{aligned}$$

(ii) $\underline{\mathsf{d}_Q = 3}$:

$$\begin{aligned}
\mathcal{Z}_{\mathsf{H-T}} &= (3\cosh\beta)^6\Big(1 + \frac{T^6}{32} + \frac{3T^4}{8}\Big), \\
\mathcal{Z}_{\mathsf{L-T}} &= 9(e^{6\mathrm{K}})\Big(1 + 10e^{-9\mathrm{K}} + 12e^{-\frac{15\mathrm{K}}{2}} + 36e^{-6\mathrm{K}} \\
&+ 16e^{-\frac{9\mathrm{K}}{2}} + 6e^{-3\mathrm{K}}\Big).
\end{aligned}$$

(iii) $\underline{\mathsf{d}_Q = 4}$:

$$\begin{aligned}
\mathcal{Z}_{\mathsf{H-T}} &= (4\cosh\beta)^6\Big(1 + \frac{T^6}{16}\Big), \\
\mathcal{Z}_{\mathsf{L-T}} &= 8(e^{6\mathrm{K}})\Big(1 + e^{-12\mathrm{K}} + 12e^{-10\mathrm{K}} + 135e^{-8\mathrm{K}} \\
&+ 216e^{-6\mathrm{K}} + 135e^{-4\mathrm{K}} + 12e^{-2\mathrm{K}}\Big).
\end{aligned}$$

(iv) $\underline{\mathsf{d}_Q = 5}$:

$$
\begin{aligned}
\mathcal{Z}_{\mathsf{H-T}} &= (5\cosh\beta)^6\Big(1+\frac{T^6}{32}\Big),\\
\mathcal{Z}_{\mathsf{L-T}} &= 5(e^{6\mathrm{K}})\Big(1+90e^{\left(-\sqrt{5}-5\right)\mathrm{K}}+90e^{\left(\sqrt{5}-5\right)\mathrm{K}}\\
&+ 240e^{\left(\frac{1}{4}\left(-\sqrt{5}-1\right)+\sqrt{5}-6\right)\mathrm{K}}+30e^{\left(\frac{1}{2}\left(-\sqrt{5}-1\right)-2\right)\mathrm{K}}\\
&+ 210e^{\left(\frac{1}{2}\left(-\sqrt{5}-1\right)+\sqrt{5}-7\right)\mathrm{K}}+12e^{\left(\frac{5}{4}\left(-\sqrt{5}-1\right)-5\right)\mathrm{K}}\\
&+ 20e^{\left(\frac{3}{2}\left(-\sqrt{5}-1\right)-6\right)\mathrm{K}}+240e^{\left(\frac{1}{4}\left(\sqrt{5}-1\right)-\sqrt{5}-6\right)\mathrm{K}}\\
&+ 120e^{\left(\frac{1}{2}\left(-\sqrt{5}-1\right)+\frac{1}{4}\left(\sqrt{5}-1\right)-3\right)\mathrm{K}}\\
&+ 120e^{\left(\frac{3}{4}\left(-\sqrt{5}-1\right)+\frac{1}{4}\left(\sqrt{5}-1\right)-4\right)\mathrm{K}}\\
&+ 60e^{\left(\frac{5}{4}\left(-\sqrt{5}-1\right)+\frac{1}{4}\left(\sqrt{5}-1\right)-6\right)\mathrm{K}}\\
&+ 30e^{\left(\frac{1}{2}\left(\sqrt{5}-1\right)-2\right)\mathrm{K}}\\
&+ 210e^{\left(\frac{1}{2}\left(\sqrt{5}-1\right)-\sqrt{5}-7\right)\mathrm{K}}\\
&+ 120e^{\left(\frac{1}{4}\left(-\sqrt{5}-1\right)+\frac{1}{2}\left(\sqrt{5}-1\right)-3\right)\mathrm{K}}\\
&+ 360e^{\left(\frac{1}{2}\left(-\sqrt{5}-1\right)+\frac{1}{2}\left(\sqrt{5}-1\right)-4\right)\mathrm{K}}\\
&+ 360e^{\left(\frac{3}{4}\left(-\sqrt{5}-1\right)+\frac{1}{2}\left(\sqrt{5}-1\right)-5\right)\mathrm{K}}\\
&+ 120e^{\left(\frac{1}{4}\left(-\sqrt{5}-1\right)+\frac{3}{4}\left(\sqrt{5}-1\right)-4\right)\mathrm{K}}\\
&+ 360e^{\left(\frac{1}{2}\left(-\sqrt{5}-1\right)+\frac{3}{4}\left(\sqrt{5}-1\right)-5\right)\mathrm{K}}\\
&+ 240e^{\left(\frac{3}{4}\left(-\sqrt{5}-1\right)+\frac{3}{4}\left(\sqrt{5}-1\right)-6\right)\mathrm{K}}\\
&+ 12e^{\left(\frac{5}{4}\left(\sqrt{5}-1\right)-5\right)\mathrm{K}}\\
&+ 60e^{\left(\frac{1}{4}\left(-\sqrt{5}-1\right)+\frac{5}{4}\left(\sqrt{5}-1\right)-6\right)\mathrm{K}}\\
&+ 20e^{\left(\frac{3}{2}\left(\sqrt{5}-1\right)-6\right)\mathrm{K}}\Big).
\end{aligned}
$$

(v) $\underline{\mathsf{d}_Q = 6}$:

$$\begin{aligned}
\mathcal{Z}_{\mathsf{H-T}} &= (6\cosh\beta)^6\Big(1+\frac{T^6}{32}\Big),\\
\mathcal{Z}_{\mathsf{L-T}} &= 36(e^{6\mathrm{K}})\Big(1+6e^{-11\mathrm{K}}+12e^{-10\mathrm{K}}+24e^{-\frac{19\mathrm{K}}{2}}\\
&+ 10e^{-9\mathrm{K}}+48e^{-\frac{17\mathrm{K}}{2}}+165e^{-8\mathrm{K}}+12e^{-\frac{15\mathrm{K}}{2}}\\
&+ 192e^{-7\mathrm{K}}+168e^{-\frac{13\mathrm{K}}{2}}+36e^{-6\mathrm{K}}+96e^{-\frac{11\mathrm{K}}{2}}\\
&+ 282e^{-5\mathrm{K}}+16e^{-\frac{9\mathrm{K}}{2}}+114e^{-4\mathrm{K}}+60e^{-\frac{7\mathrm{K}}{2}}\\
&+ 6e^{-3\mathrm{K}}+24e^{-\frac{5\mathrm{K}}{2}}+24e^{-2\mathrm{K}}\Big).
\end{aligned}$$

(b) $\mathbf{2\times 2}, \boldsymbol{E=8}$:

(i) $\underline{\mathsf{d}_Q = 2}$:

$$\begin{aligned}
\mathcal{Z}_{\mathsf{H-T}} &= (2\cosh\beta)^8\Big(1+14T^4+T^8\Big),\\
\mathcal{Z}_{\mathsf{L-T}} &= 16(e^{8\mathrm{K}})\Big(1+e^{-16\mathrm{K}}+14e^{-8\mathrm{K}}\Big).
\end{aligned}$$

(ii) $\underline{\mathsf{d}_Q = 3}$:

$$\begin{aligned}
\mathcal{Z}_{\mathsf{H-T}} &= (3\cosh\beta)^8\Big(1+\frac{3T^8}{128}+\frac{T^6}{8}+\frac{3T^4}{4}\Big),\\
\mathcal{Z}_{\mathsf{L-T}} &= 27(e^{8\mathrm{K}})\Big(1+18e^{-12\mathrm{K}}+16e^{-21\mathrm{K}/2}\\
&+ 80e^{-9\mathrm{K}}+64e^{-15\mathrm{K}/2}+56e^{-6\mathrm{K}}+8e^{-3\mathrm{K}}\Big).
\end{aligned}$$

(iii) $\underline{\mathsf{d}_Q = 4}$:

$$\begin{aligned}
\mathcal{Z}_{\mathsf{H-T}} &= (4\cosh\beta)^8\Big(1+\frac{T^8}{16}+\frac{3T^4}{4}\Big),\\
\mathcal{Z}_{\mathsf{L-T}} &= 128(e^{8\mathrm{K}})\Big(1+e^{-16\mathrm{K}}+44e^{-12\mathrm{K}}+64e^{-10\mathrm{K}}\\
&+ 294e^{-8\mathrm{K}}+64e^{-6\mathrm{K}}+44e^{-4\mathrm{K}}\Big).
\end{aligned}$$

(c) $\mathbf{4\times 1}, \boldsymbol{E=8}$:

(i) $\underline{\mathsf{d}_Q = 2}$:

$$\begin{aligned}
\mathcal{Z}_{\mathsf{H-T}} &= (2\cosh\beta)^8\Big(1+2T^4+T^8\Big),\\
\mathcal{Z}_{\mathsf{L-T}} &= 4(e^{8\mathrm{K}})\Big(1+e^{-16\mathrm{K}}+12e^{-12\mathrm{K}}+38e^{-8\mathrm{K}}\\
&+ 12e^{-4\mathrm{K}}\Big).
\end{aligned}$$

(ii) $\underline{\mathsf{d}_Q = 3}$:

$$\begin{aligned}
\mathcal{Z}_{\mathsf{H-T}} &= (3\cosh\beta)^8\Big(1+\frac{T^8}{128}\Big),\\
\mathcal{Z}_{\mathsf{L-T}} &= 3(e^{8\mathrm{K}})\Big(1+86e^{-12\mathrm{K}}+336e^{-\frac{21\mathrm{K}}{2}}\\
&+ 616e^{-9\mathrm{K}}+560e^{-\frac{15\mathrm{K}}{2}}420e^{-6\mathrm{K}}+112e^{-\frac{9\mathrm{K}}{2}}\\
&+ 56e^{-3\mathrm{K}}\Big).
\end{aligned}$$

(iii) $\underline{\mathsf{d}_Q = 4}$:

$$\begin{aligned}
\mathcal{Z}_{\mathsf{H-T}} &= (4\cosh\beta)^8\Big(1+\frac{T^8}{64}\Big),\\
\mathcal{Z}_{\mathsf{L-T}} &= 16(e^{8\mathrm{K}})\Big(1+e^{-16\mathrm{K}}+8e^{-14\mathrm{K}}+252e^{-12\mathrm{K}}\\
&+ 952e^{-10\mathrm{K}}+1670e^{-8\mathrm{K}}+952e^{-6\mathrm{K}}\\
&+ 252e^{-4\mathrm{K}}+8e^{-2\mathrm{K}}\Big).
\end{aligned}$$

(d) $\mathbf{3\times 2}, \boldsymbol{E=12}$:

(i) $\underline{\mathsf{d}_Q = 2}$:

$$\begin{aligned}
\mathcal{Z}_{\mathsf{H-T}} &= (2\cosh\beta)^{12}\Big(1+2T^6+T^{12}\Big),\\
\mathcal{Z}_{\mathsf{L-T}} &= 4(e^{12\mathrm{K}})\Big(1+e^{-24\mathrm{K}}+30e^{-20\mathrm{K}}\\
&+ 255e^{-16\mathrm{K}}+452e^{-12\mathrm{K}}+255e^{-8\mathrm{K}}+30e^{-4\mathrm{K}}\Big).
\end{aligned}$$

(ii) $\underline{\mathsf{d}_Q = 3}$:

$$\begin{aligned}
\mathcal{Z}_{\mathsf{H-T}} &= (3\cosh\beta)^{12}\Big(1+\frac{T^{12}}{2048}+\frac{3T^8}{128}\Big),\\
\mathcal{Z}_{\mathsf{L-T}} &= 9(e^{12\mathrm{K}})\Big(1+466e^{-18\mathrm{K}}+2664e^{-\frac{33\mathrm{K}}{2}}\\
&+ 7668e^{-15\mathrm{K}}+12344e^{-\frac{27\mathrm{K}}{2}}+14148e^{-12\mathrm{K}}\\
&+ 11232e^{-\frac{21\mathrm{K}}{2}}+6720e^{-9\mathrm{K}}+2592e^{-\frac{15\mathrm{K}}{2}}\\
&+ 1026e^{-6\mathrm{K}}+152e^{-\frac{9\mathrm{K}}{2}}+36e^{-3\mathrm{K}}\Big).
\end{aligned}$$

(e) $\mathbf{4\times 2}, \boldsymbol{E=16}$:

(i) $\underline{\mathsf{d}_Q = 2}$:

$$
\begin{aligned}
\mathcal{Z}_{\mathsf{H-T}} &= (2\cosh\beta)^{16}\Big(1+T^{16}+14T^{8}\Big),\\
\mathcal{Z}_{\mathsf{L-T}} &= 16(e^{16\mathrm{K}})\Big(1+e^{-32\mathrm{K}}+8e^{-28\mathrm{K}}+252e^{-24\mathrm{K}}\\
&+ 952e^{-20\mathrm{K}}+1670e^{-16\mathrm{K}}+952e^{-12\mathrm{K}}\\
&+ 252e^{-8\mathrm{K}}+8e^{-4\mathrm{K}}\Big).
\end{aligned}
$$

(f) $\mathbf{3\times 3, E=18}$:

(i) $\underline{\mathsf{d}_Q=2}$:

$$
\begin{aligned}
\mathcal{Z}_{\mathsf{H-T}} &= (2\cosh\beta)^{18}\Big(1+T^{18}+6T^{12}+9T^{10}\\
&+ 32T^{9}+9T^{8}+6T^{6}\Big),\\
\mathcal{Z}_{\mathsf{L-T}} &= 64(e^{18\mathrm{K}})\Big(1+9e^{-32\mathrm{K}}+72e^{-28\mathrm{K}}+636e^{-24\mathrm{K}}\\
&+ 1296e^{-20\mathrm{K}}+1422e^{-16\mathrm{K}}+552e^{-12\mathrm{K}}\\
&+ 108e^{-8\mathrm{K}}\Big).
\end{aligned}
$$

(II) $\boldsymbol{g=2}$

(a) $\mathbf{2\times 1+2\times 1, E=8}$:

(i) $\underline{\mathsf{d}_Q=2}$:

$$
\begin{aligned}
\mathcal{Z}_{\mathsf{H-T}} &= 2^{8}(\cosh\beta)^{6}\Big(1+T^{6}+T^{4}+T^{2}\Big),\\
\mathcal{Z}_{\mathsf{L-T}} &= 16(e^{6\mathrm{K}})\Big(1+e^{-12\mathrm{K}}+7e^{-8\mathrm{K}}+7e^{-4\mathrm{K}}\Big).
\end{aligned}
$$

(ii) $\underline{\mathsf{d}_Q = 3}$:

$$\begin{aligned}
\mathcal{Z}_{\mathsf{H-T}} &= 3^8(\cosh\beta)^6\Big(1+\frac{T^6}{32}\Big),\\
\mathcal{Z}_{\mathsf{L-T}} &= 27(e^{6\mathrm{K}})\Big(1+22e^{-9\mathrm{K}}+60e^{-\frac{15\mathrm{K}}{2}}\\
&+ 90e^{-6\mathrm{K}}+40e^{-\frac{9\mathrm{K}}{2}}+30e^{-3\mathrm{K}}\Big).
\end{aligned}$$

(iii) $\underline{\mathsf{d}_Q = 4}$:

$$\begin{aligned}
\mathcal{Z}_{\mathsf{H-T}} &= 4^8(\cosh\beta)^6\Big(1+\frac{T^6}{16}\Big),\\
\mathcal{Z}_{\mathsf{L-T}} &= 256(e^{6\mathrm{K}})\Big(1+e^{-12\mathrm{K}}+4e^{-10\mathrm{K}}+71e^{-8\mathrm{K}}\\
&+ 104e^{-6\mathrm{K}}+71e^{-4\mathrm{K}}+4e^{-2\mathrm{K}}\Big).
\end{aligned}$$

(b) $\mathbf{3\times 1+3\times 1(b_1=1), E=12}$:

(i) $\underline{\mathsf{d}_Q = 2}$:

$$\begin{aligned}
\mathcal{Z}_{\mathsf{H-T}} &= 2^{12}(\cosh\beta)^{10}\Big(1+T^{10}+T^6+T^4\Big),\\
\mathcal{Z}_{\mathsf{L-T}} &= 16(e^{10\mathrm{K}})\Big(1+e^{-20\mathrm{K}}+21e^{-16\mathrm{K}}\\
&+ 106e^{-12\mathrm{K}}+106e^{-8\mathrm{K}}+21e^{-4\mathrm{K}}\Big).
\end{aligned}$$

(ii) $\underline{\mathsf{d}_Q = 3}$:

$$
\begin{aligned}
\mathcal{Z}_{\mathsf{H-T}} &= 3^{12}(\cosh\beta)^{10}\Big(1+\frac{T^{10}}{512}+\frac{T^7}{32}+\frac{T^6}{32}\Big),\\
\mathcal{Z}_{\mathsf{L-T}} &= 81(e^{10\mathrm{K}})\Big(1+114e^{-15\mathrm{K}}+572e^{-\frac{27\mathrm{K}}{2}}+1266e^{-12\mathrm{K}}\\
&+ 1716e^{-\frac{21\mathrm{K}}{2}}+1530e^{-9\mathrm{K}}+816e^{-\frac{15\mathrm{K}}{2}}\\
&+ 438e^{-6\mathrm{K}}+84e^{-\frac{9\mathrm{K}}{2}}+24e^{-3\mathrm{K}}\Big).
\end{aligned}
$$

(c) $\mathbf{3\times 1+3\times 1(b_1=2), E=12}$:

(i) $\underline{\mathsf{d}_Q=2}$:

$$
\begin{aligned}
\mathcal{Z}_{\mathsf{H-T}} &= 2^{12}(\cosh\beta)^{10}\Big(1+T^{10}+T^6+4T^5+T^4\Big),\\
\mathcal{Z}_{\mathsf{L-T}} &= 32(e^{10\mathrm{K}})\Big(1+13e^{-16\mathrm{K}}+48e^{-12\mathrm{K}}+58e^{-8\mathrm{K}}\\
&+ 8e^{-4\mathrm{K}}\Big).
\end{aligned}
$$

(ii) $\underline{\mathsf{d}_Q=3}$:

$$
\begin{aligned}
\mathcal{Z}_{\mathsf{H-T}} &= 3^{12}(\cosh\beta)^{10}\Big(1+\frac{T^{10}}{512}+\frac{T^7}{32}+\frac{T^6}{32}\Big),\\
\mathcal{Z}_{\mathsf{L-T}} &= 81(e^{10\mathrm{K}})\Big(1+114e^{-15\mathrm{K}}+572e^{-\frac{27\mathrm{K}}{2}}+1266e^{-12\mathrm{K}}\\
&+ 1716e^{-\frac{21\mathrm{K}}{2}}+1530e^{-9\mathrm{K}}+816e^{-\frac{15\mathrm{K}}{2}}+438e^{-6\mathrm{K}}\\
&+ 84e^{-\frac{9\mathrm{K}}{2}}+24e^{-3\mathrm{K}}\Big).
\end{aligned}
$$

(d) $\mathbf{2\times 2+2\times 1, E=12}$:

(i) $\underline{\mathsf{d}_Q=2}$:

$$
\begin{aligned}
\mathcal{Z}_{\mathsf{H-T}} &= 2^{12}(\cosh\beta)^{10}\Big(1+T^{10}+3T^{6}+3T^{4}\Big),\\
\mathcal{Z}_{\mathsf{L-T}} &= 32(e^{10\mathrm{K}})\Big(1+e^{-20\mathrm{K}}+9e^{-16\mathrm{K}}+54e^{-12\mathrm{K}}\\
&+ 54e^{-8\mathrm{K}}+9e^{-4\mathrm{K}}\Big).
\end{aligned}
$$

(ii) $\underline{\mathsf{d}_Q = 3}$:

$$
\begin{aligned}
\mathcal{Z}_{\mathsf{H-T}} &= 3^{12}(\cosh\beta)^{10}\Big(1+\frac{T^{10}}{512}\Big),\\
\mathcal{Z}_{\mathsf{L-T}} &= 27(e^{10\mathrm{K}})\Big(1+342e^{-15\mathrm{K}}+1700e^{-\frac{27\mathrm{K}}{2}}\\
&+ 3870e^{-12\mathrm{K}}+5040e^{-\frac{21\mathrm{K}}{2}}+4620e^{-9\mathrm{K}}\\
&+ 2520e^{-\frac{15\mathrm{K}}{2}}+1260e^{-6\mathrm{K}}+240e^{-\frac{9\mathrm{K}}{2}}+90e^{-3\mathrm{K}}\Big).
\end{aligned}
$$

(III) $\boldsymbol{g = 3}$:

(a) $\boldsymbol{2\times 1+2\times 1+2\times 1, E = 12}$:

(i) $\underline{\mathsf{d}_Q = 2}$:

$$
\begin{aligned}
\mathcal{Z}_{\mathsf{H-T}} &= 2^{12}(\cosh\beta)^{8}\Big(1+T^{8}+T^{6}+T^{2}\Big),\\
\mathcal{Z}_{\mathsf{L-T}} &= 64(e^{8\mathrm{K}})\Big(1+e^{-16\mathrm{K}}+16e^{-12\mathrm{K}}\\
&+ 30e^{-8\mathrm{K}}+16e^{-4\mathrm{K}}\Big).
\end{aligned}
$$

(ii) $\underline{\mathsf{d}_Q = 3}$:

$$\begin{aligned}
\mathcal{Z}_{\mathsf{H-T}} &= 3^{12}(\cosh\beta)^8\Big(1+\frac{T^8}{128}\Big), \\
\mathcal{Z}_{\mathsf{L-T}} &= 243(e^{8\mathrm{K}})\Big(1+86e^{-12\mathrm{K}}+336e^{-\frac{21\mathrm{K}}{2}}+616e^{-9\mathrm{K}} \\
&+ 560e^{-\frac{15\mathrm{K}}{2}}+420e^{-6\mathrm{K}}+112e^{-\frac{9\mathrm{K}}{2}}+56e^{-3\mathrm{K}}\Big).
\end{aligned}$$

Table 2.3: Computed ground state degeneracy ($n_{\mathsf{g.s.}}$) for square lattices with $g > 1$. The g denotes "genus" (see text).

g	E	$n_{\mathsf{g.s.}}$	Type	a_1	b_1	a_2	b_2	a_3	b_3	a_4	b_4	a_5
2	8	4^g	2 I	2×1	1	2×1						
	10	4^g	2 I	3×1	1	2×1						
	12	4^g	2 I	3×1	1	3×1						
	16	4^g	2 I	3×2	1	2×1						
	18	4^g	2 I	3×2	1	3×1						
	24	4^g	2 I	3×2	1	3×2						
	24	4^g	2 I	5×2	1	2×1						
	12	$4^g \times 2$	2 I	3×1	2	3×1						
	12	$4^g \times 2$	II+I	2×2	1	2×1						
	14	$4^g \times 2$	II+I	2×2	1	3×1						
	20	$4^g \times 2$	I+II	3×2	1	2×2						
	20	$4^g \times 2$	II+I	4×2	1	2×1						
	22	$4^g \times 2$	II+I	4×2	1	3×1						
	24	$4^g \times 2$	2 I	3×2	2	3×2						
	24	$4^g \times 2$	II+I	3×3	2	3×1						
	16	$4^g \times 2^3$	2 II	2×2	1	2×2						
	24	$4^g \times 2^3$	II+I	3×3	1	3×1						
	24	$4^g \times 2^3$	2 II	4×2	1	2×2						
3	12	4^g	3 I	2×1	1	2×1	1	2×1				
	14	4^g	3 I	3×1	1	2×1	1	2×1				
	16	4^g	3 I	3×1	1	3×1	1	2×1				
	16	4^g	3 I	3×1	2	3×1	1	2×1				
	18	4^g	3 I	3×1	1	3×1	1	3×1				
	18	4^g	3 I	3×1	2	3×1	1	3×1				
	18	4^g	3 I	3×1	1	3×1	2	3×1				
	18	4^g	3 I	3×1	2	3×1	2	3×1				
	20	4^g	3 I	3×2	1	2×1	1	2×1				
	24	4^g	3 I	3×2	1	3×1	1	3×1				
	24	4^g	3 I	3×2	2	3×1	2	3×1				
	16	$4^g \times 2$	2 I+II	2×1	1	2×1	1	2×2				
	18	$4^g \times 2$	2 I+II	3×1	1	2×1	1	2×2				
	20	$4^g \times 2$	2 I+II	3×1	1	3×1	1	2×2				
	20	$4^g \times 2^2$	2 II+I	2×2	1	2×2	1	2×1				
	22	$4^g \times 2^2$	2 II+I	2×2	1	2×2	1	3×1				
	24	$4^g \times 2^4$	3 II	2×2	1	2×2	1	2×2				
4	16	4^g	4 I	2×1	1	2×1	1	2×1	1	2×1		
	18	4^g	4 I	2×1	1	2×1	1	2×1	1	3×1		
	24	4^g	4 I	3×2	1	2×1	1	2×1	1	2×1		
	20	$4^g \times 2$	II+3 I	2×2	1	2×1	1	2×1	1	2×1		
5	20	4^g	5 I	2×1	1	2×1	1	2×1	1	2×1	1	2×1
	24	$4^g \times 2$	II + 4 I	2×2	1	2×1	1	2×1	1	2×1	1	2×1

Table 2.4: Computed ground state degeneracy ($n_{\mathsf{g.s.}}$) of defective square lattices. The g denotes "genus". By "2$\star$" we mean there are 2 defects of type "$\star$" (see text).

g	E	$n_{\mathsf{g.s.}}$	Type	a_1	b_1	a_2	b_2	a_3	b_3	a_4
1	11	4^g	I	3×2 $\star$						
	15	4^g	II	4×2 $\star$						
	19	4^g	I	5×2 $\star$						
	23	4^g	I	6×2 $\star$						
	23	4^g	I	4×3 $\star$						
	16	$4^g \times 2$	II	3×3 2$\star$						
	17	$4^g \times 2$	II	3×3 $\star$						
	19	$4^g \times 2$	I	5×2 $\star\star$						
	22	$4^g \times 2$	I	6×2 2$\star$						
2	15	4^g	2 I	3×2 $\star$	1	2×1				
	17	4^g	2 I	3×2 $\star$	1	3×1				
	21	4^g	2 I	4×2 $\star$	1	3×1				
	22	4^g	2 I	3×2 $\star$	1	3×2 $\star$				
	23	4^g	2 I	3×2 $\star$	1	3×2				
	23	4^g	2 II	4×2 $\star$	1	2×2				
	23	4^g	II+I	3×3 $\star$	2	3×1				
	23	4^g	2 I	5×2 $\star$	1	2×1				
	23	$4^g \times 2$	II+I	3×3 $\star$	1	3×1				
3	19	4^g	3 I	3×2 $\star$	1	2×1	1	2×1		
	23	4^g	3 I	3×2 $\star$	1	3×1	1	3×1		
	23	4^g	3 I	3×2 $\star$	2	3×1	2	3×1		
4	23	4^g	4 I	3×2 $\star$	1	2×1	1	2×1	1	2×1

Table 2.5: Computed departure from the minimal ground state degeneracy, $\mathsf{N}^0_{\mathsf{M}} = D^0_{\mathsf{M}}/n^{\mathsf{min}}_{\mathsf{g.s.}}$, where D^0_{M} denotes the ground state degeneracy for $\mathsf{d}_Q = \mathsf{M}$, and $n^{\mathsf{min}}_{\mathsf{g.s.}}$ is equal to d_Q^{2g-1} ($2\mathsf{d}_Q^{2g-1}$) for odd (even) d_Q.

g	E	Type	a_1	b_1	a_2	b_2	a_3	b_3	a_4	N^0_3	N^0_4	N^0_5	N^0_6	N^0_7	N^0_8	N^0_9	N^0_{10}	N^0_{11}	N^0_{12}	N^0_{13}	N^0_{14}
1	4	I	2×1							1	2	1	1	1	2	1	1	1	2	1	1
	6	I	3×1							3	1	1	3	1	1	3	1	1	3	1	1
	8	I	4×1							1	2	1	1	1	4	1	1	1	2	1	1
	8	II	2×2							3^2	4^2	5^2	6^2	7^2	8^2	9^2	10^2	11^2	12^2	13^2	14^2
	12	I	3×2							3	2	1									
	16	II	4×2							3^2	2×4^2										
	18	II	3×3							3^4											
2	8	2 I	2×1	1	2×1					1	2	1	1	1	2	1	1	1	2	1	1
	12	2 I	3×1	1	3×1					3	1	1									
	12	2 I	3×1	2	3×1					3	2	1									
	12	II+I	2×2	1	2×1					1	4	1									
	16	2 II	2×2	1	2×2					3^2	2×4^2										
	18	2 I	3×2	1	3×1					3											
3	12	3 I	2×1	1	2×1	1	2×1			1	2	1									
	16	3 I	3×1	1	3×1	1	2×1			1	1										
	16	2 I+II	2×1	1	2×1	1	2×2			1	4										
	18	2 I+II	3×1	1	2×1	1	2×2			1											
4	16	4 I	2×1	1	2×1	1	2×1	1	2×1	1	2										
	18	4 I	2×1	1	2×1	1	2×1	1	3×1	1											

References

[1] X.-G. Wen *Quantum Field Theory of Many-Body Systems* (Oxford University Press, Oxford, 2004).

[2] For an explicit statement of the perceptive lore, see, e.g., page 8 of [1] for a remark concerning the quite deep standard manifestation of these degeneracies in the rich quantum arena: "The existence of topologically-degenerate ground states proves the existence of topological order. Topological degeneracy can also be used to perform fault-tolerant quantum computations (Kitaev, 2003)."

[3] A. Yu. Kitaev, Ann. of Phys. **303**, 2 (2003); arXiv:quant-ph/9707021 (1997).

[4] B. Terhal, Rev. Mod. Phys. **87**, 307 (2015).

[5] J. Haah, Phys. Rev. A **83**, 042330 (2011).

[6] J. Haah, Comm. Math. Phys. **324(2)**, 351 (2013).

[7] Specifically, on a cube of size $L \times L \times L$ endowed with periodic boundary conditions, the degeneracy of Haah's Code of [5, 6] is equal to $2^{\eta(L)}$ with η set by the degree (in t) of the polynomial that constitutes the greatest common divisor of the below three polynomials,

$$\frac{\eta+2}{4} = \deg \gcd\{1+(1+t)^L, 1+(1+\omega t)^L, \\ 1+(1+\omega^2 t)^L\}, \tag{2.71}$$

where $\omega = e^{i2\pi/3}$. This degeneracy varies between 4 and an exponential in L and can exhibit capricious jumps as the lattice size is varied. For instance, (i) when $L = 2^n$ (with n a natural number) the degeneracy is 2^{4L-2} while (ii) when $L = 2^n + 1$, the degeneracy is four [5, 6].

[8] R. Peierls, Proc. Cambridge Phil. Soc. **32**, 477 (1936); L. D. Landau and E. M. Lifshitz, Statistical Physics - Course of Theoretical Physics Vol 5 (Pergamon, London, 1958); J. Frolich, B. Simon, and T. Spencer, Commun. Math. Phys. **50**, 79 (1976); R. Peierls, Contemporary Physics **33**, 221 (1992).

[9] L. D. Landau, Zh. Eksp. Teor. Fiz. **7**, 19 (1937).

[10] J. Bardeen, L. N. Cooper, and J. R. Schrieffer, Physical Review **106**, 162 (1957).

[11] V. L. Ginzburg and L. D. Landau, Zh. Eksp. Teor. Fiz. **20**, 1064 (1950).

[12] F. Wegner, J. Math. Phys. **12**, 2259 (1971).

[13] S. Elitzur Phys. Rev. D **12**, 3978 (1975).

[14] J. M. Kosterlitz and D. J. Thouless, Journal of Physics C: Solid State Physics **6**, 1181 (1973); V. L. Berezinskii, Sov. Phys. JETP **32**, 493 (1971); V. L. Berezinskii, Sov. Phys. JETP **34**, 610 (1972).

[15] N. D. Mermin and H. Wagner, Phys. Rev. Lett. **17**, 1133 (1966).

[16] P. C. Hohenberg, Phys. Rev. **158**, 383 (1967).

[17] S. Coleman, Commun. Math. Phys. 31: 259 (1973).

[18] Z. Nussinov, arXiv:cond-mat/0105253 (2001).

[19] D. C. Tsui, H. L. Stormer, and A. C. Gossard, Phys. Rev. Lett. 48, 1559 (1982).

[20] R. B. Laughlin, Phys. Rev. Lett. 50, 1395 (1983).

[21] E. Fradkin, Field Theories of Condensed Matter Physics, second Edition, (Cambridge University Press, Cambridge, 2013).

[22] V. Kalmeyer and R. B. Laughlin, Phys. Rev. Lett. **59**, 2095 (1987); V. Kalmeyer and R. B. Laughlin, Phys. Rev. B **39**, 11879 (1989); X.-G. Wen, F. Wilczek, and A. Zee, Phys. Rev. B **39**, 11413 (1989); H. Yao and S. A. Kivelson, Phys. Rev. Lett. **99**, 247203 (2007); L. Messio, B. Bernu, and C. Lhuillier, Phys. Rev. Lett. **108**, 207204 (2012); Yin-Chen He, D. N. Sheng, and Yan Chen, Phys. Rev. Lett. **112**, 137202 (2014).

[23] A. Yu. Kitaev, Ann. of Phys. **321**, 2 (2006); arXiv:cond-mat/0506438 (2005).

[24] Z. Nussinov and J. van den Brink, Rev. Mod. Phys. **87**, 1 (2015); arXiv:1303.5922 (2013).

[25] M. A. Levin and X.-G. Wen, Phys. Rev. B **71**, 045110 (2005).

[26] X.-G. Wen and Q. Niu, Phys. Rev. B **41**, 9377 (1990).

[27] X.-G. Wen, Phys. Rev. B **40**, 7387 (1989).

[28] X.-G. Wen, Int. J. Mod. Phys. B **4**, 239 (1990).

[29] G. Ortiz, Z. Nussinov, J. Dukelsky, and A. Seidel, Phys. Rev. B **88**, 165303 (2013).

[30] Y. Aharonov and D. Bohm, Phys. Rev. **115**, 485 (1959).

[31] M. Oshikawa and T. Senthil, Phys. Rev. Lett. **96**, 060601 (2006).

[32] E. Sagi, Y. Oreg, A. Stern, and B. I. Halperin, Phys. Rev. B **91**, 245144 (2015).

[33] E. Cobanera and G. Ortiz, Phys. Rev. A **89**, 012328 (2014); Phys. Rev. A **91**, 059901 (2015).

[34] X.-G. Wen, Int. J. Mod. Phys. B **5**, 1641 (1991).

[35] Z. Nussinov and G. Ortiz, Ann. of Phys.(N.Y.) **324**, 977 (2009); arXiv:cond-mat/0702377 (2007).

[36] Z. Nussinov and G. Ortiz, Proceedings of the National Academy of Sciences, **106**, 16944 (2009); arXiv:cond-mat/0605316 (2006).

[37] Z. Nussinov and G. Ortiz, Phys. Rev. B **77**, 064302 (2008).

[38] S. Mandal, R. Shankar, and G. Baskaran, J. Phys. A: Math. Theor. **45**, 335304 (2012).

[39] S. A. Kivelson, D. S. Rokhsar, and J. P. Sethna, Phys. Rev. B 35, 8865 (1987); D. S. Rokhsar and S. A. Kivelson, Phys. Rev. Lett. 61, 2376 (1988); R. Moessner and K. S. Raman, arXiv:0809.3051 (2008); F. S. Nogueira and Z. Nussinov, Physical Review B **80**, 104413 (2009).

[40] M. Sato, Phys. Rev. D **77**, 045013 (2008).

[41] T. H. Hansson, V. Oganesyan, and S. L. Sondhi, Annals of Physics **313**, 497 (2004).

[42] C. D. Batista and Z. Nussinov, Phys. Rev. B **72**, 045137 (2005).

[43] Z. Nussinov, G. Ortiz, and E. Cobanera, Annals of Physics **327**, 2491 (2012).

[44] D. Arovas, J. R. Schrieffer, and F. Wilczek, Phys. Rev. Lett. **53**, 722 (1984).

[45] S. B. Bravyi and A. Yu. Kitaev, arXiv:quant-ph/9811052 (1998).

[46] N. Read and S. Sachdev, Phys. Rev. Lett. **66**, 1773 (1991).

[47] R. Moessner and S. L. Sondhi, Phys. Rev. Lett. **86**, 1881 (2001).

[48] G. Misguich, D. Serban, and V. Pasquier, Phys. Rev. Lett. **89**, 137202 (2002).

[49] L. Balents, M. P. A. Fisher, and S. M. Girvin, Phys. Rev. B **65**, 224412 (2002).

[50] O. I. Motrunich and T. Senthil, Phys. Rev. Lett. **89**, 277004 (2002).

[51] O. I. Motrunich, Phys. Rev. B **67**, 115108 (2003).

[52] M. Freedman, C. Nayak, K. Shtengel, K. Walker, and Z. Wang, Ann. Phys. (N.Y.) **310**, 428 (2004).

[53] C. Nayak, S. H. Simon, A. Stern, M. Freedman, and S. D. Sarma, Rev. Mod. Phys. **80**, 1083 (2008).

[54] J. Alicea, Reports on Progress in Physics **75**, 076501 (2012).

[55] X.-G. Wen, Int. J. Mod. Phys. B **6**, 1711 (1992).

[56] B. I. Halperin, Phys. Rev. B **25**, 2185 (1982).

[57] A. Kitaev and J. Preskill, Phys. Rev. Lett. **96**, 110404 (2006); M. Levin and X. -G. Wen, Phys. Rev. Letts. **96**, 110405 (2006).

[58] C. D. Batista and G. Ortiz, Adv. in Phys. **53**, 1 (2004).

[59] E. Cobanera, G. Ortiz, and Z. Nussinov, Phys. Rev. B **87**, 041105(R) (2013).

[60] Apart from the models that we will introduce in the current chapter, holographic degeneracies also appear in short range Ising, $O(n)$, non-Abelian gauge background, tiling [18, 43, 61–63], and other models. Indeed, holographic entropies have also been reported on fractal structures realized on lattices [64, 65].

[61] Z. Nussinov, Phys. Rev. B **69**, 014208 (2004).

[62] M. Sadrzadeh and A. Langari, Europhysics Journal B **88**, 259 (2015).

[63] I. Klich, S. -H. Lee, and K. Iida Nature Communications **5**, 3497 (2014).

[64] M. E. J. Newman and C. Moore, Phys. Rev. E **60**, 5068 (1999).

[65] B. Yoshida, Phys. Rev. B **88**, 125122 (2013); Ann. of Phys. **338**, 134 (2013).

[66] E. Cobanera, G. Ortiz, and Z. Nussinov, Phys. Rev. Lett. **104**, 020402 (2010); E. Cobanera, G. Ortiz, and Z. Nussinov, Adv. in Phys. **60**, 679 (2011); Z. Nussinov and G. Ortiz, Europhysics Letters **84**, 36005 (2008); Z. Nussinov and G. Ortiz, Phys. Rev. B **79**, 214440 (2009); G. Ortiz, E. Cobanera, and Z. Nussinov, Nuclear Physics B **854**, 780 (2011).

[67] R. Costa-Santos and B. M. McCoy, Nuclear Phys. B **623(3)**, 439 (2002).

[68] In any particular fixed gauge, the degeneracy is 4^g (see, e.g., Eq. (187) of [35] for a derivation). The factor of $2^{\mathsf{N}_{\mathsf{site}}-1}$ is the number of independent gauge fixes as can be seen as follows. The operators $A^{\mu=x}$ of Eq. (2.7) connect one gauge fix to another. There are $\mathsf{N}_{\mathsf{site}}$ such operators, and they are not independent of each other. Specifically, the local gauge symmetry operators $A^{\mu=x}$ adhere to the single global constraint of Eq. (2.12).

[69] A, Mishra, M, Ma, F.-C. Zhang, S. Guertler, L.-H. Tang, and S. Wan. Phys. Rev. Lett. **93**, 207201 (2004).

[70] Cenke Xu and J. E. Moore, Nucl. Phys. B **716**, 487 (2005).

[71] C. Xu and J. E. Moore, Phys. Rev. Lett. **93**, 047003 (2004).

[72] A. Pakman and A. Parnachev, JHEP **0807**, 097 (2008).

[73] S. Ryu and T. Takayanagi, Phys. Rev. Lett. **96**, 181602 (2006).

[74] L. McGough and H. Verlinde, JHEP **1311**, 208 (2013).

Chapter 3

Why Are All Dualities Conformal? Theory and Practical Consequences

This chapter contains the materials published in a paper [2].

3.1 Introduction

The utility of weak- and strong-coupling expansions and of dualities in nearly all branches of physics can hardly be overestimated. This chapter is devoted to several inter-related fundamental questions. Mainly:

(1) What information does the existence of finite order complementary weak- and strong-coupling series expansion of given physical quantities (e.g., partition functions, matrix elements, etc.) provide?

(2) To what extent can dualities be employed to *partially solve* those various problems? By *partial solvability*, we mean the ability to compute a specific physical quantity with complexity polynomial in the size of the system, given partial information that is determined by

[2] Z. Nussinov, G. Ortiz, and M-S. Vaezi, Nuclear Physics B **892**, 132 (2015).

other means.

As we will demonstrate in this chapter, a universal problem deeply binds to the above two inquiries, and raises the critical question

(3) Why do numerous dualities in very different fields always turn out to be *conformal transformations*?

To set the stage, we briefly recall general notions concerning dualities. Consider a theory of (dimensionless) coupling strength g for which weak- and strong-coupling expansions may, respectively, be performed in powers of g and $1/g$ or in other monotonically increasing/decreasing functions $f_+(g)/f_-(g)$. Common wisdom asserts that as ordinary expansion parameters (e.g., g and $1/g$) behave very differently, weak- and strong-coupling series cannot, generally, be simply compared. On a deeper level, if these expansions describe different phases (as they generally do) then the series must become non-analytic (in the thermodynamic limit) at finite values of g (where transitions occur) and thus render any equality between them void. A duality may offer insightful *information* on a strong coupling theory by relating it to a system at weak coupling that may be perturbatively examined. As is well known, when they are present, self-dualities are manifest as an equivalence of the coefficients in the two different series; this leads to an invariance under an inversion that is qualitatively (and in standard field theories, e.g., QED/Electroweak/QCD is exactly) of the canonical form "$g \leftrightarrow 1/g$" (or, more generally, $f_+(g) \leftrightarrow f_-(g)$). For example, in vacuum QED with Lagrangian density $\mathcal{L} = [\epsilon_0 \vec{E}^2/2 - \vec{B}^2/(2\mu_0)]$, the ratio $g = \epsilon_0\mu_0$ of the couplings in front of the $\vec{E}^2$ and $\vec{B}^2$ terms relates to a $g \leftrightarrow 1/g$ reciprocity. This reciprocity is evident from the invariance of Maxwell's equations in vacuum under the exchange of electric and magnetic fields [1], $\vec{E} \to \vec{B}$; $\vec{B} \to -\vec{E}$ and the Lagrangian density that results. In Yang-Mills (YM) theories, such an exchange between dual fields has led to profound insights from analogies between the Meissner effect and the behavior of vortices in superconductors to confinement

and flux tubes – a hallmark of QCD [2–5]. Abstractions of dualities in electromagnetism and in YM theories produced powerful tools such as those in Hodge and Donaldson theories [6].

In both classical and quantum models, dualities (and the $f_+(g) \leftrightarrow f_-(g)$ inversion) are generated by *linear transformations* (appearing, e.g., as unitary transformations or more general isometries relating one local theory to another in fundamental "bond-algebraic" [7–13] incarnations or, in the standard case, Fourier transformations [14–18]). Such linear transformations lead to an *effective* inversion of the coupling constant g. Dual models share, for instance, their partition functions (and thus the same series expansion). As realized by Kramers and Wannier (KW) [19–25], self-dualities provide structure that enables additional information allowing, for instance, the exact computation of phase transition points. This does not imply that the full partition function is determined with complexity polynomial in the size of the system, that is, it is *solvable* via self-dualities *alone* (and indeed as we illustrate in this chapter, self-dualities do not suffice).

Now here is a main point – that concerning question (3) – which we wish to highlight in this chapter. In diverse arenas, the weak- and strong-coupling expansion parameters $f_+(g)$ and $f_-(g)$ *are related to one another via conformal transformations* that are of the fractional linear type. Amongst many others, prevalent examples are afforded by $SL(2,\mathbb{Z})$ dualities in YM theories as well as those in Ising models and Ising lattice gauge theories. In all of these examples, the transformations linking $z \equiv f_+(g)$ to $w \equiv f_-(g) \equiv F(z)$ are particular special cases of conformal (or fractional linear (Möbius)) transformations. That is, in these,

$$z \to F(z) = w = \frac{az+b}{cz+d}, \tag{3.1}$$

with a, b, c, and d complex coefficients, and determinant

$$\Delta = \det \begin{pmatrix} a & b \\ c & d \end{pmatrix} = ad - bc \neq 0. \tag{3.2}$$

A well known mathematical property of fractional linear maps is their composition property: Given any two fractional linear functions $F_k = (a_k z + b_k)/(c_k z + d_k)$ (with $k = 1, 2$), direct substitution demonstrates that $F_1(F_2(z)) = (a'z + b')/(c'z + d')$ (i.e., yet another fractional linear transformation) where

$$\begin{pmatrix} a' & b' \\ c' & d' \end{pmatrix} = \begin{pmatrix} a_1 & b_1 \\ c_1 & d_1 \end{pmatrix} \cdot \begin{pmatrix} a_2 & b_2 \\ c_2 & d_2 \end{pmatrix}. \tag{3.3}$$

This group multiplication property will be of great utility in our analysis of dualities. Fractional linear maps, as is commonly known by virtue of the trivial equality (valid when $c \neq 0$)

$$F(z) = \frac{az + b}{cz + d} = \frac{a}{c} - \frac{\Delta}{c(cz + d)}, \tag{3.4}$$

which may be expressed as compositions of transformations of the (formal) forms: translation ($z \to z + b$), scaling/rotation ($z \to az$), and inversion ($z \to 1/z$). As each of these individual operations generally map circles and lines onto themselves so do the general transformations of Eq. (3.4). This may be understood as a consequence of a projective transformation from the Riemann sphere onto the complex plane. Relating Lorentz transformations to Möbius transformations is one of the principal ideas underlying twistor theory [26]. Envisioning *standard dualities* [27] as particular induced maps on the Euclidean S^2 sphere will be an outcome of the current work.

The set of all conformal self-mappings of the upper half complex plane forms a group, with $SL(2,\mathbb{Z})$ a subgroup ("full modular group") that consists of all the fractional linear transformations with a, b, c, and d integers, and determinant $\Delta = 1$. In the aforementioned YM theories, e.g., [1, 28], an $SL(2,\mathbb{Z})$ structure follows from a canonical invariance of the form $z \to (z+1)$ (stemming from charge quantization). As we will detail in the current chapter, in Ising models and Ising gauge theories, a canonical form of the duality is given by

$$\begin{pmatrix} a & b \\ c & d \end{pmatrix} = \begin{pmatrix} -1 & 1 \\ 1 & 1 \end{pmatrix}, \quad \Delta = -2. \tag{3.5}$$

The transformation of Eq. (3.5) may trivially be associated to one with $\Delta = 1$ [29] by a uniform scaling $(a, b, c, d) = (-1, 1, 1, 1) \to 2^{-1/2}\mathrm{i}(-1, 1, 1, 1)$ which does not change the ratio in Eq. (3.1). More widely, any fractional linear transformation of the form of Eq. (3.1) with a finite determinant may similarly be related to one with $\Delta = 1$ by a uniform scaling of all four elements of the matrix. In general, we are interested in duality mappings as applied to matrix elements, partition functions or path integrals, while the typical scenario in YM theories focuses on mappings of the action (or Hamiltonian).

In what will follow, we will first address question (3) and illustrate that disparate duality transformations must be of the form of Eq. (3.1). When applied to the expansion parameters, we will then demonstrate that these *fractional linear maps lead to linear constraints between the strong- and weak-coupling series coefficients*. A main message of this chapter is that these conformal transformations of Eq. (3.1), leading to linear relations among series coefficients, will allow a broad investigation of questions (1) and (2) above. Specifically, we will examine arbitrarily large yet *finite size* systems for which *no* phase transitions appear. As is well known, *analyticity enables a full determination of functions* over entire domains given their

values in only a far more restricted regime (even if only of vanishing measure). For a finite size system, the weak-coupling (W-C) and strong-coupling (S-C) expansions describe the same analytic function and are everywhere convergent and may thus be equated to one another. Thus, a trivial yet practical consequence is, contrary to some lore, that *the naturally perturbative* W-C *and the seemingly more involved* S-C *expansions are equally hard*. We will apply this approach to the largest Ising model systems for which the exact expansions are known to data on both finite size cubic and square lattices. We further test other aspects of our methods on Ising and generalized Wegner models. The substitution of Eq. (3.1) relates the W-C and S-C expansion parameters in general dual models. We will more generally: (1') Equate the W-C and S-C expansions to find *linear constraints* on the expansion coefficients, and (2') When possible, invoke self-duality to obtain yet further linear equations that those coefficients need to satisfy. This analysis will lead to the concept of *partial solvability*: The linear equations that we will obtain will enable us to *localize NP hardness* of finding the exact partition function coefficients (or other quantities) to that of evaluating only a fraction of these coefficients. The remainder of these coefficients can be then trivially found by the linear relations that are derived from the duality of Eq. (3.1).

A highly non-trivial consequence of our work is that of *relating mathematical identities to dualities* such as those broadly generated by Eq. (3.1). Specifically, as a concrete example in this chapter, we will illustrate how the relations that we obtain connecting the W-C and S-C expansions lead to *new combinatorial geometry equalities* in general dimensions. As a particular example we will do this by noting that, in Ising and generalized Wegner models, the expansion coefficients are equal to the number of geometrical shapes of a given magnitude of the d-dimensional surface areas. The equality between the W-C and S-C expansions then lead to identities connecting these numbers.

3.2 General constraints on duality transformations

For the Ising, Ising gauge, and several other theories that we study in this chapter, the mapping between the W-C and S-C coupling expansion parameters is afforded by the particular Möbius transformation

$$F(z) = \frac{1-z}{1+z} \tag{3.6}$$

associated with Eq. (3.5). This transformation trivially satisfies Babbage's equation

$$F(F(z)) = z \tag{3.7}$$

for all z. For self-dual models, such as the $D = 2$ Ising model or $D = 4$ Ising gauge theories, we can easily find the critical (self-dual) point, z^*, by solving the equation $F(z^*) = z^*$. We will term theories obeying Eq. (3.7) as those that exhibit a "one-" duality. In general, one may find such transformations, represented by a function $F(z)$, in terms of some parameter z (a coupling constant which can be complex-valued). Richer transformations appear in diverse arenas including Renormalization Group (RG) calculations. Based on these considerations we may have

$$\begin{cases} F(z^*) = z^*, & \text{Self-dual fixed point} \\ F(F(z)) = z, & \text{Self-duality/duality} \\ F(\cdots F(F(z^*))\cdots) = z^*, & \text{RG fixed points.} \end{cases} \tag{3.8}$$

More general transformations $F_1(F_2(\cdots F_n(z)\cdots))$ may yield linear equations in a manner identical to those appearing for the Ising theories studied in the current chapter. Expansion parameters z in self-dual theories satisfy $F(F(z)) = z$; this yields a *constraint on all possible self-dualities*. Solutions are afforded by fractional linear (conformal) maps

$$F(z) = \frac{az+b}{cz-a}, \tag{3.9}$$

with the determinant of Eq. (3.2) being non-zero, $a^2 + bc \neq 0$. As we will further expand on elsewhere, another related duality appearing in Ising and all Potts models is given by

$$F_1(z) = \frac{az+b}{cz+d}, \quad F_2(z) = \frac{-dz+b}{cz-a}, \tag{3.10}$$

with determinant $ad - bc \neq 0$ such that

$$F_1(F_2(z)) = z \tag{3.11}$$

is satisfied. In fact, as we will next establish in Section 3.3, all "two-" dualities satisfying Eq. (3.11) must be of the form of Eqs. (3.10). Specifically, all duality mappings that can be made meromorphic by a change of variables, *can only be of the fractional linear type*. This *uniqueness* may rationalize the appearance of fractional linear (dual) maps in disparate arenas ranging from statistical mechanics models, such as the ones that we study here, to S-dualities in, e.g., YM theories.

Thus far, we focused on "one-" and "two-dualities" for which the coupling constants satisfy either Eq. (3.7) or Eq. (3.11), respectively. Our calculations may be extended to "n-duality"

transformations for which

$$F_1(F_2(\cdots F_n(z)\cdots)) = z. \tag{3.12}$$

As the reader may verify, replicating the considerations invoked in the next section leads to the conclusion that if they are meromorphic each of the functions F_k (with $1 \leq k \leq n$) in Eq. (3.12) must be of the fractional linear (conformal) form

$$F_k(z) = \frac{a_k z + b_k}{c_k z + d_k}, \tag{3.13}$$

with a_k, b_k, c_k and d_k being constants.

In general, whether a function F solving Eq. (3.7) for all z is meromorphic in appropriate coordinates or not, it is impossible that any such function $F(z)$ obeying Eq. (3.7) will map the entire complex plane (or Riemann sphere) onto a subset $\mathcal{M}$ of the complex plane (or Riemann sphere). This subset $\mathcal{M}$ could be a disk or strip or any other subset of the complex plane. That is, it is impossible that a solution to Eq. (3.7) will be afforded by a function F which for all complex z, will map $z \to F(z) \in \mathcal{M}$. The proof of this latter assertion is trivial and will be performed by contradiction: Consider a point $z' \notin \mathcal{M}$, then a single application of F on z' leads to an image $F(z') \in \mathcal{M}$. As for all points z (including those that lie in $\mathcal{M}$) the image $F(z)$ is in $\mathcal{M}$, we have $F(F(z')) \in \mathcal{M}$. However, as stated in the beginning of our proof, $z' \notin \mathcal{M}$. This thus shows that $F(F(z')) \neq z'$. In other words, Eq. (3.7) cannot be satisfied by such a function. Thus, if we regard the map $z \to F(z)$ as a finite "time evolution" (or "flow" in the parlance of RG), the function $F(z)$ must "evolve" z as an "*incompressible fluid*" with area preserving dynamics in the complex plane (or Riemann sphere). This flow must be of period two in order to satisfy Eq. (3.7).

3.3 Meromorphic duality transformations must be conformal

Charles Babbage, "the father of the computer", [30] and others since, e.g, [31,32], have shown that the functional equation problem of Eq. (3.7) enjoys an infinite number of solutions. This observation can be summarized as follows: Given a particular solution f to Babbage's equation, $f(f(x)) = x$, a very general class of solutions can be written as

$$F(x) = \phi^{-1}(f(\phi(x))), \tag{3.14}$$

where ϕ is an *arbitrary* (or in a physics type nomenclature,"gauge like") function with a well defined inverse ϕ^{-1}. In other words, if we have a particular solution we can find other solutions using a function ϕ with and inverse defined in a specific domain. That is,

$$\begin{aligned} F(F(x)) &= \phi^{-1}(f(\phi(\phi^{-1}(f(\phi(x)))))) = \phi^{-1}(f(f(\phi(x)))) = \phi^{-1}(\phi(x)) \\ &= x. \end{aligned} \tag{3.15}$$

To make Babbage's observation clear, we note that if, as an example, we examine the Möbius transformation (Figure 3.1) of Eq. (3.6), $f(x) = (1-x)/(1+x)$, and consider $\phi(x) = x^2$ and a particular branch $\phi^{-1}(x) = \sqrt{x}$ for complex x (or the standard $\sqrt{x}$ function for real $x \geq 0$) then it is clearly seen that $F = \sqrt{(1-x^2)/(1+x^2)}$ is also a solution to the equation $F(F(x)) = x$. Similarly, if we choose $\phi(x) = e^{-2x}$ then $\phi^{-1}(f(\phi(x))) = -\frac{1}{2}\ln((1-e^{-2x})/(1+e^{-2x}))$ which the astute reader will recognize as the transformation of Eq. (3.49).

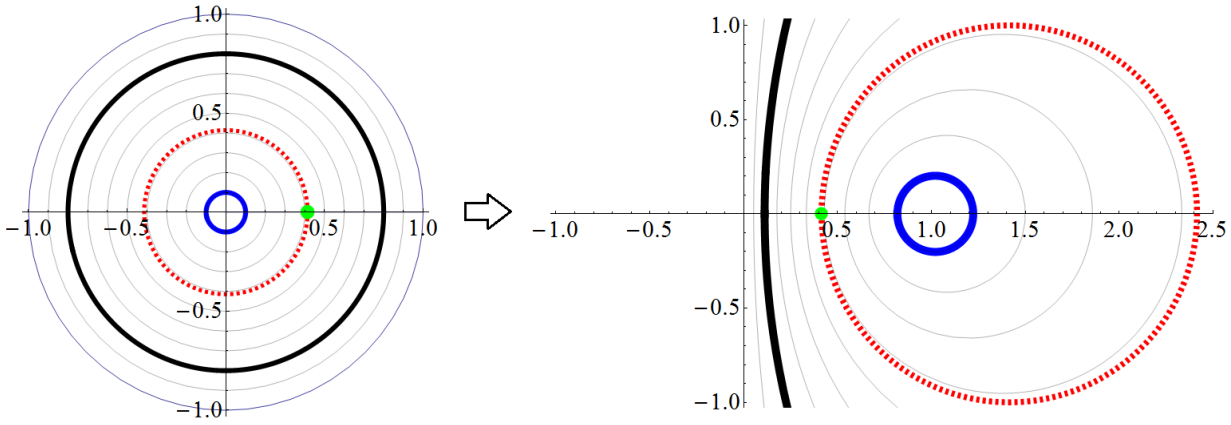

Figure 3.1: The Möbius transformation of Eq. (3.6) embodying the duality of the Ising model, with $|z| \leq 1$, as a conformal map in the complex plane that maps circles onto new shifted circles with a different radius (see Eq. (3.4)). Let us consider a circle of radius r with its center at the origin. Using the transformation above, it would be mapped to a new circle of radius $2r/(1-r^2)$ with its center shifted to the point $(1+r^2)/(1-r^2)$ (on the real axis). Three of such circles with different colors are shown in the figure above on the lefthand side. On the righthand side we see these three circles (with the same color as on the lefthand side) after transformation. The green dot represents the self-dual point ($z^* = \sqrt{2}-1$).

We now turn to a rather trivial yet as far as we are aware *new result* concerning this old equation that we establish here. We assert that if there exists a transformation ϕ that maps complex numbers z on the Riemann sphere, $z \to \phi(z)$, such that the resulting function F is meromorphic then *any such function F solving Eq. (3.7) must be of the fractional linear form (a particular conformal map)* of Eq. (3.9). Of course, a broad class of functions of the form of Eq. (3.14) may be generated by choosing arbitrary ϕ that have an inverse yet all possible rational functions will be of the fractional linear form. For instance, the function $F = \sqrt{(1-x^2)/(1+x^2)}$ discussed in the example above is, obviously, not of a fractional linear form.

Proof: The proof below is done by contradiction. A general meromorphic function on the Riemann sphere is a rational function, i.e.,

$$F(z) = \frac{P(z)}{Q(z)}, \tag{3.16}$$

with $P(z)$ and $Q(z)$ relatively prime polynomials. (If the polynomials P and Q are not relatively prime then we can obviously divide both by any common factors that they share to make them relatively prime in the ratio appearing in Eq. (3.16)). As a first step, we may find the solution(s) w to the equation

$$F(w) = z. \tag{3.17}$$

Unless both $P(w)$ and $Q(w)$ are linear in w, there generally will be (by the fundamental theorem of algebra) more than one solution to this equation (or, alternatively, a single solution may be multiply degenerate). That is, unless P and Q are both linear in w, the polynomial

$$W_z(w) = P(w) - zQ(w) \tag{3.18}$$

will be of order higher than one ($m > 1$) in w and will, for general z, have more than one different (non-degenerate) zero. When varying z over all possible complex values, it is impossible that the polynomial $W_z(w)$ will always have only degenerate zero(s) for the relatively prime $P(w)$ and $Q(w)$ (we prove this in the rather simple *(Multiplicity) Lemma* below).

We denote the general zeros of the polynomial $W_z(w)$ by $w_1, w_2, \cdots, w_m$. That is,

$$W_z(w_1) = W_z(w_2) = \cdots = W_z(w_m) = 0. \tag{3.19}$$

Now if $F(F(z)) = z$, then all solutions $\{z_{ji}\}$ to the equations $F(z_{ji}) = w_i$ (for which the polynomial (in z), $W_{w_i}(z) \equiv P(z) - w_i Q(z)$ vanishes) will, for all i, solve the equation

$$F(F(z_{ji})) = z. \tag{3.20}$$

In the last equation above, on the righthand side there is a single (arbitrary) complex number z whereas on the lefthand side there are *multiple* (see, again, the (Multiplicity) Lemma) viable different solutions z_{ji}. Thus, at least one of the solutions in this set $z_{ji} \neq z$. We denote one such solution by Z. Putting all of the pieces together, the equation $F(F(z)) = z$ cannot be satisfied for all complex z (in particular, it is not satisfied for $z = Z$). Thus, both $P(z)$ and $Q(z)$ must be linear in z, and the fractional linear form of Eq. (3.9) follows once it is restricted to this class.

Replicating the above steps *mutatis mutandis* for "two-dualities" satisfying Eq. (3.11) similarly leads to the conclusion that if the *transformations are meromorphic they must be given by ratios of linear functions (and thus conformal).* In this case, F_1 can be a general fractional linear transformation with a finite determinant and further constraints on F_2 are afforded by the requirement that Eq. (3.11) is indeed obeyed. The calculation then leads to the result of Eq. (3.10). We will elaborate on this restriction in Section 3.4.

(Multiplicity) Lemma:

We prove (by contradiction) that it is impossible for $W_z(w)$ (Eq. (3.18)) to have an m-th order ($m > 1$) degenerate root for all z. Assume, on the contrary, that

$$W_z(w) = A(z)(w - B(z))^m = P(w) - zQ(w), \tag{3.21}$$

with $A(z)$ and $B(z)$ functions of z, $m > 1$, and $P(w)$, $Q(w)$, relatively prime polynomials of w. At $z + \delta z$ (with infinitesimal δz), the degenerate root is given by

$$w = B(z + \delta z) \equiv B(z) + \delta B. \tag{3.22}$$

That is, by definition,

$$0 = W_{z+\delta z}(B(z) + \delta B). \tag{3.23}$$

We next use the Taylor expansion

$$0 \;\; = \;\; W_z(B(z)) + \delta B \; \frac{\partial W_z(w)}{\partial w}\Big|_{w=B(z),z} + \delta z \; \frac{\partial W_z(w)}{\partial z}\Big|_{w=B(z),z}. \tag{3.24}$$

Given the above form of $W_z(w)$, its partial derivative $\partial W_z/\partial w = 0$ at $w = B(z)$, for $m > 1$. Similarly, $W_z(w = B(z)) = 0$. Lastly, from Eq. (3.18)

$$\frac{\partial W_z(w)}{\partial z}\Big|_{w=B(z),z} = -Q(B(z)). \tag{3.25}$$

Putting all of the pieces together,

$$0 = -\delta z \; Q(B(z)). \tag{3.26}$$

Therefore, $w = B(z)$ is a root of $Q(w)$. As the root of $Q(w)$ is independent of z, this implies that the assumed multiply degenerate root (i.e., $B(z)$) of $W_z(w)$ is independent of z, i.e. $B(z) = B$. Recall (Eq. (3.18)) that $W_z(w) = P(w) - zQ(w)$. As $w = B$ is (for all z) a root of both $W_z(w)$ and $Q(w)$, it follows that $w = B$ is also a root of $P(w)$. It follows that both $P(w)$ and $Q(w)$ share a root (and a factor of $(w - B)$ when factorized to their zeros), e.g., when written as

$$P(w) = C\prod_a (w - p_a), \quad Q(w) = D\prod_b (w - q_b), \tag{3.27}$$

with C and D constants and with $\{p_a\}$ and $\{q_b\}$ the roots of $P(w)$ and $Q(w)$ respectively, at least one of the zeros ($\{p_a\}$) of $P(w)$ must be equal to one of the zeros ($\{q_b\}$) of $Q(w)$. Thus, $P(w)$ and $Q(w)$ are not relatively prime if $m > 1$. This, however, is a contradiction and therefore establishes our assertion and proves this Lemma.

3.4 Most general meromorphic n-dualities

Thus far, we largely focused on "two-"dualities satisfying Eq. (3.7). The ideas underlying our proof in Section 3.3 illustrated that all meromorphic dualities must be of the fractional linear form, Eq. (3.1). As elaborated, when applied to "two-"dualities satisfying Eq. (3.7), the most general meromorphic solution is that of Eq. (3.9). Similarly, more general dualities for which Eq. (3.11) is obeyed enjoy more solutions (such as those afforded by Eq. (3.10)).

We now explicitly solve the general case of Eq. (3.12). As proven, the fractional linear transformations, Eq. (3.13), are the only possible meromorphic solutions. We thus confine our attention to these. In what follows, we will invoke the composition property of Eq. (3.3).

On the right hand side of Eq. (3.12), the function z may be expressed in matrix form as

$$\begin{pmatrix} \gamma & 0 \\ 0 & \gamma \end{pmatrix}, \tag{3.28}$$

with γ an arbitrary complex number. This is so as the matrix elements ($a = \gamma,\ b = 0 = c,\ d = \gamma$) are such that, rather trivially, the associated fractional linear function of Eq. (3.1) is $(\gamma \cdot z + 0 \cdot 1)/(0 \cdot z + \gamma \cdot 1) = z$. If all functions F_k, in Eq. (3.12) are of the same form of Eq. (3.1), then when the representation of Eq. (3.28) is inserted we will trivially have

$$\begin{pmatrix} a & b \\ c & d \end{pmatrix}^n \equiv M^n = \begin{pmatrix} \gamma & 0 \\ 0 & \gamma \end{pmatrix}, \tag{3.29}$$

whose solutions are straightforward. When diagonalized by a unitary transformation, the matrix M must only have n-th roots of γ. Thus,

$$M = \gamma^{1/n} \mathcal{U}^\dagger \begin{pmatrix} e^{2\pi \mathsf{i} k_1/n} & 0 \\ 0 & e^{2\pi \mathsf{i} k_2/n} \end{pmatrix} \mathcal{U} \equiv \gamma^{1/n} \tilde{\mathsf{M}}, \tag{3.30}$$

with $k_{1,2}$ arbitrary integers and $\mathcal{U}$ any 2×2 unitary matrix. The latter may, of course, most generally be written as $\mathcal{U} = \exp[-\mathsf{i}\theta \vec{\sigma} \cdot \hat{n}/2]$ with $\vec{\sigma} = (\sigma^1, \sigma^2, \sigma^3)$, the triad of Pauli matrices, θ an arbitrary real number and $\hat{n} = ((\hat{n})_1, (\hat{n})_2, (\hat{n})_3)$ a unit vector. The factorization of $\gamma^{1/n}$ was performed in Eq. (3.30) because, as we briefly remarked earlier, a uniform scaling of all four elements of the general 2×2 matrix does not alter the fractional linear transformation of Eq. (3.1). All possible dualities are exhausted by *the space spanned by all of the matrices* $\tilde{\mathsf{M}}$ of the form of Eq. (3.30), and a duality with real $\hat{n}$ can then be interpreted as an induced

map on the Euclidean S^2 sphere (or, more precisely, one of its hemispheres as we will explain shortly).

In the case of $n = 2$ (i.e., that of Eq. (3.7)), the only non-trivial solution (i.e., non-identity matrix) solution of the form of Eq. (3.30) is formed by having $(k_2 - k_1) \equiv 1 \pmod 2$. When this occurs, Eq. (3.30) becomes

$$\tilde{\mathsf{M}} = \mathcal{U}^\dagger \sigma^3 \mathcal{U} = \vec{\sigma} \cdot \hat{n}. \tag{3.31}$$

The solution of Eq. (3.31) is, of course, identical to that of Eq. (3.9) once we set $\gamma^{1/n}\,\hat{n} = ((b+c)/2, \mathrm{i}(b-c)/2, a)$. For example, the Ising model duality of Eq. (3.6) is associated with the unit vector $\hat{n} = 2^{-1/2}(1, 0, -1)$. We thus see how the particular solutions that we obtained earlier are a particular case of this more general approach. For "two-"dualities with real $\hat{n}$, any point on the southern hemisphere (i.e., one with $(\hat{n})_3 < 0$) is associated with a different transformation. This is so as scaling the global multiplication of the matrix by (-1) (associated with $\hat{n} \to -\hat{n}$) does not alter the fractional linear transformation of Eq. (3.1). This space spanned by the hemisphere is, of course, identical to that of the $\mathcal{R}P^2$ group associated with nematic liquid crystals having a two-fold homotopy group, $\Pi_1(\mathcal{R}P^2) = \mathbb{Z}_2$ and two associated possible defect charges. Geometrically, we may thus understand dualities by thinking of the space spanned by the group elements.

In a similar vein, in the n-duality solution of Eq. (3.30), the eigenvalues of M are any two roots of the identity (or stated equivalently, any two elements of the cyclic group $\mathbb{Z}_n$ (which, on its own, form the center of the group $SU(n)$) multiplying $\gamma^{1/n}$. We now return to the general problem posed by Eq. (3.12). Repeating our arguments thus far, it is readily seen that the most general meromorphic solution is afforded by the fractional linear maps of Eq.

(3.13) with the n-th 2×2 matrix (associated with the fractional linear map F_n) set by the inverse of all others. That is, rather explicitly,

$$\begin{pmatrix} a_n & b_n \\ c_n & d_n \end{pmatrix} = \left[\begin{pmatrix} a_1 & b_1 \\ c_1 & d_1 \end{pmatrix} \cdot \begin{pmatrix} a_2 & b_2 \\ c_2 & d_2 \end{pmatrix} \cdots \begin{pmatrix} a_{n-1} & b_{n-1} \\ c_{n-1} & d_{n-1} \end{pmatrix} \right]^{-1}. \tag{3.32}$$

3.5 Multiple coupling constants

The considerations of Sections 3.3 and 3.4 can be extended to not only two but also to many coupling constants $\vec{z} = (z_1, z_2, \cdots, z_{\mathsf{q}})$, $\mathsf{q} \geq 1 \in \mathbb{N}$. In the particular case of two coupling constants, the duality mapping will be of the form $\vec{z} = (z_1, z_2) \rightarrow \vec{w} \equiv (F_1(z_1, z_2), F_2(z_1, z_2)) \equiv \vec{F}(\vec{z})$, where the functions $F_1(z_1, z_2)$ and $F_2(z_1, z_2)$ must be fractional linear maps of two complex variables [33].

To obtain the proper fractional linear map in several variables, one has to remember that it is important to preserve the composition property of these maps, that is, the application of two of these maps should generate another fractional linear map. Consider a fractional linear map $\vec{F}^{(1)}(\vec{z})$ involving two complex variables

$$w_1 = F_1^{(1)}(z_1, z_2) = \frac{a_1^{(1)} z_1 + a_2^{(1)} z_2 + a_3^{(1)}}{c_1^{(1)} z_1 + c_2^{(1)} z_2 + c_3^{(1)}}, \tag{3.33}$$

$$w_2 = F_2^{(1)}(z_1, z_2) = \frac{b_1^{(1)} z_1 + b_2^{(1)} z_2 + b_3^{(1)}}{c_1^{(1)} z_1 + c_2^{(1)} z_2 + c_3^{(1)}}, \tag{3.34}$$

where all the coefficients $a_j^{(1)}, b_j^{(1)}, c_j^{(1)}$ $(j = 1, 2, 3)$ are complex numbers. Then, it is straightforward to verify that the composition of these generalized fractional linear maps,

$\vec{F}^{(2)}(\vec{F}^{(1)}(\vec{z}))$, generates another fractional linear map and induces a, non-Abelian in general, group structure. That is, we may associate with each fractional linear map a 3×3 matrix $M^{(1)}$ given by

$$M^{(1)} = \begin{pmatrix} a_1^{(1)} & a_2^{(1)} & a_3^{(1)} \\ b_1^{(1)} & b_2^{(1)} & b_3^{(1)} \\ c_1^{(1)} & c_2^{(1)} & c_3^{(1)} \end{pmatrix}, \tag{3.35}$$

with a determinant $\Delta \neq 0$. As can be explicitly verified, the composition of maps corresponds to matrix multiplication. Moreover, we can re-scale all coefficients by the (in general, complex) factor $1/\sqrt[3]{\Delta}$ without affecting the map, so that the re-scaled (associated) matrix has a determinant equal to unity. The subset of 3×3 complex matrices with determinant 1 forms a group denoted $SL(3, \mathbb{C})$.

The fixed points of the transformation, $\vec{z}^* = (z_1^*, z_2^*)$, solve the equations

$$z_1^* = \frac{a_1^{(1)} z_1^* + a_2^{(1)} z_2^* + a_3^{(1)}}{c_1^{(1)} z_1^* + c_2^{(1)} z_2^* + c_3^{(1)}}, \tag{3.36}$$

$$z_2^* = \frac{b_1^{(1)} z_1^* + b_2^{(1)} z_2^* + b_3^{(1)}}{c_1^{(1)} z_1^* + c_2^{(1)} z_2^* + c_3^{(1)}}. \tag{3.37}$$

When these are satisfied

$$z_2^* = \frac{c_1^{(1)} (z_1^*)^2 + (c_3^{(1)} - a_1^{(1)}) z_1^* - a_3^{(1)}}{a_2^{(1)} - c_2^{(1)} z_1^*}, \tag{3.38}$$

and z_1^* is the solution of a cubic equation (there are obviously three such cubic equation solutions). Armed with the above, we now investigate the extension Babbage's equation of

Eq. (3.7) with two variables $z_{1,2}$. That is, we now explicitly solve the equation

$$\vec{z} \;=\; \vec{F}^{(1)}(\vec{F}^{(1)}(\vec{z})). \tag{3.39}$$

There are several solutions to this equation. An important class, characterized by non-zero values of $b_1^{(1)}$ and $c_1^{(1)}$ is given by

$$M^{(1)} = \begin{pmatrix} a_1^{(1)} & \frac{(1+a_1^{(1)})(1+b_2^{(1)})}{b_1^{(1)}} & -\frac{(1+a_1^{(1)})(a_1^{(1)}+b_2^{(1)})}{c_1^{(1)}} \\ b_1^{(1)} & b_2^{(1)} & -\frac{b_1^{(1)}(a_1^{(1)}+b_2^{(1)})}{c_1^{(1)}} \\ c_1^{(1)} & \frac{c_1^{(1)}(1+b_2^{(1)})}{b_1^{(1)}} & -1-a_1^{(1)}-b_2^{(1)} \end{pmatrix}. \tag{3.40}$$

This solution constitutes a generalization of Eq. (3.9) to the case of $\mathsf{q}=2$ complex variables for "two-"dualities.

The generalization of these ideas to $\mathsf{q}>2$ is formally straightforward leading to the $SL(\mathsf{q}+1,\mathbb{C})$ group structure. The geometry of these mappings is a very interesting mathematical problem beyond the scope of the current chapter.

3.6 "Partial solvability"- a non-trivial practical outcome of dualities

We will now examine *constraints that stem from the fractional linear maps* that we found, i.e., a particular set of conformal transformations. A highlight of the remainder of this chapter is that the results of Eqs. (3.9, 3.10, 3.13, 3.30, 3.32) allow for the *partial solvability* of many different theories. How this is done in practice will be best illustrated by detailed

calculations. To make the concepts concrete and relatively simple to follow, we will employ, in Sections 3.7 and thereafter, as lucid examples some of the best studied statistical mechanics models, Ising models and generalized Ising-type lattice gauge theories and focus on $n = 2$ dualities with a single coupling constant ($\mathsf{q} = 1$). In this section, we wish to sketch the central idea behind this technique.

Let us consider an arbitrarily large yet *finite size* system for which no phase transition occurs and thus the partition function $\mathcal{Z}$ (or any other function) is an *analytic* function of all couplings and/or temperature. For such a finite size system, the W-C and S-C expansions (or, correspondingly, high- and low-temperature expansions) of $\mathcal{Z}$, can often be written as finite order series (i.e., polynomials) in the respective expansion parameters $z \equiv f_+(g)$ and $w \equiv f_-(g)$. That is, we consider the general finite order W-C and S-C series for the partition function $\mathcal{Z}$ (or any other analytic function)

$$\mathcal{Z}_{\mathsf{W-C}} = Y_+(z) \sum_n C_n \, z^n, \quad \mathcal{Z}_{\mathsf{S-C}} = Y_-(w) \sum_{n'} C'_{n'} \, w^{n'}, \tag{3.41}$$

where $Y_\pm$ are analytic functions and $w = F_2(z)$ (for which, according to Eq. (3.11), $z = F_1(w)$). As in Eq. (3.41), the two expansions converge to the very same function $\mathcal{Z}$, we trivially have, by the transitive axiom of algebra, two equivalent relations,

$$\begin{aligned} Y_+(z) \sum_n C_n \, z^n &= Y_-(F_2(z)) \sum_{n'} C'_{n'} \left(F_2(z)\right)^{n'}, \\ Y_-(z) \sum_{n'} C'_{n'} \, z^{n'} &= Y_+(F_1(z)) \sum_n C_n \left(F_1(z)\right)^n, \end{aligned} \tag{3.42}$$

for the finite number of series coefficients $\{C_n\}$ and $\{C'_{n'}\}$. According to the simple results of Section 3.3, the functions $F_{1,2}$ appearing in the arguments of $Y_\pm$ and in the expansion itself are of the fractional linear type, i.e., functions of the form of Eq. (3.10). Now, here is

the crux of our argument: When the functions of Eq. (3.10) are inserted, Eqs. (3.42) may give rise to constraints amongst the coefficients $\{C_n\}$ and $\{C'_{n'}\}$ and thus *partially solve* for the function $\mathcal{Z}$ with *no additional input*.

Similarly to the "n-duality" mappings of Section 3.2, the general methods of partial solvability introduced above may be trivially extended to this more general case. This, in particular, may also enable the examination of not only W-C and S-C series but also the matching of partition functions on finite size systems which in the thermodynamic limit will have multiple phases (and associated series for thermodynamic quantities and partition functions). If Eq. (3.12) applies in systems having a certain number of such regimes in each of which the partition function may be expressed as a different finite order series of the form of Eq. (3.41), i.e.,

$$\mathcal{Z}_h = Y_h(z) \sum_n C_n \; z^n, \tag{3.43}$$

with $1 \leq h \leq m$, where m is the number of finite order representations of the partition function $\mathcal{Z}$, then we will be able to find analogs of Eqs. (3.42). These, as before, will lead to partial solvability.

As the discussion above is admittedly abstract, we will now turn to concrete examples in the next few sections. One of the most pragmatic consequences of our approach, detailed in Section 3.10 and 3.14 is that the complexity of determining the W-C and S-C series expansions may be trivially identical. This lies diametrically opposite to the maxim that S-C series expansions are in many instances far harder to determine than perturbative W-C expansions [34].

3.7 Series expansions of Ising models

To demonstrate our concept, we will first use standard expansions [22–24,35,36] of the Ising models of Eq. (3.44) and their generalizations. The Hamiltonian

$$H = -\sum_{\langle \mathsf{ab} \rangle} J_{\mathsf{ab}} s_{\mathsf{a}} s_{\mathsf{b}}, \tag{3.44}$$

$s_{\mathsf{a}} = \pm 1$. In the remainder of this chapter, we will consider this and various other models on hypercubic lattices Λ of $N = L^D$ sites in D dimensions (with even length L), endowed with periodic boundary conditions. Unless stated otherwise, we will focus on uniform ferromagnetic systems ($J_{\mathsf{ab}} = J > 0$ for all lattice links $\langle \mathsf{ab} \rangle$). In Subsection 3.14.4 we consider other boundary conditions, system sizes and lattice aspect ratios, and show that our results are essentially unchanged for large systems with random $J_{\mathsf{ab}} = \pm J$.

In the notation of earlier sections, the coupling constant is $(g \equiv) K \equiv \beta J$ with β the inverse temperature. Defining $\tilde{T} \equiv \tanh K (\equiv f_+(K))$, the identity $\exp[K s_{\mathsf{a}} s_{\mathsf{b}}] = \cosh K [1 + (s_{\mathsf{a}} s_{\mathsf{b}}) \tilde{T}]$ leads to a high-temperature (H-T), or W-C, expansion for the partition function

$$\mathcal{Z}_{\mathsf{H-T}} = (\cosh K)^{DN} \sum_{\{s\}} \prod_{\langle \mathsf{ab} \rangle} \Big[1 + \Big(s_{\mathsf{a}} s_{\mathsf{b}} \Big) \tilde{T} \Big]. \tag{3.45}$$

The sum $\sum_{\{s\}} (s_{\mathsf{a}} s_{\mathsf{b}}) \cdots (s_{\mathsf{m}} s_{\mathsf{n}}) = 2^N$ if s_{k} at each site k appears an even number of times and vanishes otherwise. Thus,

$$\mathcal{Z}_{\mathsf{H-T}} = 2^N (\cosh K)^{DN} \sum_{l=0}^{DN/2} C_{2l} \tilde{T}^{2l}, \tag{3.46}$$

where $C_{l'}$ is the number of (not necessarily connected) *loops* of total perimeter $l' = 2l$ ($l = 1, 2, \cdots$) that can be drawn on the lattice and $C_0 = 1$. For each such loop, i.e., $\Gamma = (\mathsf{ab}) \cdots (\mathsf{mn})$ formed by the bonds (nearest neighbor pair products $\{(s_{\mathsf{a}} s_{\mathsf{b}})\}$) appearing in Eq. (3.46), there is a complementary loop $\overline{\Gamma} = \Lambda - \Gamma$ for which the sum of Eq. (3.46) remains unchanged. Consequently, the H-T series coefficients are trivially symmetric, $C_{DN-l'} = C_{l'}$.

We next briefly review the low-temperature (L-T), or S-C, expansion. There are two degenerate ground states (with $s_{\mathsf{a}} = +1$ for all sites a or $s_{\mathsf{a}} = -1$) of energy $E_0 = -JDN$. All excited states can be obtained by drawing closed surfaces marking domain wall boundaries. The domain walls have a total $(D-1)$ dimensional surface area s', the energy of which is $E = E_0 + 2s'J$. Taking into account the two-fold degeneracy, the L-T expansion of the partition function in powers of $(f_-(K) \equiv) e^{-2K}$ is

$$\mathcal{Z}_{\mathsf{L-T}} = 2e^{KDN} \sum_{l=0}^{DN/2} C'_{2l} e^{-4Kl}, \tag{3.47}$$

with $C'_{s'}$ the number of (not necessarily connected) closed *surfaces* of total area $s' = 2l$ ($C'_0 = 1$). That is, the L-T expansion is in terms of $(D-1)$-dimensional "surface areas" enclosing D-dimensional droplets. Geometrically, there are no closed surfaces of too low areas s'. Thus, in the L-T expansion of Ising ferromagnets,

$$C'_{s'} = 0, \ \ s' = 2i, \tag{3.48}$$

where $1 \leq i \leq D-1$. The L-T coefficients exhibit a trivial *complementarity symmetry* akin to that in the H-T series. Given any spin configuration $\{s_{\mathsf{a}}\}$, there is a unique correspondence with a staggered spin configuration $s'_{\mathsf{a}} = (-1)^{\sum_{\alpha=1}^{D} a_\alpha} s_{\mathsf{a}}$ where a_α are the (integer) Cartesian components of the hypercubic lattice site a (i.e., $\mathsf{a} = (a_1, a_2, \cdots, a_D)$). Domain

walls associated with such staggered configuration are inverted relative to those in the original spin configuration s_{a}. That is, if a particular domain wall appears in s_{a} then it will not appear in s'_{a} and vice versa. As a result, $C'_{DN-s'} = C'_{s'}$ (for the even L hypercubic lattices that we consider).

3.8 Equating weak (H-T) and strong (L-T) coupling series

We will now follow the program outlined in Section 3.6. Our approach is to compare H-T and L-T series expansions of the Ising (and other arbitrary) models by means of a duality mapping. In the Ising model, the Möbius transformation (that satisfies the "one-" duality condition of Eq. (3.7))

$$\tilde{T} = \frac{1 - e^{-2K}}{1 + e^{-2K}}, \; e^{-2K} = \frac{1 - \tilde{T}}{1 + \tilde{T}}, \tag{3.49}$$

relates expansions in $\tilde{T}$ to those in e^{-2K}. In either of the expansion parameters $f_{\pm}(K)$ (i.e., $\tilde{T}$ or e^{-2K}), Eqs. (3.49) are examples of the fractional linear transformations discussed above. $\tilde{T}$ is the magnetization of a single Ising spin immersed in an external magnetic field of strength $h = K/\beta$ when there is a minimal coupling (a Zeeman coupling) between the dual fields: the Ising spin and the external field. This transformation may be applied to Ising models in *all dimensions* D – not only to the $D = 2$ model for which the KW correspondence holds. These transformations emulate, yet are importantly *different from*, a $g \leftrightarrow 1/g$ correspondence (the latter never enables an equality of two finite order polynomials

in the respective expansion parameters). Employing the second of Eqs. (3.49),

$$\mathcal{Z}_{\mathsf{L-T}} = 2\Big(\frac{1+\tilde{T}}{1-\tilde{T}}\Big)^{DN/2}\Big[1+\sum_{l=1}^{DN/2} C'_{2l}\Big(\frac{1-\tilde{T}}{1+\tilde{T}}\Big)^{2l}\Big]. \tag{3.50}$$

By virtue of Eq. (3.46), this can be cast as a finite order series in $\tilde{T}$ multiplying $(\cosh K)^{DN}$. Indeed, by invoking $1-\tilde{T}^2 = \frac{1}{(\cosh K)^2}$ and the binomial theorem,

$$\begin{aligned}\mathcal{Z}_{\mathsf{L-T}} &= 2(\cosh K)^{DN}\sum_{m=0}^{DN}\tilde{T}^m\Big[\binom{DN}{m} \\ &+ \sum_{l=1}^{DN/2} C'_{2l}\; A^D_{\frac{m}{2},l}\Big]\end{aligned} \tag{3.51}$$

where

$$A^D_{k,l} = \sum_{i=0}^{2l}(-1)^i\binom{2l}{i}\binom{DN-2l}{2k-i}. \tag{3.52}$$

Analogously,

$$\begin{aligned}\mathcal{Z}_{\mathsf{H-T}} &= \frac{e^{KDN}}{2^{(D-1)N}}\sum_{m=0}^{DN} e^{-2Km}\Big[\binom{DN}{m} \\ &+ \sum_{l=1}^{DN/2} C_{2l}\; A^D_{\frac{m}{2},l}\Big]\end{aligned} \tag{3.53}$$

Equating Eqs. (3.46) and (3.51) and Eqs.(3.47) and (3.53) and invoking Eq. (3.48) leads to a linear relation among expansion coefficients,

$$W^D V + P = 0, \tag{3.54}$$

where V and P are, respectively, $DN-$component and $(DN+D-1)-$component vectors defined by

$$\begin{aligned} V_i &= \begin{cases} C_{2i} & \text{when } i \leq \frac{DN}{2}, \\ C'_{2(i-\frac{DN}{2})} & \text{when } i > \frac{DN}{2}, \end{cases} \\ P_i &= \begin{cases} \binom{DN}{2i} & \text{when } i \leq \frac{DN}{2}, \\ \binom{DN}{2(i-\frac{DN}{2})} & \text{when } \frac{DN}{2} < i \leq DN, \\ 0 & \text{when } i > DN. \end{cases} \end{aligned} \tag{3.55}$$

In Eq. (3.54), the rectangular matrix

$$W^D = \begin{pmatrix} M^D_{DN\times DN} \\ T^D_{(D-1)\times DN} \end{pmatrix}, \tag{3.56}$$

where the $DN \times DN$ matrix M^D is equal to

$$M^D = \begin{pmatrix} -2^{N-1}\mathbb{1}_{\frac{DN}{2}\times\frac{DN}{2}} & A^D_{\frac{DN}{2}\times\frac{DN}{2}} \\ A^D_{\frac{DN}{2}\times\frac{DN}{2}} & -2^{(D-1)N+1}\mathbb{1}_{\frac{DN}{2}\times\frac{DN}{2}} \end{pmatrix}, \tag{3.57}$$

with a square matrix $A^D_{\frac{DN}{2}\times\frac{DN}{2}}$ whose elements $A^D_{k,l}$ $(1 \leq k,l \leq DN/2)$ are given by Eq. (3.52). Constraints (3.48) are captured by T^D in Eq. (3.56), $T^D = \begin{pmatrix} O_{(D-1)\times\frac{DN}{2}} & B^D_{(D-1)\times\frac{DN}{2}} \end{pmatrix}$, where the matrix elements $B^D_{k,l} = 1$, if $k = l$, and $B^D_{k,l} = 0$ otherwise; O is a $(D-1)\times\frac{DN}{2}$ null matrix. Apart from the direct relations captured by Eq. (3.54) that relate the H-T and L-T series coefficients to each other, there are additional constraints including those (i) originating from equating coefficients of odd powers of $\tilde{T}$ and e^{-2K} to zero and (ii) of trivial symmetry related to complimentary loops/surfaces in the H-T and L-T expansion that we discussed earlier, $C_i = C_{DN-i}$ and $C'_i = C'_{DN-i}$. It may be verified that these

restrictions are already implicit in Eq. (3.54). Notably, as the substitutions $i \leftrightarrow (2k-i)$, $(2l) \leftrightarrow (DN-2l)$ in Eq. (3.52) show, Eqs. (3.51) and (3.53) are, respectively, invariant under the two independent symmetries $C'_{2l} \leftrightarrow C'_{DN-2l}$ and $C_{2l} \leftrightarrow C_{DN-2l}$ and thus the linear relations of Eq. (3.54) adhere to these symmetries. Thus, the equalities between the lowest (small $2l$) and highest (i.e., $(DN-2l)$) order coefficients are a consequence of the duality given by Eq. (3.49) that relates expansions in the W-C and S-C parameters.

The total number of unknowns (series coefficients) in Eq. (3.54) is $U = DN$ with 1/2 of these unknowns being the H-T expansion coefficients and the other 1/2 being the L-T coefficients (the components V_i). In Subsection 3.14.1 (in particular, Table 3.2 therein), we list the rank (R) of the matrix W^D appearing in Eq. (3.54) for different dimensions D and number of sites N. As seen therein, for the largest systems examined the ratio R/U tends to 3/4 suggesting that in *all* D only $\sim 1/4$ of the combined L-T and H-T coupling series coefficients need to be computed by combinatorial means. The remaining $\sim 3/4$ are determined by Eq. (3.54). This fraction might seem trivial at first sight. If, for instance, the first 1/2 of the H-T coefficients C_{2l} are known (i.e., those with $l \leq DN/4$) then the remaining H-T coefficients C_{2l} (with $l > DN/4$) can be determined by the symmetry relation $C_{DN-2l} = C_{2l}$ and once all of the H-T series coefficients are known (and thus the partition function fully determined), the partition function may be written in the form of Eq. (3.47) and the L-T coefficients $\{C'_{2l}\}$ extracted. Thus by the symmetry relations alone knowing a 1/4 of the coefficients alone suffices. The symmetry relations are a rigorous consequence of the duality relations for any value of N. As the duality relations may include additional information apart from symmetries, it is clear that $R/U \geq 3/4$ for finite N (i.e., knowing more than a 1/4 of the coefficients is not necessary in order to evaluate all of the remaining H-T and L-T coefficients with the use of duality). For a given aspect ratio, the smaller N is (and the smaller the number of unknowns U), the additional relations of Eqs. (3.48) carry larger

relative weight and the ratio R/U may become larger. Thus, 3/4 is its lower bound. Indeed, this is what we found numerically for all (non self-dual) systems that we examined (see Subsection 3.14.1). As D increases, the lowest non-vanishing orders in the L-T expansion become more separated and Eqs. (3.54) become more restrictive for small N systems [37].

The H-T and L-T series are of the form of Eqs. (3.46) and (3.47) for all geometries that share the same minimal D dimensional hypercube (i.e., of minimal size $L = 2$) of 2^D sites. Thus, equating the series gives rise to linear relations of the same form for both a hypercube of size $N = L^D$ (with general even L) as well as a tube of $N/2^{D-1}$ hypercubes stacked along one Cartesian direction. However, although the derived linear equations are the same, the partition functions for systems of different global lattice geometries are generally dissimilar (indicating that the linear equations can never fully specify the series). Thus, the set of coefficients not fixed by the linear relations depends on the global geometry.

Parity and boundary effects may influence the rank R of the matrix W^D in Eq. (3.54). As demonstrated in Subsection 3.14.4 for $D = 2$ lattices in which (at least) one of the Cartesian dimensions L is *odd*, as well as systems with non-periodic boundary conditions, $R/U \sim 2/3$. That is, in such cases $\sim 1/3$ of the coefficients need to be known before Eq. (3.54) can be used to compute the rest. As explained in Subsection 3.14.4, symmetry and duality arguments can be enacted to show that in these cases, $R/U \geq 2/3$ for finite N, i.e., its lower bound is 2/3. A further restriction is that of discreteness – the coefficients C_{2l}, C'_{2l} (counting the number of loops/surfaces of given perimeter/surface area) must be non-negative integers for the ferromagnetic Ising model.

Let us illustrate the concepts above with a minimal periodic 2×2 ferromagnetic ($J > 0$) system with Hamiltonian $H = -2J[s_1 s_2 + s_1 s_3 + s_2 s_4 + s_3 s_4]$. From Eqs. (3.46, 3.47)

$$\begin{aligned} \mathcal{Z}_{\mathsf{H-T}} &= 16 \cosh^8 K[1 + C_2 \tilde{T}^2 + C_4 \tilde{T}^4 + C_6 \tilde{T}^6 + C_8 \tilde{T}^8], \\ \mathcal{Z}_{\mathsf{L-T}} &= 2e^{8K}[1 + C_2' e^{-4K} + C_4' e^{-8K} \\ &\quad + C_6' e^{-12K} + C_8' e^{-16K}]. \end{aligned} \tag{3.58}$$

Invoking Eqs. (3.55,3.56), $V^\dagger = (C_2, C_4, C_6, C_8, C_2', C_4', C_6', C_8')$,
$P^\dagger = (28, 70, 28, 1, 28, 70, 28, 1, 0)$, and

$$W = \begin{pmatrix} -8 & 0 & 0 & 0 & 4 & -4 & 4 & 28 \\ 0 & -8 & 0 & 0 & -10 & 6 & -10 & 70 \\ 0 & 0 & -8 & 0 & 4 & -4 & 4 & 28 \\ 0 & 0 & 0 & -8 & 1 & 1 & 1 & 1 \\ 4 & -4 & 4 & 28 & -32 & 0 & 0 & 0 \\ -10 & 6 & -10 & 70 & 0 & -32 & 0 & 0 \\ 4 & -4 & 4 & 28 & 0 & 0 & -32 & 0 \\ 1 & 1 & 1 & 1 & 0 & 0 & 0 & -32 \\ 0 & 0 & 0 & 0 & 1 & 0 & 0 & 0 \end{pmatrix}.$$

There are $U = 8$ unknown coefficients in Eq. (3.54); the rank (R) of the matrix W is eight. Thus, in this minimal finite system, the Eqs. (3.54) are linearly independent ($R/U = 1$) and all coefficients may be determined ($C_2 = C_6 = 4, C_4 = 22, C_8 = 1, C_2' = C_6' = 0, C_4' = 6, C_8' = 1$).

Generally, not all coefficients may be determined by duality alone. As we discussed, in the large system limit, $R/U \to 3/4$. A 4×4 example appears in Subsection 3.14.5.

3.9 Partial solvability and binary spin glasses

If $J_{\mathsf{ab}} = \pm J$ independently on each lattice link $\langle \mathsf{ab} \rangle$, then Eqs. (3.48) need not hold. Instead of Eq. (3.54), we have (see Subsection 3.14.2)

$$S^D V + Q = 0. \tag{3.59}$$

This less restrictive equation (by comparison to Eq. (3.54)), valid for all $J_{\mathsf{ab}} = \pm J$, is of course still satisfied by the ferromagnetic system. For the matrix S^D, a large system value of $R/U \sim 3/4$ is still obtained (see Table 3.3, Subsection 3.14.2). The partition functions for different $J_{\mathsf{ab}} = \pm J$ realizations will be obviously different. Nevertheless, all of these systems will share these linear relations [38]. Unlike the ferromagnetic system, the integers $C_{l'}, C'_{s'}$ may be negative. Computing the partition function of general binary spin glass $D = 2$ Ising models is a problem of *polynomial* complexity in the system size. When $D \geq 3$, *the complexity becomes that* of an NP complete problem [39, 40]. Therefore, our equations partially solve and "*localize*" NP-hardness to only a fraction of these coefficients; the remaining coefficients are determined by linear equations. The complexity of computing $\binom{n}{m}$, required for each element of S^D, is $\mathcal{O}(n^2)$. Our equations enable a polynomial (in N) consistency checks of partition functions. In performing the expansions of Eqs. (3.46) and (3.47), the complexity of determining the number of loops (or surfaces) of given size l' (or s') (i.e., the coefficients $C_{l'}$ or $C'_{s'}$) increases rapidly with l' (or s').

Our relations may be applied to systematically simplify the calculation of these coefficients. As we now explain, the situation becomes exceedingly transparent in the Ising models discussed thus far. For these theories, the coefficients are symmetric: $C_{l'} = C_{DN-l'}$, $C'_{s'} = C'_{DN-s'}$. By virtue of these symmetries that are embodied in the duality relations of Eq. (3.59), it is clear that if the lower 1/2 of the H-T coefficients $\{C_{l' \leq DN/2}\}$ (or, similarly, the lower 1/2 of L-T coefficients. i.e., $\{C'_{s' \leq DN/2}\}$), i.e., a 1/4 of the combined H-T and L-T series coefficients, were known then the remaining H-T (or L-T) coefficients are trivially determined. Then, armed with either the full H-T (or L-T) series, the exact partition functions can be equated $\mathcal{Z}_{\mathsf{H-T}} = \mathcal{Z}_{\mathsf{L-T}}$ and written in the form of Eqs. (3.46) and (3.47) to determine the remaining unknown L-T (or H-T) coefficients. That is, once the partition functions are known, the series expansions (and thus coefficients) are uniquely determined. By construction, Eq. (3.59) incorporates, of course, the relation

$$\mathcal{Z}_{\mathsf{H-T}} = \mathcal{Z}_{\mathsf{L-T}} \tag{3.60}$$

which forms the core of our analysis. Thus, as the symmetry is a consequence of the duality relations, it is clear that knowing a 1/4 of the combined H-T and L-T coefficients suffices to determine all of them via Eq. (3.59), i.e., that the required fraction of coefficients to find all of the others via duality satisfies the inequalty $(1 - R/U) \leq 1/4$. As the asymptotic ratio of $R/U \sim 3/4$ suggests, and as we have verified, knowing the first 1/4 of both the H-T and L-T coefficients (i.e., those with $l' \leq DN/4$ and $s' \leq DN/4$) instead of 1/2 of the H-T (or L-T) coefficients discussed above, suffices to completely determine all other coefficients. As the difficulty of evaluating coefficients increases rapidly with their order, systematically computing this 1/4 lowest order coefficients ($\{C_{l' \leq DN/4}\}, \{C'_{s' \leq DN/4}\}$) is less

numerically demanding than computing the first 1/2 of all the H-T coefficients ($\{C_{l' \leq DN/2}\}$), or calculating the first 1/2 all of the L-T coefficients ($\{C'_{s' \leq DN/2}\}$).

3.10 Generating "hard"' series expansions from their "easier" counterparts

The central idea underlying our approach is that, for finite size systems, the H-T and L-T series expansions are different representations of the very same partition function, Eq. (3.60). This equality followed from the analyticity of the partition function on any (arbitrary size yet) finite size system. As the astute reader noted throughout all earlier sections, this relation forms the nub of the current study. It is worthwhile to step back and ask what the practical implications of our results are for disparate H-T and L-T series expansions (or other W-C and S-C series). First and foremost, Eq. (3.60) implies, of course, that the generation of the H-T and L-T series on finite size lattice are equally hard, as obtaining one immediately yields the other.

As stated by certain insightful textbooks, e.g., [34, 41–43], the H-T and L-T expansions differ in their conceptual premise. For instance, as [34] notes, "the derivation of a high-temperature expansion is, in principle, straightforward", since it just amounts to counting the number of closed loops, while, as befits the more meticulous examination of the ground states and myriad possible excitations about them, it may seem that "the generation of lengthy low-temperature series is a highly specialized art". Much work has been devoted to a finite lattice method that improves the bare H-T and L-T series (as in, e.g., the H-T loop tallying briefly reviewed in Section 3.7) [43–46]. Many specialized texts [41, 42] laud

the simplifying features of general H-T expansions vis a vis their L-T counterparts, including commending their features such as "smoothness" [41], the uniform sign of the H-T coefficients in disparate theories, and their applicability to gapless systems [41, 42]. In a more recent detailed exposition [43], it was noted that "while the high-temperature series are well-behaved the situation at low temperatures is less satisfactory, in particular above two dimensions". In a related vein, we remark that the H-T series are well known to naturally relate to one of the oldest and simplest expansions — that of the virial coefficients [47] as well as large-n expansions [48]. Thus, with all of the above, it would generally seem that H-T and L-T qualitatively differ. However, as seen by Eq. (3.60) and the linear equations that we derived in earlier sections connecting the H-T and L-T expansions, the complexity of deriving either expansion on all general finite size lattices is the same. Thus for finite size lattices with finite order H-T and L-T series related by a transformation of their expansion parameter, the general maxim concerning the different intrinsic complexity of the H-T and L-T expansions does not hold.

Concretely, we may derive H-T coefficients from L-T coefficients and vice versa from the simple relation of Eq. (3.60). In the case of the Ising model that formed much of the focus of the current study, from Eq. (3.54) we have that

$$C_{2k} = \frac{1}{2^{N-1}}\left[\sum_{l=1}^{DN/2} A^{D}_{k,l} C'_{2l} + \binom{DN}{2k}\right]. \tag{3.61}$$

In [49], we apply our method to derive the H-T expansions from their L-T counterparts on finite size periodic two- and three-dimensional lattices [50].

It is notable that our method *applies to non-trivial systems such as the three-dimensional Ising model*. Our relations enable *a consistency check of proposed series solutions* and the

derivation of the entire series from a knowledge of only a fraction of coefficients. Indeed, we verified that the L-T series provided in [50] satisfy the linear equations of Eq. (3.54) (and our derived H-T series adhere to the same relations). As we explained in Section 3.8 for regular uniform coupling systems, and in Section 3.9 for less constrained non-uniform systems, a partial knowledge of both the L-T and/or H-T series may enable a construction of the full partition function.

As we have reiterated earlier and do so once again here, our approach applies to arbitrarily large yet finite size lattices.

3.11 New combinatorial geometry relations from dualities

Mathematical identities are system independent and enable the general transformation of one set of objects into another. As such, they are reminiscent of dualities. Symbolically, let us consider particular partition functions (or "generating functions") $\{\mathcal{Z}_1\}$ that encode all quantities that we wish to determine in a particular set of systems. If certain identities universally apply, we may invoke these relations to transform each function into an equivalent dual, and formally rewrite

$$\{\mathcal{Z}_1\} = \{\mathcal{Z}_2\} \tag{3.62}$$

for the two sets of functions. In Eq. (3.62), $\{\mathcal{Z}_2\}$ can be interpreted as the set of generating functions of very different problems or physical systems. As such, dualities and, in particular,

the universal relations that we obtained from conformal transformations linking dual systems may encode very general mathematical relations.

In what follows, we concretely demonstrate that dualities may lead to an extensive number of (new) mathematical relations such as those connecting the number of surfaces and volumes of a particular size. These relations are already contained in our previously derived Eqs. (3.59). The key conceptual point is that dualities between different types of partition functions (irrespective of the general coupling constants associated with a large set of such functions) can hold generally by virtue of mathematical identities.

Wegner's duality [51] relates interactions between $\{s_{\mathsf{a}}\}$ on the boundaries of "d dimensional cells" to generalized Ising gauge type models with interactions between $\{s_{\mathsf{a}}\}$ on the boundaries of "$(D-d)$ dimensional cells". These generalized Ising lattice gauge theories are given by the Hamiltonian

$$H = -\sum_{\square_d} K_d \prod_{\mathsf{a}\in\partial\square_d} s_{\mathsf{a}}, \tag{3.63}$$

with $s_{\mathsf{a}} = \pm 1$ and K_d general coupling constants. Here, a "$d = 1$ dimensional cell" corresponds to a (one-dimensional) nearest neighbor edge (i.e., one whose boundary is $\langle \mathsf{ab} \rangle$) associated with standard $s_{\mathsf{a}} s_{\mathsf{b}}$ interactions that we largely focused on thus far (i.e., the Ising model Hamiltonian of Eq. (3.44). The case of $d = 2$ corresponds to a product of four s_{a}'s at the centers of the four edges which form the boundary of a two-dimensional plaquette (as in standard hypercubic lattice gauge theories). That is, $d = 2$ corresponds to the lattice gauge Hamiltonian

$$H = -\sum_{\square_2} K_{d=2} \, (U_{\mathsf{ab}} U_{\mathsf{bc}} U_{\mathsf{cd}} U_{\mathsf{da}}), \tag{3.64}$$

where the link variables $U_{\mathsf{ab}} = \pm 1$, and with $\square_2$ being the standard "$d = 2$ dimensional" cells (i.e., square plaquettes) whose one-dimensional boundary $\partial\square_2$ is the formed by the nearest neighbor one-dimensional links (ab), (bc), (cd), and (da). The case of $d = 3$ corresponds to the product of six s_{a}'s at the center of the six two-dimensional faces which form the boundary of a three-dimensional cube, etc. The Hamiltonian is the sum of products of $(2d)$ s_{a}'s on the boundaries of all of the d dimensional hypercubes in the lattice (in a lattice of $\tilde{N}$ sites there are $N_c = \tilde{N}\binom{D}{d}$ such hypercubes and $N_s = \tilde{N}\binom{D}{d-1}$ Ising variables s_{a} at the centers of their faces). If the dimensionless interaction strength for a d dimensional cell is K_d then the couplings in the two dual models will be related by Eqs. (3.49) or, equivalently, $\sinh 2K_d \sinh 2K_{D-d} = 1$. The $D = 3, d = 1$ duality corresponds to the duality between the $D = 3$ Ising model and the $D = 3$ Ising gauge theory. The $D = 2, d = 1$ case is that of the KW self-duality. For general d, Wenger derived his duality from an equivalence between the H-T and L-T coefficients.

We now turn to *new, and rather universal, geometrical results* obtained by our approach that hold in general dimensions. If the ground state degeneracy is 2^{N_g} (e.g., $N_g = 1$ for the standard ($d = 1$) Ising models, $N_g = \tilde{N} + 2$ in $D = d = 2$ Ising gauge theories with periodic boundary conditions), then we find [52] that, *irrespective of the coupling constants*, the H-T and L-T series for these models are given by Eqs. (3.46) and (3.47) with the following substitutions

$$N = \frac{N_c}{D}, \quad C_{2l} = 2^{N_s - N} C_{2l}^{(d)}, \quad C'_{2l} = 2^{N_g - 1} C_{2l}^{\prime(d)}. \tag{3.65}$$

Thus, Eq. (3.59) obtained for standard ($d = 1$) Ising models also holds for general d following this substitution. *In systems with d dimensional cells, $C_{2l}^{(d)}$ and $C_{2l}^{\prime(d)}$ denote, respectively, the number of closed surfaces of total d and $(D - d)$ dimensional surface areas equal to $2l$.*

By building on our earlier results, we observe that, when the hypercubic lattice length L is even, *Eq.* (3.59) *universally relates, in any dimension* D *(and for any* d*)*, these numbers to each other leaving only $\sim 1/4$ of these undetermined. By comparison to Eq. (3.59), additional geometrical conditions that hold for $d = 1$ (Eqs. (3.48)) produce the slightly more restrictive Eq. (3.54). Similar additional constraints appear for $d > 1$. A KW type self-duality present for $D = 2d$ leads to linear equations that relate $\{C_{2l}^{(d)}\}$ (the number of surfaces of total $D/2$-dimensional surface area $(2l)$) to themselves. We next explicitly discuss the $D = 2$, $d = 1$ case (i.e, the standard $D = 2$ Ising model). Similar considerations hold for any $D = 2d$ system.

3.12 Dualities versus self-dualities

More information can be gleaned for self-dual systems, e.g., the KW self-duality of the $D = 2$ Ising model. In this model, $C_{2l} \sim C'_{2l}$ (as C_{2l} and C'_{2l} are both the number of closed $d = 1$ dimensional loops of length $2l$) when Eqs. (3.54) are applied to large systems ($L \gg l$), see Subsection 3.14.3. Consequently, the number of coefficients that need to be explicitly evaluated is nearly $1/2$ of those obtained by matching the H-T and L-T expansions without invoking self-duality (see Subsection 3.14.1): $R/U \sim 7/8$ of the coefficients are determined by self-duality once $\sim 1/8$ of the coefficients are provided. We caution that the relation $C_{2l} \sim C'_{2l}$ is only asymptotically correct in the limit of large system sizes. Consequently, we find in Subsection 3.14.3 that R/U asymptotically approaches $7/8$ from below (and not from above as it would have if this relation were exact for finite size systems [53]) as N becomes larger.

3.13 Summary

We demonstrated that *all meromorphic duality transformations on the Riemann sphere (satisfying a generalized form of Babbage's equation) must be a conformal map of the fractional linear type* (and simple generalizations in the case of multiple coupling constants), in the appropriate coupling constants. The bulk of our analysis was focused on investigating the consequences of such general duality maps. As we demonstrated in this chapter, these maps may lead to linear constraints relating finite order series expansions of two dual models. We speculate that in models with numerous isometries (e.g., $N = 4$ supersymmetric YM theories [54]), much of the theory might become encoded in relations analogous to the linear equations studied here. Employing Cramer's rule and noting that the determinants of the matrices appearing therein are volumes of polytopes spanned by vectors comprising the columns of these matrices, relates series amplitudes to *polyhedral volumes* (see Subsection 3.14.6). In $N = 4$ supersymmetric YM theories, polyhedral volume correspondences for scattering amplitudes led to a flurry of recent activity [55].

A main theme of our approach is that the analyticity of any quantity ensures that its different series expansions must match for all values of the coupling constants. Consequently, a main outcome of our study is that the *mere existence* of two or more such finite order series expansions of a theory, related by dualities (of the form of Eq. (3.1)), may "partially solve" that theory. By *partial solvability* we allude to the ability to compute, with complexity polynomial in the system size, the full partition function $\mathcal{Z}$, for instance, given partial information (e.g., a finite fraction $(1 - R/U)$ of all series coefficients in the examples discussed in this chapter). Stated equivalently, we saw how to systematically exhaust all of the

information that duality relations between disparate systems provides. This yields restrictive linear equations on the combined set of series coefficients of the dual systems. These equations allow for more than the computation of one set of (e.g., low-temperature (L-T) or strong-coupling (S-C)) coefficients in terms of the other half (e.g., high-temperature (H-T) or weak-coupling (W-C)). In Ising models and generalized Ising gauge (i.e., Wegner type) theories on even length hypercubic lattices in general dimensions D, only $\sim 1/4$ of the coefficients were needed as an input to fully determine the partition functions; in the self-dual planar Ising model only $\sim 1/8$ of the coefficients were needed as an input – the self-duality determined all of the remaining coefficients by linear relations. For an Ising chain, the H-T series expansion contains only one (two) term(s) for open (periodic) boundary conditions, i.e., $\mathcal{Z} = 2(2\cosh K)^{L-1} (\mathcal{Z} = [(2\cosh K)^L + (2\sinh K)^L])$, thus trivially all coefficients are determined. As Ising models on varied $D > 1$ lattices and random Ising spin glass systems all solve a common set of linear equations, our analysis demonstrates that properties such as *critical exponents cannot* be determined by dualities alone. To avoid confusion, we briefly elaborate on this point. Although all of the properties may, of course, be determined by the series coefficients (especially when investigated via powerful tools such as Padé approximants [56] and numerous others), the information supplied by the duality relations *on their own* does not suffice to establish the exact critical exponents — some direct calculations of the coefficients must be invoked. Our linear relations might nevertheless prove useful in evaluating critical exponents more efficiently as they allow for a double pincer approach in which the H-T and L-T series inform about each other.

For the even size hypercubic lattices with periodic boundary conditions studied in this chapter there are no closed loops (surfaces) of an odd length. Consequently, $C_{l'} = C'_{s'} = 0$ for odd l' or odd s' as we have invoked. If we were to formally allow for additional odd l' or s' coefficients then the ratio $R/U = 1/2$ instead of the values of R/U that we derived

(see Table 3.1). However, when the conditions $C_{l'} = 0$ for odd l' are imposed for the H-T coefficients these lead (via duality) to non-trivial constraints on the L-T series coefficients $C_{l'} = f_{l'}(\{C'_{s'}\}) = 0$ with $f_{l'}$ linear functions. (Similarly, a vanishing of the L-T series coefficients leads to non-trivial relations amongst the H-T coefficients.) These constraints lead to $R/U > 1/2$ and to the universal geometric equalities discussed earlier. We earlier obtained lower bounds on R/U using a complementarity symmetry; the linear constraints may relate to the complementarity of the coefficients. From *a practical point of view*, we explained and showed how S-C *series expansions may be generated from their* W-C *counterparts* (and vice versa). Thus, we saw that seemingly easily perturbative W-C (or H-T) and more nontrivial S-C (or L-T) expansions are actually identically equally hard to generate. We applied these ideas [49] to concrete test cases for some of the *largest exactly known series for both two- and three-dimensional Ising models on finite size lattices* [50]. It is worth reiterating this and underscoring that this construct may be thus applied to general non-integrable systems (such as the three-dimensional Ising model, the general $D > 2$ models in Table 3.1), and numerous other theories.

Table 3.1: Partial solvability of various models. A fraction R/U of the coefficients are simple functions of a fraction $(1 - R/U)$ of coefficients of the H-T(W-C)/L-T(S-C) series.

Model	D	R/U
Ising hypercubic	> 2	$3/4$
Ising hypercubic spin-glass	> 2	$3/4$
Wegner models	> 2	$3/4$
spin-glass Wegner models	> 2	$3/4$
self-dual Ising	2	$7/8$
honeycomb and triangular Ising	2	$3/4$
Potts hypercubic ($q > 2$)	> 2	$2/3$
self-dual Ising gauge	4	$7/8$

Table 3.1 summarizes our findings for numerous models on even size lattices in D dimensions endowed with periodic boundary conditions [57]. In Subection 3.14.4, we discuss other lattice

sizes and boundary conditions. With the aid of our linear equations, the NP hardness of models such as the Ising spin glass in finite dimensions $D > 2$ is confined to a fraction $(1 - R/U)$ of determining all $\mathcal{O}(N)$ coefficients in these models. As we underscored, once these are computed, the remaining fraction R/U of the coefficients are given by rather trivial linear equations. A similar matching of series, performed in this chapter for the partition function, may be replicated for *any physical quantity*, such as matrix elements of operators, admitting a finite series expansion. Although the illustrative models shown in Table 3.1 are all classical, all of our proofs concerning the conformal character of general dualities and the restrictions that these imply are completely general and *hold for both classical and quantum systems*.

A highly nontrivial consequence of our work is the systematic derivation of new mathematical relations via dualities. In the test case of the Ising, Ising gauge, and generalized Wegner models explored in detail in this chapter, *we found an extensive set of previously unknown equalities in combinatorial geometry* given by substituting Eqs. (3.65) into Eq. (3.59).

Acknowledgements

This work was partially supported by NSF CMMT 1106293. ZN gratefully acknowledges insightful discussions with C. M. Bender, S. Kachru, P. H. Lundow, and M. Ogilvie. We are extremely appreciative to Per Hakan Lundow for further correspondence and for providing tables of series coefficients that were very instrumental for a practical application of our method.

3.14 Supplementary information

In the below, we provide explicit details and examples of our method. We will first illustrate how some of the entries in Table 3.1 were determined, study spin glass systems, examine various boundary conditions and system sizes, and relate dualities derived from dualities to polytope volume ratios.

3.14.1 Supplementary information 1: Rank of ferromagnetic Ising models in general D dimensions

We start by explicitly examining the consequences of the conformal transformation of Eq. (3.6) (see Fig. 3.1) in the main text, that implemented dualities in the Ising model. Towards that end, below, in Table 3.2, we display the rank of the matrix W^D of Eq. (3.56). As is seen, for the larger systems examined, in all spatial dimensions D, the ratio (R/U) between the rank of the matrix (R) formed by the linear relations implied by the dualities and the total number of unknown (U) series coefficients (for the combined H-T and L-T expansions) tends to $\sim 3/4$. Specifically, for any finite system size N, the rank

$$R = \frac{3}{4}DN + D, \tag{3.66}$$

while the number of unknowns,

$$U = DN. \tag{3.67}$$

The additive contribution of $D-1$ to the rank originates from the number of conditions of Eqs. (3.48) of the main text. We note that although we tabulate here results for symmetric hypercubes, similar values appear in $L_1 \times L_2 \times \cdots \times L_D$ lattices for which all sides L_i are even (and consequently all possible loop lengths l' and surface areas s' are even and lead to Eqs. (3.46) and (3.47) in the main text).

Table 3.2: Determining series coefficients by relating expansion parameters – the rank (R) of the matrix W^D (Eq. (3.54) of the main text) for periodic hypercubic lattices of $N = L \times L \times L \cdots \times L$ sites in D spatial dimensions. The total sum of the full number of coefficients $\{C_{2l}\}$ and $\{C'_{2l}\}$ in the expansions of Eqs. (3.46) and (3.51) in the main text is denoted by U.

	N	U	R	$\frac{R}{U}$	$\frac{3}{4}$
$D=2$	4	8	8	1.00000	
	16	32	26	0.81250	
	36	72	56	0.77778	
	64	128	98	0.76563	
	100	200	152	0.76000	
	144	288	218	0.75694	
	196	392	296	0.75510	
	256	512	386	0.75391	
	324	648	488	0.75309	
	400	800	602	0.75250	
	900	1800	1352	0.75111	0.75000
$D=3$	8	24	21	0.87500	
	64	192	147	0.76563	
	216	648	489	0.75463	
	512	1536	1155	0.75195	
$D=4$	16	64	52	0.81250	
	256	1024	772	0.75391	
$D=5$	32	160	125	0.78125	
$D=6$	64	384	294	0.76563	
$D=7$	128	896	679	0.75781	
$D=8$	256	2048	1544	0.75391	

As discussed in the main text, for small system size N, the conditions of Eqs. (3.48) therein are more restrictive. This further leads to the *monotonic decrease* of R/U as N is increased.

For the lowest terms, when D is large, these additional conditions play a more prominent role and the problem becomes more solvable.

3.14.2 Supplementary information 2: Rank of binary spin-glass Ising models in general D dimensions

In Table 3.2, we examined the uniform (ferromagnetic) Ising model. We now briefly turn to Ising models with general (random) signs, $J_{\mathsf{ab}} = \pm J$. In such a case, the restrictions of Eq. (3.48) of the main text no longer apply. Furthermore, while $C_0 = 1$, in the L-T expansion C_0' need not be unity (as, apart from global $\mathbb{Z}_2$ (i.e., $s_{\mathsf{a}} \to (-s_{\mathsf{a}})$ at all lattice sites a), the ground state may have additional degeneracies). Thus, the equation to be solved is

$$S^D V + Q = 0. \tag{3.68}$$

Here, V is a $(DN+1)-$component vector, and Q is a $(DN+2)-$component vector defined by

$$\begin{aligned} V_i &= \begin{cases} C_{2i} & \text{when } i \leq \frac{DN}{2}, \\ C'_{2(i-1-\frac{DN}{2})} & \text{when } i > \frac{DN}{2}, \end{cases} \\ Q_i &= \begin{cases} 0 & \text{when } i \leq \frac{DN}{2}, \\ \binom{DN}{2(i-1-\frac{DN}{2})} & \text{when } \frac{DN}{2} < i \leq DN+1, \\ 2^{N-1} & \text{when } i = DN+2. \end{cases} \end{aligned} \tag{3.69}$$

Table 3.3: The rank of the matrix S^D in Eq. (3.70) for the $\pm J$ spin glass Ising model. Similar to the more restrictive ferromagnetic Ising model (where the constraints of Eq. (3.48) in the main text apply), R/U tends to $\sim 3/4$ for large systems.

	N	U	R	$\frac{R}{U}$	$\frac{3}{4}$
$D=2$	4	9	7	0.77778	
	16	33	25	0.75758	
	36	73	55	0.75342	
	64	129	97	0.75194	
	100	201	151	0.75124	
	144	289	217	0.75087	
	196	393	295	0.75064	
	256	513	385	0.75049	
	324	649	487	0.75039	
	400	801	601	0.75031	
	900	1801	1351	0.75014	0.75000
$D=3$	8	25	19	0.76000	
	64	193	145	0.75130	
	216	649	487	0.75039	
	512	1537	1153	0.75016	
$D=4$	16	65	49	0.75385	
	256	1025	769	0.75024	
$D=5$	32	161	121	0.75155	
$D=6$	64	385	289	0.75065	
$D=7$	128	897	673	0.75028	
$D=8$	256	2049	1537	0.75012	

In Eq. (3.68), the matrix

$$S^D = \begin{pmatrix} H^D_{(DN+1)\times(DN+1)} \\ G^D_{1\times(DN+1)} \end{pmatrix}, \tag{3.70}$$

where the $(DN+1)\times(DN+1)$ matrix H^D is equal to

$$\begin{pmatrix} -2^{N-1}\mathbb{1}_{\frac{DN}{2}\times\frac{DN}{2}} & \tilde{A}^D_{\frac{DN}{2}\times(\frac{DN}{2}+1)} \\ \tilde{B}^D_{(\frac{DN}{2}+1)\times\frac{DN}{2}} & -2^{(D-1)N+1}\mathbb{1}_{(\frac{DN}{2}+1)\times(\frac{DN}{2}+1)} \end{pmatrix},$$

with matrices $\tilde{A}^D, \tilde{B}^D$, whose elements are given by $\tilde{A}^D_{k,l} = A^D_{k,l-1}$ for $1 \le k \le \frac{DN}{2}$, $1 \le l \le \frac{DN}{2}+1$ and $\tilde{B}_{k,l} = A^D_{k-1,l}$ where $1 \le k \le \frac{DN}{2}+1, 1 \le l \le \frac{DN}{2}$. The vector G is given by

$$G_{1,l} = \begin{cases} 0 & \text{when } l \le \frac{DN}{2}, \\ -1 & \text{when } l > \frac{DN}{2}. \end{cases} \tag{3.71}$$

The last row of the matrix G and the vector Q capture the constraint

$$\sum_{l=0}^{DN/2} C'_{2l} = 2^{N-1} \tag{3.72}$$

As is seen in Table 3.3, the effect of the restrictions of Eqs. (3.48) of the main text diminishes for large system sizes; the ratio $(R/U) \sim 3/4$ for $N \gg 1$ also in this case when Eqs. (3.48) of the main text can no longer be invoked. For any finite N, the rank

$$R = \frac{3}{4}DN + 1, \tag{3.73}$$

(in this case Eq. (3.48) of the main text no longer holds) while (as stated above), the number of unknowns or components of V is

$$U = DN + 1. \tag{3.74}$$

We remark that although we tabulate above the results for symmetric hypercubes, i.e., those in which along all Cartesian directions i, $L_i = L$, similar values appear for general lattices of size $L_1 \times L_2 \times \cdots \times L_D$ with even L_i (for all $1 \leq i \leq D$).

As expected, for finite N, the ratio (R/U) in the more restricted ferromagnetic case (Table 3.2) is always larger than that in the corresponding random $\pm J$ system (Table 3.3).

3.14.3 Supplementary information 3: Rank of self-dual relations for the ferromagnetic $D = 2$ Ising model

We now turn to finite size (vector) self-dualities of the $D = 2$ Ising model [58] with both periodic (p)/anti-periodic (a) boundary conditions,

$$\frac{1}{(\sinh \tilde{K})^{N/2}} \begin{pmatrix} \mathcal{Z}^{\langle p;p \rangle}(\tilde{K}) \\ \mathcal{Z}^{\langle p;a \rangle}(\tilde{K}) \\ \mathcal{Z}^{\langle a;p \rangle}(\tilde{K}) \\ \mathcal{Z}^{\langle a;a \rangle}(\tilde{K}) \end{pmatrix} =$$

$$\frac{1}{2(\sinh K)^{N/2}} \begin{pmatrix} 1 & 1 & 1 & 1 \\ 1 & 1 & -1 & -1 \\ 1 & -1 & 1 & -1 \\ 1 & -1 & -1 & 1 \end{pmatrix} \begin{pmatrix} \mathcal{Z}^{\langle p;p \rangle}(K) \\ \mathcal{Z}^{\langle p;a \rangle}(K) \\ \mathcal{Z}^{\langle a;p \rangle}(K) \\ \mathcal{Z}^{\langle a;a \rangle}(K) \end{pmatrix}, \tag{3.75}$$

where $\tilde{K}$ is the coupling dual to K (as determined by $f_+(K) = f_-(\tilde{K})$, i.e., $\sinh 2\tilde{K} \sinh 2K = 1$). Inserting Eqs. (3.46) and (3.47) of the main text into Eq. (3.75), allowing $C_0^{\langle\gamma;\delta\rangle}, C_0^{'\langle\gamma;\delta\rangle}$ to be different from unity ($\langle\gamma = p, a; \delta = p, a\rangle$), and repeating our earlier steps we obtain (with $Y_{k,l} = \frac{1}{2^{N-1}} A^{D=2}_{k-1,l-1}$),

$$\sum_{l=1}^{N+1} Y_{k,l} C_{2l-2}^{\langle\gamma;\delta\rangle} = 4C_{2k-2}^{'\langle\gamma;\delta\rangle}, \quad \sum_{l=1}^{N+1} Y_{k,l} C_{2l-2}^{'\langle\gamma;\delta\rangle} = C_{2k-2}^{\langle\gamma;\delta\rangle},$$

where $1 \leq k, l \leq N+1$. Furthermore,

$$C_{2l}^{\langle p;p\rangle} = C_{2l}^{'\langle p;p\rangle} + 2C_{2l}^{'\langle p;a\rangle} + C_{2l}^{'\langle a;a\rangle}, \tag{3.76}$$

$$C_{2l}^{\langle a;p\rangle} = C_{2l}^{\langle p;a\rangle} = C_{2l}^{'\langle p;p\rangle} - C_{2l}^{'\langle a;a\rangle}, \tag{3.77}$$

$$C_{2l}^{\langle a;a\rangle} = C_{2l}^{'\langle p;p\rangle} - 2C_{2l}^{'\langle p;a\rangle} + C_{2l}^{'\langle a;a\rangle}. \tag{3.78}$$

Setting $\mathcal{Z}^{\langle p;a\rangle} = \mathcal{Z}^{\langle a;p\rangle}$ in Eq. (3.75), we have $M^{\mathsf{self}} V = 0$, with V a $(6N+6)$ dimensional vector whose components are

$$\begin{aligned}
V_{1\leq i\leq N+1} = C_{2(i-1)}^{\langle p;p\rangle}, V_{N+1<i\leq 2N+2} = C_{2(i-N-2)}^{'\langle p;p\rangle}, \\
V_{2N+2<i\leq 3N+3} = C_{2(i-2N-3)}^{\langle p;a\rangle}, V_{3N+3<i\leq 4N+4} = C_{2(i-3N-4)}^{'\langle p;a\rangle}, \\
V_{4N+4<i\leq 5N+5} = C_{2(i-4N-5)}^{\langle a;a\rangle}, V_{5N+5<i\leq 6N+6} = C_{2(i-5N-6)}^{'\langle a;a\rangle},
\end{aligned} \tag{3.79}$$

and where M^{self} is

$$\begin{pmatrix}
-2^{N-1} & \overline{A} & O & O & O & O \\
\overline{A} & -2^{N+1} & O & O & O & O \\
O & O & -2^{N-1} & \overline{A} & O & O \\
O & O & \overline{A} & -2^{N+1} & O & O \\
O & O & O & O & -2^{N-1} & \overline{A} \\
O & O & O & O & \overline{A} & -2^{N+1} \\
-\mathbb{1} & \mathbb{1} & O & 2\mathbb{1} & O & \mathbb{1} \\
O & \mathbb{1} & -\mathbb{1} & O & O & -\mathbb{1} \\
O & \mathbb{1} & O & -2\mathbb{1} & -\mathbb{1} & \mathbb{1}
\end{pmatrix}.$$

Here, $2^{N\pm1}$ are multiples of the identity ($\mathbb{1}$) matrix, O is the null matrix, the elements of $\overline{A}$ are given by $\overline{A}_{k,l} = A^{D=2}_{k-1,l-1}$ $(1 \leq k, l \leq N+1)$ and $\mathbb{1}, O$ and A are all $(N+1) \times (N+1)$ matrices.

Table 3.4: The rank of the matrix M^{self} wherein the self-duality of the planar Ising model was invoked. The notation is identical to that in Table 3.2.

	N	U	R	$\frac{R}{U}$	$\frac{7}{8}$
$D=2$	4	30	25	0.83333	0.87500
	16	102	88	0.86275	
	36	222	193	0.86937	
	64	390	340	0.87179	
	100	606	529	0.87294	
	144	870	760	0.87356	
	196	1182	1033	0.87394	
	256	1542	1348	0.87419	
	324	1950	1705	0.87436	
	400	2406	2104	0.87448	
	576	3462	3028	0.87464	

The rank R of the matrix M^{self} is provided in Table 3.4. In the $D = 2$ self-dual Ising model the ratio $R/U \sim 7/8$. In the large system (N) limit, $C_{2l} \sim C'_{2l}$. Thus, by comparison to the non self-dual Ising models, there is indeed a reduction by a factor of two in the number of coefficients needed before the rest are trivially determined by the linear relations $M^{\mathsf{self}}V = 0$. It is noteworthy that, contrary to the behavior for non-self dual systems, the values of (R/U) are *monotonically increasing* in N, approaching their asymptotic value of $7/8$ from below.

3.14.4 Supplementary information 4: Different system sizes, aspect ratios, and boundary conditions

We now examine the analog of Eq. (3.56) of the main text for planar systems of size $L_1 \times L_2$ in which the parity of $L_{1,2}$ can be either even or odd. Systems with only even L_i were examined in the main text (and Table 3.2) to find a ratio of $R/U \sim 3/4$. As seen below, when either (or both) L_1, L_2 are odd, $R/U \sim 2/3$ (i.e., 1/3 of the coefficients are needed as an input to determine the full series by linear relations).

Table 3.5: The rank of the linear equations analogous to Eq. (3.56) of the main text when both L_1 and L_2 are odd.

L_1	L_2	N	U	R	$\frac{R}{U}$	$\frac{2}{3}$
3	3	9	24	19	0.79167	
3	9	27	75	55	0.73333	
5	5	25	70	51	0.72857	0.66667
5	9	45	128	91	0.71094	
9	9	81	234	163	0.69658	

In a system with periodic boundary conditions, when at least one of the Cartesian dimensions L_i of the lattice is odd, closed loops of odd length may appear: the H-T series is no longer constrained to be of the form of Eq. (2) of the main text with even l'. By contrast, as the total number of lattice links is even, the difference between low energy or "good"' (i.e.,

Table 3.6: Rank for $L_1 \times L_2$ lattices with even L_1 and odd L_2.

L_1	L_2	N	U	R	$\frac{R}{U}$	$\frac{2}{3}$
2	3	6	18	13	0.72222	
2	9	18	54	37	0.68519	
4	9	36	108	73	0.67593	0.66667
4	25	100	300	201	0.67000	
8	9	72	216	145	0.67130	

$s_{\mathsf{a}} = s_{\mathsf{b}}$) and high energy "bad" ($s_{\mathsf{a}} = -s_{\mathsf{b}}$) bonds $s_{\mathsf{a}} s_{\mathsf{b}}$ is even and Eq. (3.47) of the main text still holds.

In Tables 3.5 and 3.6 we provide the results for $D = 2$ periodic lattices. As seen, when at least one of the lattice dimensions is odd, $R/U \sim 2/3$. The reduction in the value of R/U relative to the even size lattice with periodic boundary conditions originates from the fact that the $\mathsf{H}-\mathsf{T}$ expansion admits both even and odd powers of $\tilde{T}$; there are more undetermined H-T coefficients. More potently, a lower bound of $R/U \geq 2/3$ can be proven by invoking the symmetries captured by the duality relations. The H-T expansion is symmetric ($C_{DN-l'} = C_{l'}$). In the H-T expansion both odd and even powers l' appear. By contrast, in the L-T expansion only even powers s' arise. The number of non-vanishing H-T series coefficients $\{C_{l'}\}$ is DN; the number of L-T expansion coefficients $C'_{s'}$ in the low temperature form of the partition function, $\mathcal{Z}_{\mathsf{L}-\mathsf{T}}$ is $\frac{DN}{2}$. Given $\{C'_{s'}\}$, by invoking duality (i.e.,by equating $\mathcal{Z}_{\mathsf{H}-\mathsf{T}} = \mathcal{Z}_{\mathsf{L}-\mathsf{T}}$) we may compute all $\{C_{l'}\}$. Thus if we compute these $\frac{DN}{2}$ L-T coefficients (a 1/3 of the combined H-T and L-T coefficients), the partition function and all remaining H-T coefficients can be fully determined.

We next turn to systems with open boundary conditions. In these systems, no odd power shows up in the H-T series expansion. By contrast, odd powers may appear in the L-T expansion (as, e.g., when there is a single $s_{\mathsf{a}} = -1$ at the boundary on a $D = 2$ lattice in which all other sites b have $s_{\mathsf{b}} = +1$ for which there are three "bad" bonds). In Table

3.7 we list the matrix rank for open boundary conditions. Once again, we find that for these $R/U \sim 2/3$. The reduction in the value of R/U by comparison to the even size lattice with periodic boundary conditions in this case has its origins in the fact that here the $\mathsf{L}-\mathsf{T}$ expansion admits both even and odd powers of (e^{-2K}); there are, once again, more undetermined coefficients. We remark that the symmetries $l' \leftrightarrow DN - l'$ and $s' \leftrightarrow DN - s'$ of the H-T and L-T expansions that were present for periodic boundary conditions no longer appear when the system has open boundaries. In the H-T expansion, only even powers appear. In the L-T expansion both odd and even orders s' are present. Thus, the number of H-T coefficients is essentially 1/2 of that of the L-T coefficients. Thus, if all of the H-T coefficients $C_{l'}$ were known (i.e., a 1/3 of all of the combined coefficients), it is clear (even without doing any calculations) that the remaining L-T coefficients $C'_{s'}$ can be determined by duality by setting $\mathcal{Z}_{\mathsf{H}-\mathsf{T}} = \mathcal{Z}_{L-T}$ and computing $\{C'_{s'}\}$. Thus, for any finite size system, the fraction of coefficients required to compute the rest via the duality relations of Eqs. (3.54) is bounded from above, i.e., $(1 - R/U) \leq 1/3$. Asymptotically, for large N, the fraction R/U approaches 2/3 from below (that the approach is from below and not from above follows from this inequality).

Defining the parity

$$\mathcal{P} \equiv \begin{cases} 0 & \text{if both } L_1 \text{ and } L_2 \text{ are even} \\ 1 & \text{otherwise} \end{cases}, \tag{3.80}$$

we find the ranks listed in Table 3.7.

Table 3.7: The rank of the linear equations for various rectangular lattices with open boundary conditions.

	L_1	L_2	N	U	R	$\frac{R}{U}$	$\frac{2}{3}$
$\mathcal{P}=0$	2	2	4	6	5	0.83333	0.66667
	2	8	16	30	23	0.76667	
	2	50	100	198	149	0.75253	
	4	4	16	34	25	0.73529	
	6	6	36	86	61	0.70930	
	10	10	100	262	181	0.69084	
$\mathcal{P}=1$	2	3	6	10	8	0.80000	
	3	3	9	16	13	0.81250	
	4	9	36	83	60	0.72289	
	4	25	100	243	172	0.70782	
	9	9	81	208	145	0.69712	

3.14.5 Supplementary information 5: Explicit test cases

In what follows, we examine specific small lattice systems via our general method.

Random $\pm J$ Ising systems on a periodic 2×2 plaquette

In the main text we examined a periodic 2×2 ferromagnetic ($J > 0$) system with Hamiltonian $H = -2J[s_1 s_2 + s_1 s_3 + s_2 s_4 + s_3 s_4]$. If instead of the ferromagnetic Hamiltonian, we have an Ising model with general (random) $J_{\mathsf{ab}} = \pm J$ on each of the links $\langle \mathsf{ab} \rangle$ then Eq. (3.48) of the main text will no longer hold. Instead of Eq. (3.54) of the main text, the equation satisfied is given by Eq. (3.68) where the DN dimensional (or, in this case, eight-dimensional) matrix M differs from W by the omission of the matrix T (the single last column of W in this 2×2 example). That is, rather explicitly, S is given by

$$\begin{pmatrix}
-8 & 0 & 0 & 0 & 28 & 4 & -4 & 4 & 28 \\
0 & -8 & 0 & 0 & 70 & -10 & 6 & -10 & 70 \\
0 & 0 & -8 & 0 & 28 & 4 & -4 & 4 & 28 \\
0 & 0 & 0 & -8 & 1 & 1 & 1 & 1 & 1 \\
1 & 1 & 1 & 1 & -32 & 0 & 0 & 0 & 0 \\
4 & -4 & 4 & 28 & 0 & -32 & 0 & 0 & 0 \\
-10 & 6 & -10 & 70 & 0 & 0 & -32 & 0 & 0 \\
4 & -4 & 4 & 28 & 0 & 0 & 0 & -32 & 0 \\
1 & 1 & 1 & 1 & 0 & 0 & 0 & 0 & -32 \\
0 & 0 & 0 & 0 & -1 & -1 & -1 & -1 & -1
\end{pmatrix}.$$

As noted in the main text, the DN dimensional vector Q in the $\pm J$ Ising system differs from P in the ferromagnetic case in that it does not have an additional $D-1$ (which equals one in this $D=2$ example) last entries being equal to zero. It is clear that the ferromagnetic system investigated above fulfills Eq. (3.68) (the ferromagnetic system satisfies one further constraint related to the last row of W). We wish to underscore that *any* 2×2 Ising system with *general* couplings $J_{\mathsf{ab}}=\pm J$ on each of the links $\langle \mathsf{ab}\rangle$ will comply with Eq. (3.68).

A periodic 4×4 ferromagnetic system

For a periodic 4×4 ferromagnetic system, there are 32 coefficients and the rank of the matrix W is 26. Thus, the coefficients are linear functions of a subset of six coefficients. Choosing

these to be, e.g., $C_2, C_4, C_6, C_4^{'}, C_6^{'}, C_8^{'}$ the remaining coefficients are given by

$$\begin{aligned}
C_8 &= 2(330 - 5C_6 - 27C_4 - 105C_2 \\
&+ C_8^{'} + 10C_6^{'} + 54C_4^{'}). \\
C_{10} &= 45C_6 + 2(160C_4 + 693C_2 \\
&- 8(-332 + C_8^{'} + 8C_6^{'} + 30C_4^{'})). \\
C_{12} &= -120C_6 - 945C_4 + 8(980 - 539C_2 \\
&+ 7C_8^{'} + 46C_6^{'} + 154C_4^{'}). \\
C_{14} &= 210C_6 + 1728C_4 + 8085C_2 \\
&- 16(-2580 + 7C_8^{'} + 40C_6^{'} + 146C_4^{'}). \\
C_{16} &= 20886 - 252C_6 - 2100C_4 - 9900C_2 \\
&+ 140C_8^{'} + 760C_6^{'} + 2952C_4^{'}. \\
C_{18} &= C_{14}, \\
C_{20} &= C_{12}, \\
C_{22} &= C_{10}, \\
C_{24} &= C_8, \\
C_{26} &= C_6, \\
C_{28} &= C_4, \\
C_{30} &= C_2, \\
C_{32} &= 1.
\end{aligned} \tag{3.81}$$

and

$$
\begin{aligned}
C_{10}^{'} &= 2144 + 8C_6 + 96C_4 + 616C_2 \\
&- 8C_8^{'} - 35C_6^{'} - 112C_4^{'}. \\
C_{12}^{'} &= 112 - 48C_6 - 448C_4 - 1904C_2 \\
&+ 28C_8^{'} + 160C_6^{'} + 567C_4^{'}. \\
C_{14}^{'} &= 120C_6 + 928C_4 + 4120C_2 - 56C_8^{'} \\
&- 350C_6^{'} - 1296(-10 + C_4^{'}). \\
C_{16}^{'} &= 2(1167 - 80C_6 - 576C_4 - 2832C_2 \\
&+ 35C_8^{'} + 224C_6^{'} + 840C_4^{'}). \\
C_{18}^{'} &= C_{14}^{'}, \\
C_{20}^{'} &= C_{12}^{'}, \\
C_{22}^{'} &= C_{10}^{'}, \\
C_{24}^{'} &= C_8^{'}, \\
C_{26}^{'} &= C_6^{'}, \\
C_{28}^{'} &= C_4^{'}, \\
C_{30}^{'} &= C_2^{'} = 0, \\
C_{32}^{'} &= 1. \qquad (3.82)
\end{aligned}
$$

In both of these $D = 2$ dimensional examples (and far more generally) the trivial reciprocity relations

$$\begin{aligned} C_{2l} &= C_{2N-2l}, \\ C'_{2l} &= C'_{2N-2l}, \end{aligned} \tag{3.83}$$

must be (and indeed are) obeyed.

3.14.6 Supplementary information 6: Cramer's rule and amplitudes as polytope volume ratios – a 2×2 test case illustration

In this Subsection, we explicitly illustrate how the computation of the remaining series coefficients from the smaller number of requisite ones using our linear equations is, trivially, related to a volume ratio of polytopes (high dimensional polyhedra). In the main text, we remarked on the two key ingredients of this correspondence: (1) given known coefficients, we may solve for the remaining ones via our linear equations by applying Cramer's rule wherein the coefficients are equal to the ratio of two determinants. (2) the determinants (appearing in Cramer's rule) as well as those of any other matrices are equal to volumes of polytopes spanned by the vectors comprising the columns or rows of these matrices.

To make this lucid, we consider the periodic 2×2 ferromagnetic system of the main text. As it was mentioned earlier, the first six rows and last two rows of matrix W are linearly independent. Thus, in this example. we may choose these rows to construct an 8×8 matrix $\bar{W}$. The corresponding vector $\bar{P}$ that needs to be solved for satisfies the equation

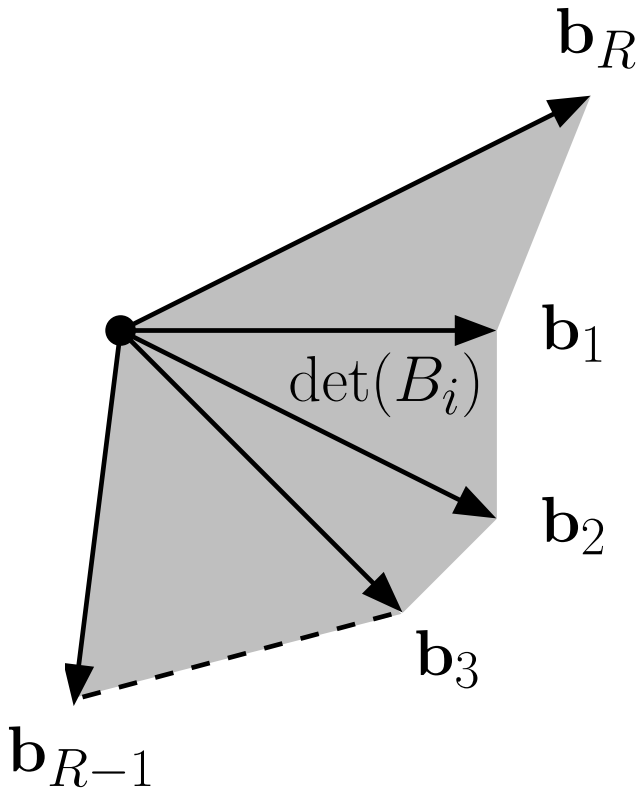

Figure 3.2: Pictorial representation of the volume spanned by the vectors forming the matrix B_i. This volume is set by the determinant of B_i.

$\bar{W}V + \bar{P} = 0$. Here,

$$\bar{P} = \begin{pmatrix} 28 \\ 70 \\ 28 \\ 1 \\ 28 \\ 70 \\ 1 \\ 0 \end{pmatrix}, \tag{3.84}$$

and

$$\bar{W} = \begin{pmatrix} -8 & 0 & 0 & 0 & 4 & -4 & 4 & 28 \\ 0 & -8 & 0 & 0 & -10 & 6 & -10 & 70 \\ 0 & 0 & -8 & 0 & 4 & -4 & 4 & 28 \\ 0 & 0 & 0 & -8 & 1 & 1 & 1 & 1 \\ 4 & -4 & 4 & 28 & -32 & 0 & 0 & 0 \\ -10 & 6 & -10 & 70 & 0 & -32 & 0 & 0 \\ 1 & 1 & 1 & 1 & 0 & 0 & 0 & -32 \\ 0 & 0 & 0 & 0 & 1 & 0 & 0 & 0 \end{pmatrix}.$$

Table 3.8: The value of the series coefficients as found by Cramer's rule. $\det(\bar{W}) = 9175040$.

i	$\det(B_i)$	$\frac{\det(B_i)}{\det(\bar{W})}$
1	36700160	4
2	201850880	22
3	36700160	4
4	9175040	1
5	0	0
6	55050240	6
7	0	0
8	9175040	1

We may invoke Cramer's rule and find all of the undetermined coefficients,

$$V_i = \frac{\det(B_i)}{\det(\bar{W})}. \tag{3.85}$$

As the denominator in Eq. (3.85) is common to all V_i, we see that V_i is essentially given by the determinant $\det B_i$. The matrix B_i is obtained by replacing the i-th column of $\bar{W}$ with $(-\bar{P})$. We summarize the results in Table 3.8. Putting all of the pieces together, we obtain

(as we must) the exact partition function,

$$\begin{aligned} V_1 &= C_2 = 4, \\ V_2 &= C_4 = 22, \\ V_3 &= C_6 = 4, \\ V_4 &= C_8 = 1, \\ V_5 &= C_2^{'} = 0, \\ V_6 &= C_4^{'} = 6, \\ V_7 &= C_6^{'} = 0, \\ V_8 &= C_8^{'} = 1. \end{aligned} \tag{3.86}$$

It is hardly surprising that Cramer's rule can be applied – that is obvious given the linear equations. What we wish to highlight is that each of the determinants appearing in Cramer's rule (Eq. (3.85)) can be interpreted as the volume of a high-dimensional parallelepiped spanned by the vectors comprising the matrix columns. In the case above, the dimension d' of each of the matrices B_i and $\bar{W}$ is equal to their rank $R = 8$. The volume of the corresponding high dimensional tetrahedron (or polytope) spanned by the vectors forming B_i is given by $(\det B_i)/d'!$. In systems in which Cramer's rule may be applied, the dimensionality d' is given by the rank of R of the system of linear equations, $d' = R$.

In Figure 3.2, we schematically depict such a high dimensional volume.

References

[1] C. Montonen and D. Olive, Phys. Lett. B **72**, 117 (1977).

[2] G. 't Hooft, Nucl. Phys. B **138**, 1 (1978).

[3] S. Mandelstam, Phys. Rept. **23**, 245 (1976).

[4] A. Casher, H. Neuberger, and S. Nussinov, Phys. Rev. D **20**, 179 (1979).

[5] E. Witten, Phys. Today **50**, 28 (1997).

[6] M. F. Atiyah, lecture notes (2007). http://www.fme.upc.edu/arxius/butlleti-digital/riemann/071218_conferencia_atiyah-d_article.pdf.

[7] Z. Nussinov and G. Ortiz, Europhys. Lett. **84**, 36005 (2008).

[8] Z. Nussinov and G. Ortiz, Phys. Rev. B **79**, 214440 (2009).

[9] E. Cobanera, G. Ortiz, and Z. Nussinov, Phys. Rev. Lett. **104**, 020402 (2010).

[10] E. Cobanera, G. Ortiz, and Z. Nussinov, Adv. Phys. **60**, 679 (2011).

[11] G. Ortiz, E. Cobanera, and Z. Nussinov, Nuc. Phys. B **854**, 780 (2011).

[12] Z. Nussinov, G. Ortiz, and E. Cobanera, Phys. Rev. B **86**, 085415 (2012).

[13] E. Cobanera, G. Ortiz, and E. Knill, Nucl. Phys. B **877**, 574 (2013).

[14] H. Nishimori and G. Ortiz, *Elements of Phase Transitions and Critical Phenomena* (Oxford University Press, New York, 2011).

[15] R. Savit, Rev. Mod. Phys., **52**, 453 (1980).

[16] F. Y. Wu and Y. K. Wang, J. Math. Phys. **17**, 439 (1976).

[17] K. Drühl and H. Wagner, Ann. Phys. (N.Y.) **141**, 225 (1982).

[18] V. A. Malyshev and E. N. Petrova, J. of Math. Sci., **21**, 877 (1983).

[19] H. A. Kramers and G. H. Wannier, Phys. Rev. **60**, 252 (1941).

[20] G. H. Wannier, Rev. Mod. Phys. **17**, 50 (1945).

[21] L. Onsager, Phys. Rev. **65**, 117 (1944).

[22] *Phase Transitions and Critical Phenomena*, vol. 3, *Series Expansions for Lattice Models*, ed. C. Domb and M. S. Green (Academic Press, London, 1974).

[23] C. Domb, Proc. Roy. Soc. **A199**, 199 (1949).

[24] J. Ashkin and W. E. Lamb, Phys. Rev. **64**, 159 (1943).

[25] J. Mitchell, B. Hsu, and V. Galitski, arXiv:1310.2252 (2013).

[26] R. Penrose, J. Math. Phys. **8**, 345 (1967).

[27] In the notation of what will follow in the current chapter, by "standard dualities" we are alluding to the typical "two-dualities" with one coupling constant g. For these, $F(F(z)) = z$ (the parameter z defining the theory, $z = f_+(g)$, is mapped back onto itself following two consecutive applications of F).

[28] C. Vafa and E. Witten, Nuclear Physics B **431**, 3 (1994).

[29] As a curiosity, we remark that up to a trivial permutation and rescaling, the matrix of Eq. (3.5) embodying a duality transformation, diagonalizes the transfer matrix of the one-dimensional Ising chain of Eq. (3.44) with nearest neighbor $J_{\mathsf{ab}} = J$ (and for which we define $K \equiv \beta J$ with β the inverse temperature). That is,

$$\begin{pmatrix} 2^{-1/2} & 2^{-1/2} \\ 2^{-1/2} & -2^{-1/2} \end{pmatrix} \begin{pmatrix} e^{K} & e^{-K} \\ e^{-K} & e^{K} \end{pmatrix} \begin{pmatrix} 2^{-1/2} & 2^{-1/2} \\ 2^{-1/2} & -2^{-1/2} \end{pmatrix} = 2 \begin{pmatrix} \cosh K & 0 \\ 0 & \sinh K \end{pmatrix}. \tag{3.87}$$

[30] C. Babbage, *Examples of the Solutions of Functional Equations* (Cambridge University Press, Reissue edition, June 13, 2013).

[31] J. F. Ritt, Annals of Mathematics, Second Series, Vol. 17, No. 3 (Mar., 1916), pp. 113-122.

[32] J. F. Ritt, Annals of Mathematics, Second Series, Vol. 20, No. 1 (Sept., 1918), pp. 13-22.

[33] That all meromorphic duality transformations must generally be of the form of Eq. (3.33) is seen by extending the arguments of Section 3.3. Here, we briefly provide simple details explaining this assertion. If each of the functions $F_1(z_1, z_2)$ and $F_2(z_1, z_2)$ is meromorphic on Riemann spheres associated with both z_1 and z_2, then (similar to Eq. (3.16)) they must be rational, $F_{1,2} = P_{1,2}(z_1, z_2)/Q_{1,2}(z_1, z_2)$. For any fixed $z_2 = \mathsf{const.}$, the proof of Section 3.3 demonstrates that the two functions $F_{1,2}(z_1, z_2 = \mathsf{const.})$ are both functions of the form of Eq. (3.1) in the variable z_1. Similarly, if z_1 is held constant, $F_{1,2}$ must become fractional linear functions in z_2. Thus the four binomials $P_1(z_1, z_2), P_2(z_1, z_2), Q_1(z_1, z_2)$ and $Q_2(z_1, z_2)$ are of order no higher than linear in both z_1 and z_2. Similarly, for any number ($\mathsf{q} \geq 1$) of variables z_i, the most general functions

$F_a(\vec{z})$ will be found to be ratios of two q-th order multinomials which are *linear* in each of the variables z_i. In what follows, we return to the case of two complex variables and show how this general form is further restricted. If bilinear (i.e., $z_1 z_2$) terms are present in any of the functions $P_{1,2}$ and $Q_{1,2}$ then a recursive application of the duality transformations (i.e., $\vec{F}(\cdots(\vec{F}(\vec{z})\cdots))$) generally leads to the appearance of higher powers of z_1 and z_2. Thus, closure under applications by $\vec{F}$ generally appears only when all four functions $P_{1,2}$ and $Q_{1,2}$ are linear in both z_1 and z_2 with *no bilinear terms* allowed. This then *only allows* for the generalized fractional linear transformations of Eq. (3.33).

[34] M. Plischke and B. Bergesen, *Equilibrium Statistical Physics*, 3rd Edition, World Scientific Publishing, 2006, see in particular sections 6.2.1 and 6.2.2 therein.

[35] G. Gallavotti and S. Miracle-Sole, Comm. Math. Phys. **7**, 274 (1968).

[36] R. A. Minlos and Ya. G. Sinai, Math. USSR Sbornik **2**, 335 (1967); Trudy Moskov. Mat. Obsc **19**, 113 (1968).

[37] If, hypothetically, in equating the H-T and L-T expansions in similar systems, the non-vanishing coefficients in the L-T expansion remain far separated and only appeared at order $l' = 2D + 2(D-1)n$ for $n = 0, 1, 2, \cdots$ then replicating our calculations leads to $R/U \sim 1 - 1/(2D)$.

[38] Information regarding even a single coefficient might differentiate amongst different $\{J_{\mathsf{ab}}\}$ realizations (all adhering to Eqs. (3.59)). For instance, $C_4 = N$ if and only if $J_{\mathsf{ab}} = +J$ for all $\langle \mathsf{ab} \rangle$.

[39] F. Barahona, J. Phys. A **15**, 3241 (1982).

[40] S. Istrail, *32nd ACM Symposium on the Theory of Computing (STOC00)*, ACM Press, Portland, Oregon, p. 87-96 (2000).

[41] C. Domb, *The Critical Point* (Taylor & Francis, London, 1996).

[42] J. Oitmaa, Ch. Hamer, and W. Zheng, *Series expansion methods for strongly interacting lattice models* (Cambridge University Press, Cambridge, 2006).

[43] A. Wipf, *Statistical Approach to Quantum Field Theory: An Introduction*, Lecture Notes in Physics, volume 864, Springer-Verlag Berlin, Heidelberg (2013).

[44] T. de Neef and I.G. Enting, J. Phys. A **10**, 801 (1977).

[45] I. G. Enting, A. J. Guttmann, and I. Jensen, J. Phys. A **27**, 6987 (1994).

[46] H. Arisue and T. Fujiwara, Phys. Rev. E **67**, 066109 (2003).

[47] J. E. Mayer and E. Montroll, J. Chem. Phys. **9**, 2 (1941).

[48] S. Chakrabarty and Z. Nussinov, Phys. Rev. B **84**, 064124 (2011).

[49] Z. Nussinov, G. Ortiz, and M-S. Vaezi, Nuclear Physics B **892**, 132 (2015), Supplemental Material to this work.

[50] R. Haggkvist and P.H. Lundow, J. Stat. Phys. **108**, 429 (2002); R. Haggkvist, A. Rosengren, D. Andren, P. Kundrotas, P.H. Lundow, and K. Markstrom, Phys. Rev. E **69**, 046104 (2004); http://www.theophys.kth.se/~phl/Data/index.html

[51] F. J. Wegner, J. of Math. Phys. **12**, 2259 (1971).

[52] For general d, $\mathcal{Z}_{\mathsf{H}-\mathsf{T}} = 2^{N_s}(\cosh K)^{N_c}\sum_{l=0}^{N_c/2} C_{2l}\tilde{T}^{2l}$, $\mathcal{Z}_{\mathsf{L}-\mathsf{T}} = 2^{N_g}e^{KN_c}\sum_{l=0}^{N_c/2} C'_{2l}e^{-4Kl}$. Comparing these expressions with Eqs. (3.46, 3.47) leads to the substitution written in the main text.

[53] If the H-T and L-T coefficients were exactly equal to each other for finite size systems N (i.e., if $C_{2l} = C'_{2l}$) then by virtue of the symmetries $C_{2l} = C_{DN-2l}$ and $C'_{2l} = C'_{DN-2l}$ (that are valid for all N), we would have $R/U > 7/8$.

[54] J. Drummond, J. Henn, and J. Plefka, JHEP **05**, 046 (2009).

[55] N. Arkani-Hamed, J. L. Bourjaily, F. Cachazo, A. B. Goncharov, A. Postnikov, and J. Trnka, arXiv:1212.5605 (2012).

[56] G. A. Jr. Baker, *Quantitative Theory of Critical Phenomena*, Academic Press (1990).

[57] Asymptotically, by virtue of self-duality, for large systems, $C_{2l} \sim C'_{2l}$ for $l \ll L$ in Eq. (3.59) (we have not re-evaluated this fraction for small systems).

[58] A. I. Bugrij and V. N. Shadura, Phys. Rev. B **55**, 11045 (1997).

Chapter 4

The Binomial Spin Glass

This chapter contains the materials of a submitted paper [3].

4.1 Introduction

Spin glasses are extremely rich systems that have continued to surprise for many decades [1–13]. They represent paradigmatic realizations of complexity that are abundant in nature and numerous combinatorial optimization problems [14]. Abstractions of spin-glass physics have led to new optimization algorithms and new insight into computational complexity [15–18], shed light on protein folding [19], and provided models of neural networks [20]. Notwithstanding this success, several fundamental questions still linger. These include [21] the character of the low-lying states and whether there are many incongruent [22] ground states. It has long been known that spin-glass systems with discrete couplings may rigorously exhibit an extensive degeneracy [23, 24], but these results do not extend to continuous

[3] M-S. Vaezi, G. Ortiz, M. Weigel, and Z. Nussinov, "The Binomial Spin Glass", Accepted by **PRL**; arXiv:1712.08602.

coupling distributions [25–29]. The possibility of vanishing spectral gaps mandates the distinction of localized and extended excitations, and only the latter can give rise to a multitude of states.

In this chapter, we connect the $\pm J$ and the Gaussian spin glass models by interpolating them via the *binomial* spin glass that has a tunable control parameter m. We establish bounds of the spectral degeneracy of the Ising system on bipartite graphs, which includes the usual Edwards-Anderson (EA) model with $\pm J$ ($m = 1$) and Gaussian ($m \to \infty$) couplings [10] (the EA model was discussed in Chapter 1, Subsection 1.2.3). We thus show that discrete (finite m) spin-glass samples exhibit an extensive ground-state degeneracy, while continuous ones ($m \to \infty$) become two-fold degenerate, while more generally the degeneracy depends on the precise way the non-commuting limits $N \to \infty$ and $m \to \infty$ are taken.

4.2 The binomial Ising spin glass model

We define the *binomial Ising spin glass* on a graph of N sites [30] by the Hamiltonian

$$H_m = -\sum_{\langle \mathsf{xy} \rangle} \mathcal{J}^m_{\mathsf{xy}} s_{\mathsf{x}} s_{\mathsf{y}} \equiv -\sum_{\alpha=1}^{\mathcal{L}} \mathcal{J}^m_\alpha z_\alpha. \tag{4.1}$$

Here, the sum is over sites x and y, defining a link $\alpha = \langle \mathsf{xy} \rangle$, $\mathcal{L}$ denotes the total number of links, and $s_{\mathsf{x}} = \pm 1$. The *binomial coupling* for each link α, $\mathcal{J}^m_\alpha \equiv \frac{1}{\sqrt{m}} \sum_{k=1}^m J^{(k)}_\alpha$, is a sum of m copies (or "layers") of binary couplings $J^{(k)}_\alpha = \pm 1$, each with probability p of being $+1$. The probability distribution of $\mathcal{J}^m_\alpha$,

$$\tilde{P}(\mathcal{J}^m_\alpha) = \sum_{j=0}^{m} \binom{m}{j} p^{m-j} (1-p)^j \delta\left(\mathcal{J}^m_\alpha - \frac{m-2j}{\sqrt{m}} \right), \tag{4.2}$$

is a binomial. In the large-m limit, the distribution (4.2) approaches a Gaussian of mean $\sqrt{m}(2p-1)$ and variance $\sigma^2 = 4p(1-p)$. In particular, for $p = 1/2$, the distribution $\tilde{P}(\mathcal{J}_\alpha^m)$ approaches the standard normal distribution usually considered for the EA model [10].

4.3 Entropy density

To understand the degeneracies in the spectrum, we study the entropy density of the ℓ-th energy level,

$$\mathcal{S}_\ell \equiv \frac{\sum\limits_{\{\mathcal{J}_\alpha^m\}} P(\{\mathcal{J}_\alpha^m\}) \ln D_\ell(\{\mathcal{J}_\alpha^m\})}{N}, \tag{4.3}$$

where D_ℓ is the degeneracy of the ℓ-th energy level [23]. $P(\{\mathcal{J}_\alpha^m\}) = \prod_{\alpha=1}^{\mathcal{L}} \tilde{P}(\mathcal{J}_\alpha^m)$ is the probability of the coupling configuration.

In what follows we embark on the derivation of an upper bound on the ground state entropy density $\mathcal{S}_0$. We restrict ourselves to bipartite graphs, where any closed loop encompasses an even number of links α. Consider two spin configurations $|\mathsf{s}\rangle \neq |\mathsf{s}'\rangle$ and evaluate their energy difference $\Delta E = E(\mathsf{s}) - E(\mathsf{s}')$. From Eq. (4.1),

$$\Delta E \;=\; -\sum_{\alpha=1}^{\mathcal{L}} \mathcal{J}_\alpha^m \Big(z_\alpha(\mathsf{s}) - z_\alpha(\mathsf{s}') \Big) = -2 \sum_{\alpha=1}^{\mathcal{L}} \mathcal{J}_\alpha^m n_\alpha, \tag{4.4}$$

with integers $n_\alpha = 0, \pm 1$ defined by $n_\alpha \equiv [z_\alpha(\mathsf{s}) - z_\alpha(\mathsf{s}')]/2$, where $z_\alpha(\mathsf{s}) = s_{\mathsf{x}} s_{\mathsf{y}}$. If $|\mathsf{s}\rangle$ and $|\mathsf{s}'\rangle$ are degenerate then $\Delta E = 0$. A degeneracy only occurs for some realizations $\{\mathcal{J}_\alpha^m\}$ of the couplings, and Eq. (4.4) can be understood as a set of conditions for the couplings to ensure this.

Consider an arbitrary reference configuration $|\mathsf{s}\rangle$ of energy $E(\mathsf{s})$ and examine its viable degeneracy with the contending $2^N - 1$ other configurations $|\mathsf{s}'\rangle$. Each of these leads to a particular set of integers $\mathsf{C}_j = \{n_\alpha\}_j$, which form the set $\{\mathsf{C}_j\}^{|\mathsf{s}\rangle}_{j=1,2^N-1}$. A subset of those, $\mathsf{Sat}_{|\mathsf{s}\rangle} = \{\mathsf{C}_{j_1}, \mathsf{C}_{j_2}, \cdots, \mathsf{C}_{j_{\mathcal{N}}}\}$, will satisfy the degeneracy condition $\Delta E = 0$ in Eq. (4.4) for some coupling realizations. There are two types of solutions to the equation $\Delta E = 0$: (i) $n_\alpha = 0, \forall \alpha$, or (ii) $n_\alpha \neq 0$, for at least one link α. It is straightforward to demonstrate that there is a single configuration $|\mathsf{s}'\rangle (\neq |\mathsf{s}\rangle)$ for which (i) $n_\alpha = 0, \forall \alpha$ (Subsection 4.6.1). This is the degenerate configuration $|\mathsf{s}'\rangle$ obtained by inverting all of the spins in $|\mathsf{s}\rangle$. To determine whether the degeneracy may be larger than two, we need to compute the probability $\mathcal{P}$ that constraints of type (ii) may be satisfied. While we cannot exactly calculate this probability for general N and m, bounds that we will derive suggest that $\lim_{N\to\infty} \lim_{m\to\infty} \mathcal{S}_\ell = 0$. As we will emphasize, different large m and N limits may yield incompatible results.

Constraints $\mathsf{C}_j \in \mathsf{Sat}_{|\mathsf{s}\rangle}$ are in *a one-to-one correspondence* with zero-energy interfaces (Subsection 4.6.2), whose *size* is equal to the number g_j of non-zero integers in the set $\{n_\alpha\}_j$. That is, given a fixed reference configuration $|\mathsf{s}\rangle$ and a degenerate one $|\mathsf{s}'\rangle$, all type (ii) solutions to Eq. (4.4) are associated with configurations where the product $s_{\mathsf{x}} s'_{\mathsf{x}}$ is equal to -1 in a non-empty set of sites $\mathsf{x} \in R$. To avoid the trivial redundancy due to global spin inversion, consider the states $|\mathsf{s}\rangle$ and $|\mathsf{s}'\rangle$ for which the spin at an arbitrarily chosen "origin" of the lattice assumes the value $+1$. These states are related via $|\mathsf{s}'\rangle = U_{\mathsf{s}'\mathsf{s}}|\mathsf{s}\rangle$, where the *domain-wall operator* $U_{\mathsf{s}'\mathsf{s}}$ is the product of Pauli matrices that flip the sign of the spins s'_{x} at the sites x where $|\mathsf{s}\rangle$ and $|\mathsf{s}'\rangle$ differ. Regions R are bounded by zero-energy domain walls that are interfaces dual to the links with $n_\alpha = \pm 1$, i.e., surrounding the areas R where the spins in $|\mathsf{s}\rangle$ an $|\mathsf{s}'\rangle$ have opposite orientation. Each satisfied constraint $\mathsf{C}_j \in \mathsf{Sat}_{|\mathsf{s}\rangle}$ is associated with a state $|\mathsf{s}'\rangle = U_{\mathsf{s}'\mathsf{s}}|\mathsf{s}\rangle$ that is degenerate with $|\mathsf{s}\rangle$ for some coupling realization(s).

We next formalize the counting of *independent domain walls* or clusters of free spins to arrive at an asymptotic bound on their number [Eq. (4.9)]. This will, in turn, provide a bound on the degeneracy. We define a *complete* set of *independent* constraints $\overline{\mathsf{Sat}}_{|\mathsf{s}\rangle} \subset \mathsf{Sat}_{|\mathsf{s}\rangle}$, of cardinality $\mathcal{M}$, to be composed of *all* constraints $\mathsf{C}_{\bar{\mathsf{j}}} \in \mathsf{Sat}_{|\mathsf{s}\rangle}$ that lead to *linearly independent equations* of the form of Eq. (4.4), $\Delta E = E(\mathsf{s}) - E(\mathsf{s}_{\bar{\mathsf{j}}}) = 0$, on the coupling constants $\{J_\alpha^m\}$ (Subsection 4.6.2). All constraints in $\mathsf{Sat}_{|\mathsf{s}\rangle}$ are a consequence of the linearly independent subset of constraints $\overline{\mathsf{Sat}}_{|\mathsf{s}\rangle}$. Each constraint $\mathsf{C}_{\bar{\mathsf{j}}} \in \mathsf{Sat}_{|\mathsf{s}\rangle}$ is associated with a domain wall operator $U_{\mathsf{s}_{\bar{\mathsf{j}}}\mathsf{s}}$ that generates a degenerate state $|\mathsf{s}_{\bar{\mathsf{j}}}\rangle = U_{\mathsf{s}_{\bar{\mathsf{j}}}\mathsf{s}}|\mathsf{s}\rangle$. If for a given coupling realization $\{\mathcal{J}_\alpha^m\}$ there are $M(\{\mathcal{J}_\alpha^m\}) \leq \mathcal{M}$ such independently satisfied constraints, then the states

$$|\bar{n}_1 \bar{n}_2 \cdots \bar{n}_M\rangle \equiv U_{\mathsf{s}_{\bar{1}}\mathsf{s}}^{\bar{n}_1} U_{\mathsf{s}_{\bar{2}}\mathsf{s}}^{\bar{n}_2} \cdots U_{\mathsf{s}_{\bar{M}}\mathsf{s}}^{\bar{n}_M} |\mathsf{s}\rangle, \tag{4.5}$$

($\bar{n}_i = 0, 1$) will include all of the spin configurations degenerate with $|\mathsf{s}\rangle$. Taking global spin inversion into account, the degeneracy of $|\mathsf{s}\rangle$ is

$$D_{\ell(|\mathsf{s}\rangle,\{\mathcal{J}_\alpha^m\})} \leq 2^{M(\{\mathcal{J}_\alpha^m\})+1}, \tag{4.6}$$

where, for a system defined by the coupling constants $\{\mathcal{J}_\alpha^m\}$, the index $\ell(|\mathsf{s}\rangle, \{\mathcal{J}_\alpha^m\}))$ denotes the level ℓ the state $|\mathsf{s}\rangle$ belongs to. The set $\{|\bar{n}_1 \bar{n}_2 \cdots \bar{n}_M\rangle\}$ may contain additional states not degenerate with $|\mathsf{s}\rangle$ (Subsection 4.6.3).

After averaging over disorder, the expected number of the linearly independent satisfied constraints $\overline{\mathsf{Sat}}_{|\mathsf{s}\rangle}$ is

$$\langle M \rangle_m \equiv \sum_{\{\mathcal{J}_\alpha^m\}} \sum_{\mathsf{C}_{\bar{\mathsf{j}}} \in \overline{\mathsf{Sat}}_{|\mathsf{s}\rangle}} P(\{\mathcal{J}_\alpha^m\}) \delta^{\{\mathcal{J}_\alpha^m\}}(\mathsf{C}_{\bar{\mathsf{j}}}) \equiv \sum_{\mathsf{C}_{\bar{\mathsf{j}}} \in \overline{\mathsf{Sat}}_{|\mathsf{s}\rangle}} \mathcal{P}(\mathsf{C}_{\bar{\mathsf{j}}}). \tag{4.7}$$

Here, $\mathcal{P}(\mathsf{C}_{\bar{\jmath}})$ is the probability that a linearly independent constraint $\mathsf{C}_{\bar{\jmath}}$ is satisfied. The Kronecker $\delta^{\{\mathcal{J}_\alpha^m\}}(\mathsf{C}_{\bar{\jmath}})$ equals 1 if $\mathsf{C}_{\bar{\jmath}}$ is satisfied for the couplings $\{\mathcal{J}_\alpha^m\}$ and is zero otherwise. Let us bound the probability $\mathcal{P}(\mathsf{C}_{\bar{\jmath}})$ by taking the form (4.2) of the coupling distribution into account. From the definition of the couplings $\{\mathcal{J}_\alpha^m\}$, the sum in Eq. (4.4) can effectively be read as including a sum over layers $k = 1, \ldots, m$, which hence includes $g_{\bar{\jmath}}m$ non-zero terms. For general $m \geq 1$, and even $g_{\bar{\jmath}}m$, the probability that half of the nonzero integers $n_\alpha J_\alpha^{(k)}$ in Eq. (4.4) are $+1$ and the remainder are -1 is

$$\mathcal{P}(\mathsf{C}_{\bar{\jmath}}) = \binom{g_{\bar{\jmath}}m}{\frac{g_{\bar{\jmath}}m}{2}} \frac{1}{2^{g_{\bar{\jmath}}m}} < \frac{1}{\sqrt{g_{\bar{\jmath}}m}}. \tag{4.8}$$

(Eq. (4.4) cannot be satisfied for odd $g_{\bar{\jmath}}m$.) From asymptotic analysis [31] and Eq. (4.8), the probability $\mathcal{P}(\mathsf{C}_{\bar{\jmath}})$ scales (for large m) as (and, for any m, is bounded by) $1/\sqrt{g_{\bar{\jmath}}m}$. Denoting by $g_{\min}$ the smallest possible value of $g_{\bar{\jmath}}$ for the graph/lattice at hand,

$$\langle M \rangle_m \leq \frac{\mathcal{M}}{\sqrt{g_{\min}m}}. \tag{4.9}$$

On a general graph, the number $\mathcal{M}$ of linearly *independent* constraints $\mathsf{C}_{\bar{\jmath}}$ on the coupling constants $\{\mathcal{J}_\alpha^m\}$ cannot be larger than their total number, $\mathcal{M} \leq \mathcal{L}$, i.e., the number of links $\mathcal{L}$ on this graph. Putting all of the pieces together, Eqs. (4.6) and (4.9) imply

$$\sum_{\{\mathcal{J}_\alpha^m\}} P(\{\mathcal{J}_\alpha^m\}) \ln D_{\ell(|\mathsf{s}\rangle,\{\mathcal{J}_\alpha^m\})} \leq (1 + \frac{\mathcal{L}}{\sqrt{g_{\min}m}}) \ln 2. \tag{4.10}$$

Trying to evaluate the l.h.s. of Eq. (4.10) we must take into account that whatever $|\mathsf{s}\rangle$ we pick might be a ground state for some coupling configurations, but will be an excited state for others. Hence we cannot directly infer a bound to the average entropy $\mathcal{S}_\ell$ from (4.10). Since the inverse temperature $1/(k_B T) = \partial \ln D / \partial E$, however, the system's ground-state

degeneracy for couplings $\{\mathcal{J}_\alpha^m\}$ is typically lower than (or equal to) that of any other level ℓ (Subsection 4.6.4), i.e., $D_0 \leq D_\ell$. This monotonicity of $D(E)$ implies that, typically, $\mathcal{S}_0 N = \sum_{\{\mathcal{J}_\alpha^m\}} P(\{\mathcal{J}_\alpha^m\}) \ln D_0(\{\mathcal{J}_\alpha^m\}) \leq \sum_{\{\mathcal{J}_\alpha^m\}} P(\{\mathcal{J}_\alpha^m\}) \ln D_{\ell(|\mathsf{s}\rangle,\{\mathcal{J}_\alpha^m\})}$. Then, Eq. (4.10) yields

$$\mathcal{S}_0 \leq \left(\frac{\mathcal{L}}{N\sqrt{g_{\min} m}} + \frac{1}{N}\right) \ln 2. \tag{4.11}$$

This is the promised rigorous bound. For $p \neq 1/2$ one has a lower entropy density than that of $p = 1/2$. Thus, Eq. (4.11) constitutes a generous upper bound on $\mathcal{S}_0$ for general p. To study higher energy levels, consider the average of Eq. (4.10) over all possible 2^N reference spin configurations $|\mathsf{s}\rangle$. Performing this average and invoking the monotonicity of $D(E)$ suggests that the entropy density $\mathcal{S}_\ell$ of Eq. (4.3) of low-lying excited levels $\ell > 0$ is, typically, also bounded by the r.h.s of Eq. (4.11). For d-dimensional hypercubic lattices with periodic boundary conditions, the ratio $\mathcal{L}/N = d$ while $g_{\min} = 2d$. Thus, $\mathcal{S}_0 \leq (\sqrt{d/2m} + 1/N) \ln 2$. Eq. (4.11) further suggests that, in the thermodynamic ($N \to \infty$) limit (Subsection 4.6.5),

$$\mathcal{S}_0(m') \sim \sqrt{\frac{m}{m'}}\, \mathcal{S}_0(m) \quad \text{for finite} \quad m, m' \gg 1. \tag{4.12}$$

We now study the exact m dependence of the ground state entropies of the binomial model on the square lattice with periodic boundaries and $N = L^2$. To this end, we employed an implementation of the Pfaffian technique of counting dimer coverings of the lattice as discussed in Ref. [32], which is a generalization of earlier methods [33, 34] to fully periodic lattices. In Fig. 4.1, we present the results for the ground-state entropy, averaged over 1000

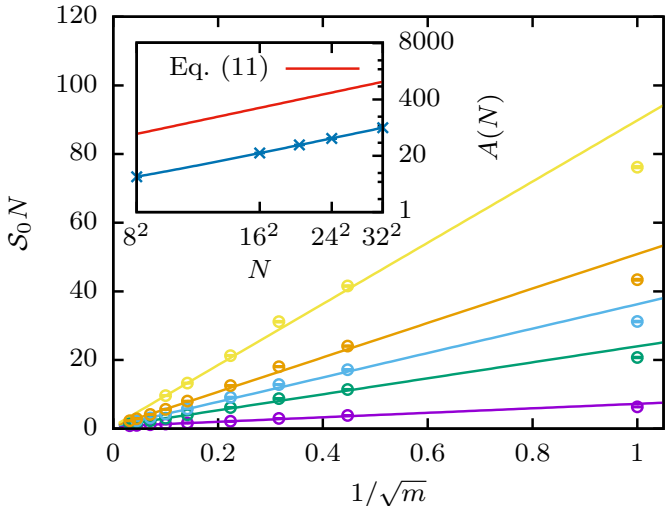

Figure 4.1: Ground-state entropy $\mathcal{S}_0 N$ of the binomial Ising spin glass with m layers, cf. Eq. (4.1), on square lattices of $N = L^2$ spins from exact ground-state calculations (from the bottom: $L = 8$, 16, 20, 24, and 32). Lines are fits of the form of (4.13) to the data for sufficiently large m. The inset shows the linear scaling of the amplitude $A(N)$. The top line indicates the constraint imposed by the upper bound (4.11).

coupling realizations for each lattice size. The data are well described by

$$\mathcal{S}_0 N = \left(\frac{A(N)}{\sqrt{m}} + 1 \right) \ln 2. \tag{4.13}$$

Linear fits in $1/\sqrt{m}$ for fixed N work well for sufficiently large m, as is illustrated by the straight lines in Fig. 4.1. Thus, for any finite N, as $m \to \infty$ the ground-state entropy is equal to $\ln 2$, implying a single degenerate ground-state pair. The slope $A(N)$ shown in the inset follows a linear behavior, $A(N) = aN + b$, and we find $a = 0.0858(4)$ and $b = 1.09(12)$. For not too small m, our data are hence fully consistent with

$$\mathcal{S}_0 = \left(\frac{a}{\sqrt{m}} + \frac{1}{N} + \frac{b}{N\sqrt{m}} \right) \ln 2. \tag{4.14}$$

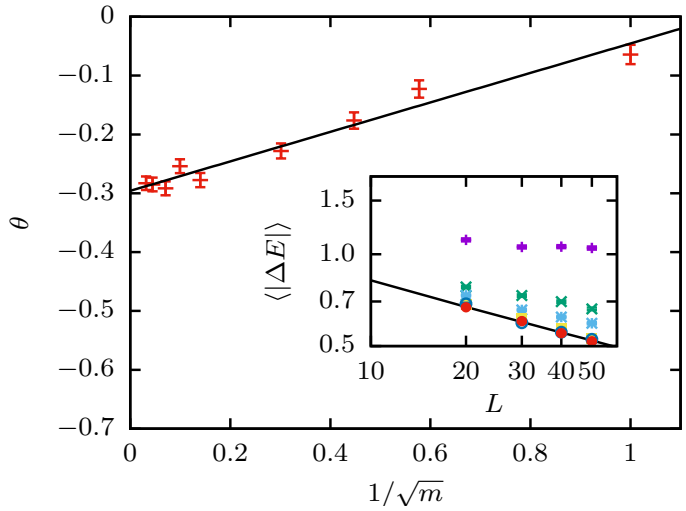

Figure 4.2: Effective spin stiffness exponents $\theta = \theta(m)$ resulting from fits of the power law $\langle|\Delta E|\rangle = BL^{\theta}$ to the defect energies for the binomial model of m layers (inset, from the top: $m = 1$, 5, 11, 51, 201, and 1001), averaged over 10 000 disorder samples. The solid line of the inset corresponds to the Gaussian model.

When $N \gg \sqrt{m} \gg 1$, Eq. (4.14) is consistent with the physically inspired (Subsection 4.6.5) scaling of Eq. (4.12). For large N, the bound of Eq. (4.11) would have been asymptotically saturated if $a \simeq 1$, far larger than the actual value of a. The behavior in the double limit $m, N \to \infty$ is subtle: (1) for $m \to \infty$, N finite, we have a single ground-state pair; (2) for $N \to \infty$, m finite, there is a finite ground-state entropy $\sim \ln 2/\sqrt{m}$; (3) for $N \to \infty$, $m \to \infty$, $\kappa = N/\sqrt{m}$ fixed, there is a finite number $2^{a\kappa}$ of ground-state pairs. Thus clearly the continuum and thermodynamic limits are not commutative in general. Note further that according to the bound $\mathcal{S}_0 \leq (\sqrt{d/2m} + 1/N) \ln 2$ for hypercubic lattices additional rich behavior is expected if the limit of high dimensions is correlated with that of large m.

4.4 Energy excitations

Let us turn to the study of excitations. By construction, cf. Eq. (4.4), for finite m the energy is "quantized" in multiples of $1/\sqrt{m}$. It is therefore natural to expect a closing of the spectral gap as $m \to \infty$. That this is indeed the case can be shown rigorously for the one-dimensional binomial spin glass in its thermodynamic limit, with different behaviors for odd and even m, see the discussion in Subsection 4.6.6. The closing of the gap is a consequence of the existence of (rare) local excitations, i.e., finite-size clusters of almost free spins (Subsection 4.6.7). Whether gapless *non-local* excitations exist and which form they take in the thermodynamic limit is a long-standing question [35]. One possible approach of investigating such excitations consists of subjecting individual samples to a system spanning perturbation by a change of boundary condition and studying how this affects the energy and configuration of the ground state. Such defect energy calculations [36] enable us to extract a scaling $\langle|\Delta E|\rangle \sim L^\theta$ of the defect energies with the spin stiffness exponent θ. Generalizing Peierls' argument [37–40] for the stability of the ordered phase, one should find $\theta > 0$ for cases where there is a finite-temperature spin-glass phase, and $\theta \leq 0$ otherwise. The latter case is expected for dimensions $d = 1$ and $d = 2$, whereas θ is positive for $d \geq 3$ [41, 42]. We employed techniques based on minimum-weight perfect matching [43, 44] to perform such calculations for the binomial model on the square lattice. The resulting disorder-averaged defect energies from *exact* ground-state calculations for samples with periodic and antiperiodic boundaries are shown in the inset of Fig. 4.2. As m increases, the decay of defect energies as a function of L becomes steeper and the data approach the behavior of the Gaussian EA model. The effective spin stiffness exponents θ extracted from fits of the type $\langle|\Delta E|\rangle = BL^\theta$ are shown in the main panel of Fig. 4.2. These exponents appear to interpolate smoothly between the limiting cases of the Gaussian model with $\theta = -0.2793(3)$

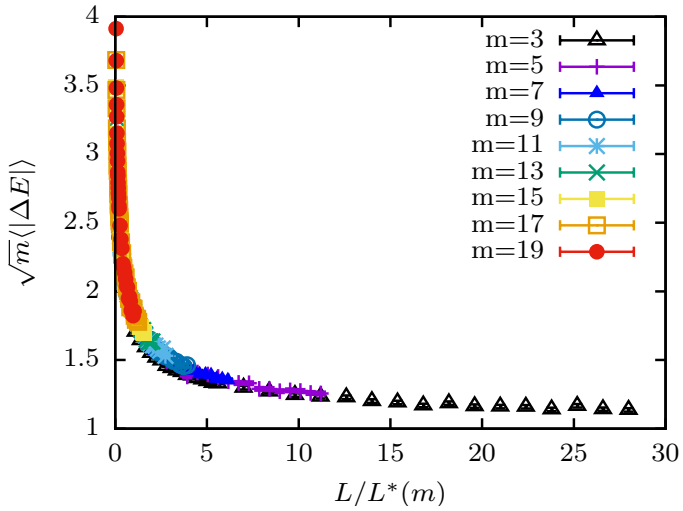

Figure 4.3: Scaling collapse of the defect energies of the binomial model for system sizes rescaled with the crossover length scale $L^*(m) \sim m^\kappa$ with $\kappa = 1.79$.

and the $\pm J$ system with $\theta = 0$ [41, 44]. Asymptotically, however, we expect that $\theta(m) = 0$ for any finite value of m when $L \gtrsim L^*(m)$. The scaling of the crossover length $L^*(m) \sim m^\kappa$ follows by considering the model with the unscaled couplings $\sqrt{m}\mathcal{J}_\alpha^m$, for which the energy gap Δ is independent of m. The discreteness of the spectrum becomes apparent once the corresponding defect energies $\sqrt{m}\langle|\Delta E|\rangle \sim L^\theta$ have decayed below the size of the gap, i.e., for

$$L \geq L^*(m) \sim m^{-1/(2\theta)},$$

such that $\kappa = -1/(2\theta)$. For the $d = 2$ system we have $\theta = -0.2793(3)$ [44], such that $\kappa = 1.790(2)$, which is in excellent agreement with the actual defect energies for our system shown in Fig. 4.3.

It is clear that if $\theta < 0$, as is the case for the Gaussian spin glass in two dimensions, excitations of a divergent length scale may entail a vanishing energy penalty. At zero temperature, the discreteness of the spectrum is then always seen at large scales $L \gtrsim L^*(m)$. On the other hand, for $\theta \geq 0$ (i.e., $d \geq 3$), the above arguments imply that the discreteness does not

matter at large scales. Also, in this case one should inspect the full probability distribution of domain wall energies and the weight it carries in the limit $\Delta E \to 0$ (Subsection 4.6.7). In how far such excitations correspond to incongruent states, however, one might only be able to infer by inspecting the configurations themselves.

4.5 Summary

In summary, we introduced and discussed the *binomial spin glass*. This class of models affords controlled access to the enigmatic continuous ($m \to \infty$) finite dimensional EA model. Its $m = 1$ realization is the quintessential discrete spin glass, the $\pm J$ model. We derived bounds on the spectral degeneracy of the binomial Ising spin glass on general graphs and suggested an asymptotic scaling that is fully supported by exact two-dimensional calculations. The behavior of defect energies suggests the existence of a crossover length $L^*(m) \sim L^{-1/2\theta}$ below which the binomial model behaves like the Gaussian system. Our results show that the existence of degeneracies depends on the particular way of taking the thermodynamic ($N \to \infty$) and continuous coupling ($m \to \infty$) limits, and limiting states with and without degeneracies can be reached by corresponding correlated limiting processes, thus accommodating theories that postulate degeneracies as well as pictures stipulating a unique ground-state pair. An intriguing prediction regards an effectively negative crossover scaling exponent in three dimensions, where hence discreteness of the spectrum is expected not to matter at large scales.

The physics of spin-glass models and, in particular, the role of degeneracies has also recently attracted attention from another side. In the context of quantum annealing [45] as implemented in the devices by D-Wave and similar machines that are being developed by

competing consortia, degeneracies are not a desired feature as the quantum annealing process does not sample such states uniformly [46]. On the other hand, continuous coupling distributions may also be undesired because of increased susceptibility to external noise implied by chaos in spin glasses [47–50]. Our binomial glasses may allow for realizations that suffer the least from these combined problems. While the present system is already a generalization of the usually considered spin-glass models, we believe that the approach of decomposing continuous couplings into discrete layers and the intriguing consequences it allowed us to uncover in terms of the general non-commutativity of the thermodynamic and continuous coupling limits is promising and we expect exciting applications to models in other fields.

Acknowledgements

This research was partially supported by the NSF CMMT under grant number 1411229.

4.6 Supplementary information

4.6.1 Supplementary information 1: The trivial ground state pair given an assignment of link variables

Given the definition of the link variable $z_\alpha \equiv s_{\mathsf{x}} s_{\mathsf{y}}$, a moment's reflection reveals that

$$s_{\mathsf{y}} = s_{\mathsf{x}} \prod_{\alpha \in \Gamma_{\mathsf{xy}}} z_\alpha, \tag{4.15}$$

where Γ_{xy} is any path on the lattice, composed of nearest-neighbor links, joining site x to site y. Thus, with $s_{\mathsf{y}}|_{|\mathsf{s}\rangle}$ denoting the value of the spin at site y in configuration $|\mathsf{s}\rangle$, we have that

$$s_{\mathsf{y}}|_{|\mathsf{s}\rangle} = s_{\mathsf{x}}|_{|\mathsf{s}\rangle} \prod_{\alpha \in \Gamma_{\mathsf{xy}}} z_\alpha|_{|\mathsf{s}\rangle} \ , s_{\mathsf{y}}|_{|\mathsf{s}'\rangle} = s_{\mathsf{x}}|_{|\mathsf{s}'\rangle} \prod_{\alpha \in \Gamma_{\mathsf{xy}}} z_\alpha|_{|\mathsf{s}'\rangle}. \tag{4.16}$$

Now, if for all links α, the values of z_α are the same in both configurations $|\mathsf{s}\rangle$ and $|\mathsf{s}'\rangle$ (i.e., if $\{z_\alpha\}|_{|\mathsf{s}\rangle} = \{z_\alpha\}|_{|\mathsf{s}'\rangle}$) then, trivially,

$$\prod_{\alpha \in \Gamma_{\mathsf{xy}}} z_\alpha|_{|\mathsf{s}\rangle} = \prod_{\alpha \in \Gamma_{\mathsf{xy}}} z_\alpha|_{|\mathsf{s}'\rangle}. \tag{4.17}$$

Taken together, Eqs. (4.16) and (4.17) imply that if, at a particular site x, the spin configurations $|\mathsf{s}\rangle$ and $|\mathsf{s}'\rangle$ share the same value of the spin, $s_{\mathsf{x}}|_{|\mathsf{s}'\rangle} = s_{\mathsf{x}}|_{|\mathsf{s}\rangle}$, then the spins must be identical at all other lattices sites y, $s_{\mathsf{y}}|_{|\mathsf{s}'\rangle} = s_{\mathsf{y}}|_{|\mathsf{s}\rangle}$. This, however, leads to a contradiction as $|\mathsf{s}'\rangle \neq |\mathsf{s}\rangle$. Therefore, if two distinct spin configurations satisfy condition (**i**) it must be

that the respective spin values at any lattice site x are different, $s_{\mathsf{x}}|_{|\mathsf{s}'\rangle} = -s_{\mathsf{x}}|_{|\mathsf{s}\rangle}$. That is,

$$s_{\mathsf{y}}|_{|\mathsf{s}'\rangle} = -s_{\mathsf{y}}|_{|\mathsf{s}\rangle}, \quad \forall \mathsf{y}. \tag{4.18}$$

Hence, if $n_\alpha = 0, \forall \alpha$ in Eq. (4.4), then there are, trivially, only two degenerate configurations ($|\mathsf{s}'\rangle \neq |\mathsf{s}\rangle$) related by a global spin inversion. The above simple proof applies for arbitrary energy levels. Replicating, *mutatis mutandis*, the above argument to a general set of (non-necessarily vanishing) integers $\{n_\alpha\}$ over all lattice links α, illustrates that any set $\{n_\alpha\}$ may correspond to exactly two unique spin configurations.

4.6.2 Supplementary information 2: Graphical Representation of the Constraints

In Section 4.3, we defined $\mathsf{Sat}_{|\mathsf{s}\rangle}$ to be the set composed of *all* constraints C_j satisfying the relation $\Delta E = E(\mathsf{s}) - E(\mathsf{s}') = 0$, in Eq. (4.4). We also defined the subset $\overline{\mathsf{Sat}}_{|\mathsf{s}\rangle} \subset \mathsf{Sat}_{|\mathsf{s}\rangle}$, comprising *all linearly independent* constraints. Here, we further introduce a restricted subset of constraints, that of *geometrically disjoint* and independent zero energy domain walls, $\overline{\mathsf{Sat}^{\mathsf{g}}}_{|\mathsf{s}\rangle} \subset \overline{\mathsf{Sat}}_{|\mathsf{s}\rangle}$. The subset $\overline{\mathsf{Sat}^{\mathsf{g}}}_{|\mathsf{s}\rangle}$ is defined by having no pair of different constraints on the coupling constants that involve links associated with the same lattice sites x.

In what follows, we provide a few simple examples illuminating the above definitions. To this end, we consider a 5×5 square lattice with binomial couplings $\{\mathcal{J}_\alpha^m\}$ (Fig. 4.4). We start with a random spin configuration $|\mathsf{s}\rangle$ (panel (a)). Panels (b) through (e), represent spin configurations $|\mathsf{s}'\rangle$ for which one or more spins are being flipped with respect to panel (a).

The energy difference in each case can be easily calculated. For example,

$$\begin{aligned}\Delta E_{a,b} &= E_a - E_b = -2(\mathcal{J}^m_{19,14} n_{19,14} \\ &+ \mathcal{J}^m_{19,18} n_{19,18} + \mathcal{J}^m_{19,20} n_{19,20} + \mathcal{J}^m_{19,24} n_{19,24}),\end{aligned} \tag{4.19}$$

gives the energy difference between spin configurations in panel (a) and (b). It is easy to see that $n_{19,18} = n_{19,20} = n_{19,24} = 1$, and $n_{19,14} = -1$. Following the same procedure we end up with,

$$\begin{aligned}\Delta E_{a,b} &= -2(-\mathcal{J}^m_{19,14} + \mathcal{J}^m_{19,18} + \mathcal{J}^m_{19,20} + \mathcal{J}^m_{19,24}), \\ \Delta E_{a,c} &= -2(\mathcal{J}^m_{8,3} + \mathcal{J}^m_{8,7} + \mathcal{J}^m_{8,9} + \mathcal{J}^m_{8,13}), \\ \Delta E_{a,d} &= -2(-\mathcal{J}^m_{7,2} + \mathcal{J}^m_{7,6} + \mathcal{J}^m_{8,3} + \mathcal{J}^m_{8,9} + \mathcal{J}^m_{8,13} \\ &\quad -\mathcal{J}^m_{12,11} - \mathcal{J}^m_{12,13} - \mathcal{J}^m_{12,17}), \\ \Delta E_{a,e} &= \Delta E_{a,b} + \Delta E_{a,d} \\ &= -2(-\mathcal{J}^m_{19,14} + \mathcal{J}^m_{19,18} + \mathcal{J}^m_{19,20} + \mathcal{J}^m_{19,24} \\ &\quad -\mathcal{J}^m_{7,2} + \mathcal{J}^m_{7,6} + \mathcal{J}^m_{8,3} + \mathcal{J}^m_{8,9} + \mathcal{J}^m_{8,13} \\ &\quad -\mathcal{J}^m_{12,11} - \mathcal{J}^m_{12,13} - \mathcal{J}^m_{12,17}).\end{aligned} \tag{4.20}$$

Now, assume $\mathsf{C_1}, \mathsf{C_2}, \mathsf{C_3}$, and $\mathsf{C_4}$ are constraints associated with $\Delta E_{a,b}, \Delta E_{a,c}, \Delta E_{a,d}, \Delta E_{a,e}$, respectively. If these constraints are satisfied, i.e., $\Delta E_{a,,b} = \Delta E_{a,c} = \Delta E_{a,d} = \Delta E_{a,e} = 0$, for certain coupling realizations, then they belong to the set $\mathsf{Sat}_{|\mathsf{s}\rangle}$. That is, $\mathsf{C_1}, \mathsf{C_2}, \mathsf{C_3}, \mathsf{C_4} \in \mathsf{Sat}_{|\mathsf{s}\rangle}$.

To understand this better, consider the case $m = 4$. From Eq. (4.2), couplings $\mathcal{J}_\alpha^4$ may acquire the values $-2, -1, 0, 1, 2$. In Fig. 4.5, we provide three examples of random coupling realizations. The spin configuration is the same as in panel (a) of Fig. 4.4. From Eq. (4.20) and Fig. 4.5, we can see that, only $\mathsf{C_3}$ in panel (a), none in panel (b), and only $\mathsf{C_1}$ in panel (c) are satisfied.

In order to create the subset $\overline{\mathsf{Sat}}_{|\mathsf{s}\rangle}$, we should note that it is not necessarily unique, since we may have different linearly independent constraints that span the same set of conditions in $\mathsf{Sat}_{|\mathsf{s}\rangle}$. In addition to that, the satisfaction of constraints depends on the coupling realizations as well. For instance, if for a given realization, $\mathsf{C_1}, \mathsf{C_2}$ and $\mathsf{C_3}$ are satisfied, trivially from Eq. (4.20) (i.e., $\Delta E_{a,e} = \Delta E_{a,b} + \Delta E_{a,d}$), $\mathsf{C_4}$ is automatically satisfied. Therefore, for such cases, $\mathsf{C_4}$ is a linear combination of $\mathsf{C_1}$ and $\mathsf{C_3}$, and one may define the subset $\overline{\mathsf{Sat}}^{(\mathsf{I})}_{|\mathsf{s}\rangle}$ for which $\mathsf{C_1}, \mathsf{C_2}, \mathsf{C_3} \in \overline{\mathsf{Sat}}^{(\mathsf{I})}_{|\mathsf{s}\rangle}$, but $\mathsf{C_4} \notin \overline{\mathsf{Sat}}^{(\mathsf{I})}_{|\mathsf{s}\rangle}$. On the other hand, there exist some realizations for which $\Delta E_{a,b} = -\Delta E_{a,d} \neq 0$, but $\Delta E_{a,e} = 0$. Meaning, $\mathsf{C_4}$ is satisfied, however, $\mathsf{C_1}$ and $\mathsf{C_3}$ are not.

The geometrically disjoint constraints may also give rise to different subsets. For instance, from Fig. 4.4, one can trivially show that the pairs $\mathsf{C_1}, \mathsf{C_2}$ and $\mathsf{C_1}, \mathsf{C_3}$ are each geometrically disjoint, however, $\mathsf{C_2}$ and $\mathsf{C_3}$ are not. Therefore, we could define two different subsets $\overline{\mathsf{Sat^g}}^{(\mathsf{I})}_{|\mathsf{s}\rangle}$ and $\overline{\mathsf{Sat^g}}^{(\mathsf{II})}_{|\mathsf{s}\rangle}$ so that $\mathsf{C_1}, \mathsf{C_2} \in \overline{\mathsf{Sat^g}}^{(\mathsf{I})}_{|\mathsf{s}\rangle}$ and $\mathsf{C_1}, \mathsf{C_3} \in \overline{\mathsf{Sat^g}}^{(\mathsf{II})}_{|\mathsf{s}\rangle}$.

These examples further illustrate the difference between $\mathcal{M}$ and $M(\{\mathcal{J}_\alpha^m\})$ in Section 4.3, where $\mathcal{M}$ is associated with the maximum number of linearly independent satisfied constraints, i.e., the cardinality of $\overline{\mathsf{Sat}}_{|\mathsf{s}\rangle}$, while $M(\{\mathcal{J}_\alpha^m\})$ denotes the number of constraints satisfied for a particular realization of coupling constants. Trivially, $M(\{\mathcal{J}_\alpha^m\}) \leq \mathcal{M}$.

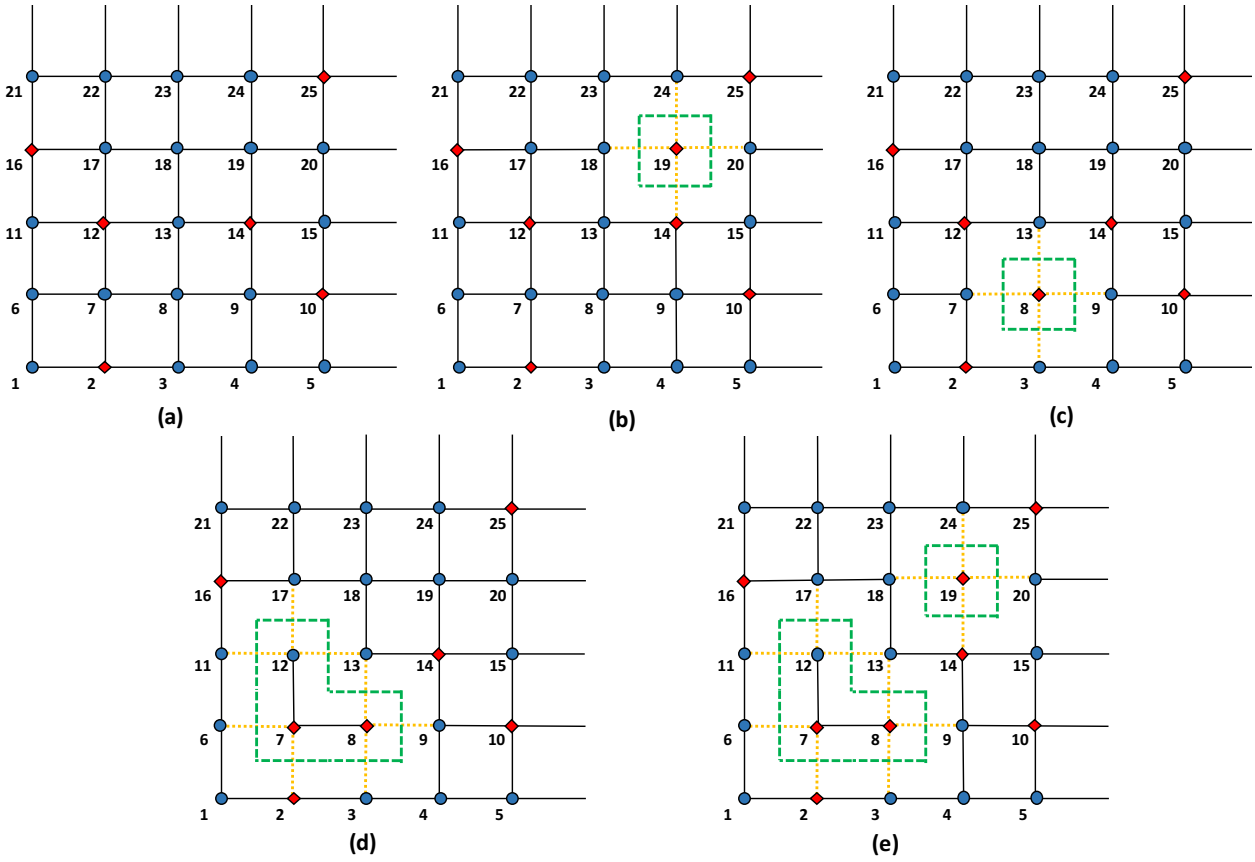

Figure 4.4: Graphical representations of the constraints. Panel (a) represents a random spin configuration. Blue solid circles and red diamonds denote spin up and down, respectively. Flipping one or more spins at different sites of panel (a) would result in new spin configurations such as in panels (b) through (e) (e.g., the spin configuration of panel (b) is obtained from flipping the spin at site 19 of panel (a)). The dashed yellow dotted lines represent the links that contribute to the energy difference. The green dashed lines crossing such links correspond to a domain wall.

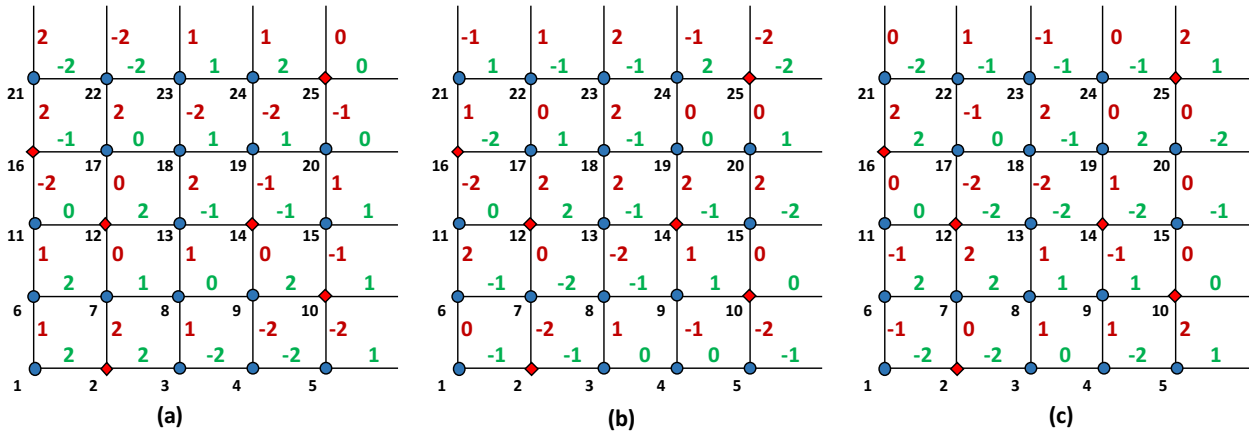

Figure 4.5: Three examples of coupling realizations for the binomial model with $m = 4$ (i.e., $\mathcal{J}_\alpha^4 = -2, -1, 0, 1, 2$). The numbers in green (brown) color provide the values of horizontal (vertical) coupling constants.

4.6.3 Supplementary information 3: Meaning of Equation (4.5)

In Eq. (4.5), we mentioned that the set $\{|\bar{n}_1\bar{n}_2\cdots\bar{n}_M\rangle\}$ includes all of the spin configurations degenerate with $|\mathsf{s}\rangle$. We also pointed out that it may contain additional states not degenerate with $|\mathsf{s}\rangle$. The latter point is usually associated with the domain walls that are not geometrically disjoint (see Subsection 4.6.2). To accentuate this consider, e.g., a 5×5 lattice with a given random spin configuration and coupling constants (see panel (a) of Fig. 4.6), in which $U_{\mathsf{ba}}, U_{\mathsf{ca}}$, and U_{da} are spin flip operators leading, respectively, to zero energy domain walls around the sites $7, 18$ and 19 (corresponding to panels (b),(c) and (d)).

From Fig. 4.6, the domain walls in panel (c) and (d) are not geometrically disjoint, where U_{ca} and U_{da} act on the *nearest neighbor* sites 18 and 19 such that the sign of the link connecting them, is altered by both operators. In such a case, even though the two states $U_{\mathsf{ca}}|\mathsf{a}\rangle \equiv |\mathsf{c}\rangle$ and $U_{\mathsf{da}}|\mathsf{a}\rangle \equiv |\mathsf{d}\rangle$ are degenerate with $|\mathsf{a}\rangle$, the state $U_{\mathsf{da}}U_{\mathsf{ca}}|\mathsf{a}\rangle \equiv |\mathsf{e}\rangle$ (i.e., from panel (e),

$U_{\mathsf{ea}} = U_{\mathsf{da}}U_{\mathsf{ca}}$) is not degenerate with $|\mathsf{a}\rangle$. One should note that in general this might not be true. That is, for some coupling realizations the state $|\mathsf{e}\rangle$ can be degenerate with $|\mathsf{a}\rangle$.

By contrast, the two spin flip operators U_{ba} and U_{da} associated with the geometrically disjoint domain walls in panel (b) and (d), respectively, do not alter the signs of any common links. Therefore, the state $U_{\mathsf{da}}U_{\mathsf{ba}}|\mathsf{a}\rangle \equiv |\mathsf{f}\rangle$ (i.e., from panel (f), $U_{\mathsf{fa}} = U_{\mathsf{da}}U_{\mathsf{ba}}$) is degenerate with $|\mathsf{a}\rangle$.

4.6.4 Supplementary information 4: The ground state entropy is bounded by the entropy of a random energy level

In deriving the bound of Eq. (4.11), we assumed that no information other than the probability distribution $P(\{\mathcal{J}_\alpha^m\})$ is provided. The configuration $|\mathsf{s}\rangle$ that we considered in Section 4.3 was an arbitrary random state. We next consider a more sophisticated problem. Suppose that the coupling constants are drawn from a binomial distribution and that once chosen a *ground state configuration* $|\mathsf{s}\rangle$ is given (i.e., the values of the spins s_{x} at all sites x in this ground state are provided). We then calculate the average of Eq. (4.7) with the condition that the (otherwise random binomial) coupling constants admit the particular configuration $|\mathsf{s}\rangle$ as *a ground state*. When applicable, the fact that $|\mathsf{s}\rangle$ is a ground state may generally yield nontrivial constraints on the coupling constants $\{J_\alpha^{(k)}\}$ (recall that $\mathcal{J}_\alpha^m \equiv \frac{1}{\sqrt{m}}\sum_{k=1}^m J_\alpha^{(k)}$). In such a situation, given the configuration $|\mathsf{s}\rangle$, we may not simply use the initial binomial distribution for the coupling constants.

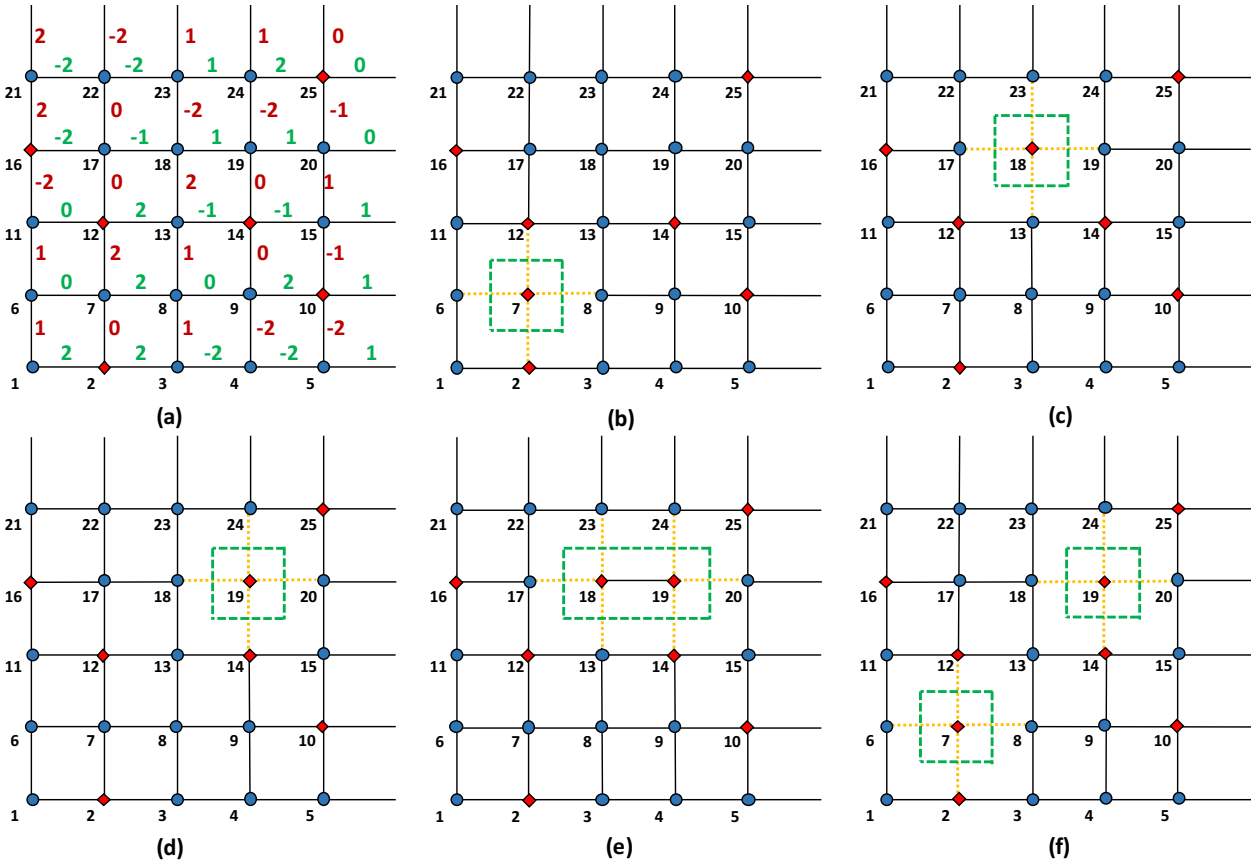

Figure 4.6: Panel (a) represents a random spin configuration with some given coupling constants. Blue solid circles and red diamonds denote spin up and down, respectively. The numbers in green (brown) color provide the values of horizontal (vertical) coupling constants. Flipping one or more spins at different sites of panel (a) would result in new spin configurations such as in panels (b) through (f). The dashed yellow dotted lines represent the links that contribute to the energy difference. The green dashed lines crossing such links correspond to a domain wall. Please note that the values associate with different links in each panel is the same as in panel (a).

We now trivially demonstrate that if the energy density associated with the high temperature limit is unique then Eq. (4.11) constitutes an upper bound on the average ground state entropy density even if such information was provided for each realization of $\{J_\alpha^{(k)}\}$. This assertion follows as the entropy $S_\ell(\{J_\alpha^{(k)}\})$ associated with any energy $E = E_\ell$ is typically larger than the ground state entropy,

$$S_0 \leq S_\ell. \tag{4.21}$$

The proof of Eq. (4.21) is rather elementary and relies on a trivial symmetry of the spectrum. Let us denote the two sublattices forming the large bipartite lattice by A and B. If we flip all spins in sublattice A (i.e., $s_{\mathsf{x}\in\mathsf{A}} \to -s_{\mathsf{x}\in\mathsf{A}}$) and do not alter those in sublattice B ($s_{\mathsf{y}\in\mathsf{B}} \to s_{\mathsf{y}\in\mathsf{B}}$), then all nearest-neighbor links (i.e., the products $s_{\mathsf{x}}s_{\mathsf{y}}$ for nearest neighbor sites x and y) on the original lattice change their sign, $z_\alpha \to -z_\alpha$. This single sublattice spin inversion constitutes a one-to-one mapping of the Ising spin states, that changes the sign of the total energy ($E \to -E$). We may thus conclude that as a function of the energy E, the entropy density $\mathcal{S} = S(\{J_\alpha^{(k)}\})/N$ for a system with fixed couplings $\{J_\alpha^{(k)}\}$ satisfies the simple relation $\mathcal{S}(E_\ell) = \mathcal{S}(-E_\ell)$ where E_ℓ is the energy of the ℓ-th level. It follows that the energy $E = 0$ is an extremum of the entropy density $\mathcal{S}(E) \equiv \mathcal{S}(E_\ell)$. Consequently, for any fixed couplings $\{J_\alpha^{(k)}\}$,

$$\frac{1}{T} = N\frac{\partial \mathcal{S}}{\partial E} \geq 0. \tag{4.22}$$

(The factor of N appears in the above equation since $\mathcal{S}$ is the entropy density). Thus, $E \leq 0$ for any positive temperature T. In what follows we discuss what occurs if there is a *unique* high temperature limit for each set of coupling constants. In such a case, the entropy density $\mathcal{S}(E)$ (averaged over all realization of the coupling constants) is maximal at $E = 0$. The

semi-positive definite nature of the derivative in Eq. (4.22) implies (as in all common systems satisfying the third law of thermodynamics) that the entropy is lowest at $T = 0$. Since the state $|\mathsf{s}\rangle$ for which we performed the analysis was arbitrary (and corresponds to an energy $E_{|\mathsf{s}\rangle}$ for which the entropy density is greater than or equal to that of the ground state), we see that Eq. (4.22) must hold even if information is provided as to the explicit ground state configuration $|\mathsf{s}\rangle$ for each particular realization of the couplings $\{J_\alpha^{(k)}\}$. We thus observe that even if given such additional information, the ground state entropy density must satisfy the bound of Eq. (4.11).

4.6.5 Supplementary information 5: Asymptotic Scaling of the Entropy Density

We now motivate a scaling that the rigorous bound of Eq. (4.11) suggests Eq. (4.12) as an approximate asymptotic relation for large N and m. In Section 4.6.2 of this supplemental material, we defined the subset $\overline{\mathsf{Sat}^{\mathsf{g}}}_{|\mathsf{s}\rangle} \subset \overline{\mathsf{Sat}}_{|\mathsf{s}\rangle}$ composed of geometrically disjoint constraints. If there are n_g such constraints (or associated zero energy domain walls when these constraints are satisfied) then the degeneracy will be trivially bounded from below by 2^{n_g}. This bound is established by noting that, since no spin is common to two domain walls, all of the spins in each of these n_g domain walls may be flipped independently of all others. When applied to domain walls in $\overline{\mathsf{Sat}^{\mathsf{g}}}_{|\mathsf{s}\rangle}$ then, in the notation of Eq. (4.5), each binary string of length n_g will correspond to a different configuration that is degenerate with the reference state $|\mathsf{s}\rangle$. This is to be contrasted with the set of zero energy domain walls $\overline{\mathsf{Sat}}_{|\mathsf{s}\rangle}$ for which various binary strings of the form of Eq. (4.5) may correspond to states that are *not* degenerate with $|\mathsf{s}\rangle$.As m grows, by Eq. (4.8), both the number of satisfied constraints and the number of independent zero energy domain walls may diminish as $1/\sqrt{m}$. When

fewer walls appear in $\overline{\mathsf{Sat}}_{|\mathsf{s}\rangle}$, it may become increasingly rare for different walls in this subset to share the same lattice sites. If this occurs then, for large m, we will have the asymptotic relation $\overline{\mathsf{Sat}^{\mathsf{g}}}_{|\mathsf{s}\rangle} \sim \overline{\mathsf{Sat}}_{|\mathsf{s}\rangle}$. In such a case, in the large N limit, $\mathcal{S} \sim n_g/N \ln 2$. The number n_g and the probability of these zero energy domain walls decay, for $m \gg 1$, as $1/\sqrt{m}$ (or $1/\sqrt{m'}$ for $m' \gg 1$). Similarly, if a finite fraction of the M domain walls in $\overline{\mathsf{Sat}}_{|\mathsf{s}\rangle}$ does not remain geometrically disjoint such that, asymptotically, one may only generate q^M (with $q < 2$) degenerate states (Eq. (4.5)) given M independent domain walls, then $\mathcal{S} \sim \frac{M}{N} \ln q$. Either way, we anticipate that in the thermodynamic limit that Eq. (4.12) will hold.

4.6.6 Supplementary information 6: One-dimensional Binomial Spin Glass

Let us start with the simplest one-dimensional binomial spin glass system (which by a simple change of variables ($s_{\mathsf{x}} \to s'_{\mathsf{x}} \equiv s_{\mathsf{x}} \prod_{\mathsf{u}<\mathsf{x}} \mathsf{sign}(\mathcal{J}^m_{\mathsf{u},\mathsf{u}+1})$) may be transformed onto a random Ising ferromagnet with couplings $|\mathcal{J}^m_{\mathsf{x}',\mathsf{x}'+1}|$). Here, the ground state energy $E_0 = -\sum_x |\mathcal{J}^m_{\mathsf{x},\mathsf{x}+1}|$. In an open chain of N sites, the lowest excitation consists of identifying the weakest link, $|\mathcal{J}^m_{\mathsf{x}',\mathsf{x}'+1}| \equiv \min_{\mathsf{x}}\{|\mathcal{J}^m_{\mathsf{x},\mathsf{x}+1}|\}$ and flipping all spins $s_{\mathsf{x}} \to -s_{\mathsf{x}}$ for which $\mathsf{x} > \mathsf{x}'$ (or consistently doing the same thing and only flipping all spins to the left of x'); this generates a state that has an energy $E_0 + \Delta E_{\min}$ with $\Delta E_{\min} = 2|\mathcal{J}^m_{\mathsf{x}',\mathsf{x}'+1}|$. (On a periodic chain, we may similarly identify the two weakest links and flip all spins lying between those two links leading to an energy cost $\Delta E_{\min}$ that is twice the sum of the moduli of these two weakest links.) Calculations of the density of states and all ensuing thermodynamic properties are trivial [51]. For instance, the disorder averaged entropy in the low temperature, $T \ll 1$, limit of the binary model is $[S_{m=1}(T)] \sim k_B(\ln 2 + (N-1)(1+2\beta)e^{-2\beta})$, with $\beta = 1/(k_B T)$. The exponential suppression becomes $e^{-2\beta/\sqrt{m}}$ and $e^{-4\beta/\sqrt{m}}$ for odd and even m, respectively.

Thus the excitation gap scales as $m^{-1/2}$ (*yet differently for odd and even* m). By contrast, the low-T entropy of the continuum model is $[S_{m\to\infty}(T)] \sim k_B(\ln 2 + \frac{N-1}{\sqrt{2\pi}}(k_BT - \frac{(k_BT)^3}{8}))$, indicating the vanishing of the spectral gap in the thermodynamic limit. In that limit, these lowest excitations differ, relative to the ground state, by an extensive number of flipped spins.

4.6.7 Supplementary information 7: Distribution of excitations

Given any *ground state* configuration on a hypercubic lattice in d dimensions, one may compute the probability distribution for excitations of energy $\Delta E_{\mathsf{x}} = |\Delta E_{\mathsf{x}}| = 2\sum_{\mathsf{y}} n_{\mathsf{xy}}\mathcal{J}_\alpha^m$ generated by flipping a single spin x. Here, the sum is over all sites y that are nearest neighbor of site x and $n_{\mathsf{xy}} = -\mathsf{sign}(s_{\mathsf{x}}s_{\mathsf{y}}) = \pm 1$. Given the probability distribution for the links $\{\mathcal{J}_\alpha^m\}$, one may compute the probability distribution associated with a finite sum of these links $2\sum_{\mathsf{y}} n_{\mathsf{xy}}\mathcal{J}_\alpha^m$ in the ground state. The latter sum is that over a finite number of links (with bounded mean and variance) and thus for any $\epsilon > 0$ (no matter how small), the probability that $|\Delta E_{\mathsf{x}}| < \epsilon$ is strictly smaller than unity. In order for the system to have a spectral gap that is greater than ϵ, it must be that *for each of the* N *lattice sites* x, the energy penalty $|\Delta E_{\mathsf{x}}| > \epsilon$. Given that the condition $|\Delta E_{\mathsf{x}}| > \epsilon$ must, in the thermodynamic limit, be satisfied an infinite number of times, while for any single x the probability that this condition is satisfied is strictly smaller than one, it is essentially impossible to have a gap larger than any arbitrary positive number ϵ. From this, it follows that the gapless local excitations must be appear. If the local energy penalties in the ground state were independent of one another then the probability that all local flips result in an energy penalty larger than ϵ would the product of the probabilities of having $|\Delta E_{\mathsf{x}}| > \epsilon$ for all sites x. Although the local flip are not independent of one another (since they all relate to flips relative to the same special

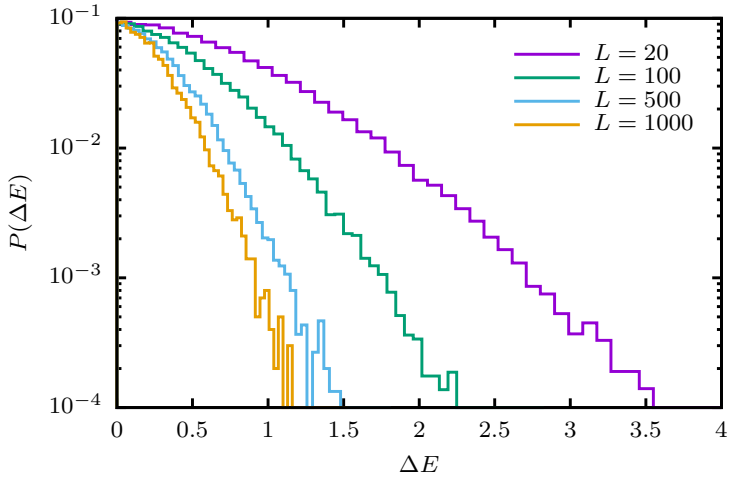

Figure 4.7: Distribution of defect energies $|\Delta E|$ for the 2D Gaussian system and a number of different system sizes. The curves collapse if rescaled by $L^{-\theta}$ with the value $\theta \approx -0.28$ of the stiffness exponent.

state- the ground state), it seems highly unlikely $|\Delta E_{\mathsf{x}}| > \epsilon$ for all x when the probability of having a local energy penalty larger than ϵ for any single x is strictly smaller than one.

We now explicitly discuss a measure that, in general dimensions, may provide physical insight – the *distribution* of such individual defect energies (i.e., the distribution of domain wall energies in our binomial Ising spin system). In Fig. 4.7, we plot this distribution in the continuous $m = \infty$ Gaussian limit. If $f(\epsilon, \tilde{l})$ denotes the cumulative probability that the energy penalty of a domain wall (of size $\tilde{l}$) is smaller than ϵ, then the probability that amongst $\mathcal{N}_{\tilde{l}}$ *independent* domain walls, no singe domain wall entails an energy cost lower than ϵ will be bounded from above by $e^{-f(\epsilon,\tilde{l})\mathcal{N}_{\tilde{l}}}$ as we briefly elaborate on now. Since, by definition, $f(\epsilon, \tilde{l})$ is the cumulative probability that the energy cost of a random wall of size $\tilde{l}$ is smaller than ϵ (i.e., $Prob.(|\Delta E| \leq \epsilon) = f(\epsilon, \bar{l})$), the probability that amongst $\mathcal{N}_{\tilde{l}}$ *independent* domain walls, we explicitly have that the probability that no single domain wall has an energy cost larger than ϵ is, trivially, $[Prob.(|\Delta E| > \epsilon)]^{\mathcal{N}_{\tilde{l}}} = (1 - f(\epsilon, \tilde{l}))^{\mathcal{N}_{\tilde{l}}} \leq e^{-\mathcal{N}_{\tilde{l}} f(\epsilon,\tilde{l})}$ (where we invoked

$e^{-f} \geq (1-f)$ for all $f \geq 0$). For small $f \to 0^+$ (associated with $\epsilon \to 0^+$ in $d \geq 3$), this general inequality is replaced by an equality (i.e., $[Prob.(|\Delta E| > \epsilon)]^{\mathcal{N}_{\tilde{l}}} = e^{-\mathcal{N}_{\tilde{l}} f(\epsilon,\tilde{l})}$).

Thus, if the area ($d = 2$) or volume ($d = 3$) of the entire lattice is $||\Lambda||$, then whenever the sum

$$\lim_{\epsilon \to 0^+} \lim_{\tilde{l}_0 \to \infty} \lim_{N \to \infty} \sum_{||\Lambda||^{1/d} - \tilde{l}_0 \geq \tilde{l} \geq \tilde{l}_0} f(\epsilon, \tilde{l}) \mathcal{N}_{\tilde{l}} = \infty \tag{4.23}$$

then gapless (or degenerate) states of diverging $\tilde{l}$ may appear. This is so because flipping all of the spins links one ground state to its conjugate. The inequality $||\Lambda||^{1/d} - \tilde{l}_0 \geq \tilde{l} \geq \tilde{l}_0$ in Eq. (4.23) means that the an extensive number of spin flips is needed to connect a given spin configuration to either of the two members of the degenerate ground state pair.

Since $\theta_{d=2} < 0$ then (as is further underscored in the full distribution of Fig. 4.7), in two dimensions nearly all large domain walls entail a *vanishing* energy penalty. In $d = 2$, $\lim_{\epsilon \to 0^+} \lim_{\tilde{l} \to \infty} f(\epsilon, \tilde{l}) = 1$ and the probability of obtaining, in the thermodynamic limit, degenerate states that differ by an extensive number of flipped spins is unity. The existence of gapless states in $d = 2$ is hardly surprising; such gapless states may be trivially constructed by the insertion of random domain walls of divergent size into a ground state. Indeed, in $d = 2$ (where the typical energy cost $\mathcal{O}(\tilde{l}^{\theta})$ vanishes as $\tilde{l} \to \infty$), knowledge of the detailed distribution of the energy cost as a function of the domain wall size $\tilde{l}$ is unnecessary for establishing gapless states. However, in $d \geq 3$ (where $\theta_d > 0$), the lowest energy states are related to *the asymptotic low energy limit* of the domain wall energy distribution (a distribution that, in these higher dimensions, is associated with a divergent average energy $\mathcal{O}(\tilde{l}^{\theta_d})$ when $\tilde{l} \to \infty$). A gap (for states that differ from one another by an extensive number of flipped spins) is potentially possible if the sum of Eq. (4.23) vanishes. Thus, we stress that

in $d \geq 3$, knowledge of the cumulative probability distribution $f(\epsilon, \tilde{l})$ can be of paramount importance. We reserve the analysis of the $d = 3$ domain wall energy distribution for future work.

References

[1] D. L. Stein and C. M. Newman, *Spin Glasses and Complexity* (Princeton University Press, 2013).

[2] K. H. Fischer and J. A. Hertz, Spin Glasses (Cambridge University Press, Cambridge, 1991).

[3] D. L. Stein and C. M. Newman, Complex Systems **20**, 115 (2011).

[4] J. A. Mydosh, *Spin Glasses: An Experimental Introduction* (Taylor and Francis, London, Washington D. C., 1993).

[5] V. Cannella and J. A. Mydosh Phys. Rev. B **6**, 4220 (1972).

[6] H. Nishimori, *Statistical Physics of Spin Glasses and Information Processing: An Introduction* (Oxford University Press, Oxford, 2011).

[7] H. Nishimori and G. Ortiz *Elements of Phase Transitions and Critical Phenomena* (Oxford University Press, Oxford, 2011).

[8] P. W. Anderson, Physics Today **41**(1), 9 (1988); **41**(3), 9 (1988); **41**(6), 9 (1988); **41**(9), 9 (1988); Physics Today **42**(7), 9 (1989); **42**(9), 9 (1989); **43**(3), 9 (1990).

[9] J. Lukic, A. Galluccio, E. Marinari, Olivier C. Martin, and G. Rinaldi, Phys. Rev. Lett. **92**, 117202 (2004).

[10] S. Edwards and P. W. Anderson, J. Phys. F **5**, 965 (1975).

[11] D. Sherrington and S. Kirkpatrick Phys. Rev. Lett. **35**, 1792 (1975).

[12] K. Binder and A. P. Young, Rev. Mod. Phys., **58**, 80 (1986).

[13] G. Parisi, Phys. Rev. Lett. **43**, 1754 (1979); G. Parisi, J. Phys. A **13**, L115 (1980; G. Parisi, J. Phys. A **13**, 1101 (1980); G. Parisi, J. Phys. A **13**, 1887 (1980); G. Parisi, Phys. Rev. Lett. **50**, 1946 (1983).

[14] F. Barahona, J. Phys. A **15**, 3241 (1982).

[15] M. Mezard, G. Parisi, and M. A. Virasoro, Europhys. Lett. **1**, 77 (1985).

[16] M. Mezard, G. Parisi, and M. A. Virasoro, *Spin Glass Theory and Beyond* (World Scientific, Singapore, 1987).

[17] M. Mezard, G. Parisi, and R. Zecchina, Science **297**, 812 (2002).

[18] A. Braunstein, M. Mezard, and R. Zecchina, Random Structures and Algorithms **27**, 201 (2005).

[19] J. D. Bryngelson and P. G. Wolynes, Proceedings of the Natl. Acad. of Science (USA) **84**, 7524 (1987).

[20] J. J. Hopfield, Proc. Natl. Acad. Sci. USA **79,** 2554 (1982); D. J. Amit, H. Gutfreund, and H. Sompolinsky, Phys. Rev. Lett. **55**, 1530 (1985); J. J. Hopfield and D. W. Tank, Science **233**, 625 (1986); H. Sompolinky, Physics Today **41** (12), 70 (1988).

[21] C. M. Newman and D. L. Stein, Comm. Math. Phys. **224**, 205 (2001).

[22] Given any Ising spin configuration one may inspect the sign of each of the links z_α on the lattice. If there is an extensive (volume proportional) number of links z_α that are of

different signs in two different Ising spin configurations $|\mathsf{s}\rangle$ and $|\mathsf{s}'\rangle$ then the two states are said to be "incongruent" relative to one another [3].

[23] J. E. Avron, G. Roepstorff, and L. S. Schulman, J. Stat. Phys. **26**, 25 (1981).

[24] M. Loebl and J. Vondrak, Discrete Mathematics **271** (1-3), 179 (2003).

[25] J. W. Landry and S. N. Coppersmith, Phys. Rev. B **65**, 134404 (2002).

[26] E. Marinari and G. Parisi, Phys. Rev. B **62**, 11677 (2000).

[27] H. Rieger, *Frustrated Systems: Ground State Properties via Combinatorial Optimization*, Lecture Notes in Physics Vol. 501 (Springer-Verlag, Heidelberg, 1998).

[28] J. Houdayer and O. Martin, Phys. Rev. Lett. 83, 1030 (1999).

[29] R. N. Bhatt and A. P. Young, Phys. Rev. B **37**, 5606 (1988).

[30] We exclude classical systems with topological degeneracy, M.-S. Vaezi, G. Ortiz, and Z. Nussinov, Phys. Rev. B **93**, 205112 (2016).

[31] Notice that one can write the asymptotic form

$$\mathcal{P}(\mathsf{C}_{\bar{\jmath}}) \sim \sqrt{\frac{2}{\pi g_{\bar{\jmath}} m}}, \tag{4.24}$$

for large m after applying Stirling's approximation.

[32] A. Galluccio, M. Loebl, and J. Vondrak, Phys. Rev. Lett. **84**, 5924 (2000).

[33] J. A. Blackman, J. R. Goncalves, and J. Poulter, Phys. Rev. E **58**, 1502 (1998).

[34] L. Saul and M. Kardar, Phys. Rev. E **48**, R3221 (1993).

[35] N. Kawashima and H. Rieger, in Frustrated Spin Systems, edited by H. T. Diep (World Scientific, Singapore, 2005), chap. 9, p. 491.

[36] M. Cieplak and J. R. Banavar, Phys. Rev. B **27**, 293 (1983).

[37] R. Peierls, Proc. Camb. Phil. Soc. **32**, 477 (1936).

[38] R. B. Griffiths, Phys. Rev. **136**, A437 (1964).

[39] G. Ortiz, E. Cobanera, and Z. Nussinov, Nuc. Phys. B **854**, 780 (2011); see Appendix E in particular.

[40] C. Bonati, European Journal of Physics **35**, 035002 (2014).

[41] A. K. Hartmann and A. P. Young, Phys. Rev. B **64**, 180404 (2001).

[42] S. Boettcher, European Physics Journal B **38**, 83 (2004).

[43] I. Bieche, R. Maynard, R. Rammal, and J. P. Uhry, J. Phys. A **13**, 2553 (1980).

[44] H. Khoshbakht and M. Weigel, Phys. Rev. B **97**, 064410 (2018).

[45] A. B. Finnila, M. A. Gomez, C. Sebenik, C. Stenson, and J. D. Doll, Chem. Phys. Lett. **219**, 343 (1994).

[46] S. Mandrà, Z. Zhu, and H. G. Katzgraber, Phys. Rev. Lett. **118**, 070502 (2017).

[47] A. J. Bray and M. A. Moore, Phys. Rev. Lett. **58**, 57 (1987).

[48] C. K. Thomas, D. A. Huse, and A. Middleton, Phys. Rev. Lett. **107**, 047203 (2011).

[49] D. Hu, P. Ronhovde, and Z. Nussinov, Philosophical Magazine **92**, 406 (2012).

[50] Z. Zhu, A. J. Ochoa, S. Schnabel, F. Hamze, and H. G. Katzgraber, Phys. Rev. A **93**, 012317 (2016).

[51] In order to attain any state, a number of links $\{\mathcal{J}_\alpha^m\}$ must be flipped relative to a ground state. The probability for obtaining a particular energy amounts to a convolution on the probability distribution of the links. The latter convolution readily becomes a trivial product after Fourier transformation.